DIFFUSION IN THE INTERMETALLIC COMPOUND NiAL

Thesis

Submitted for the

Degree of Doctor of Philosophy

by BARRY RUSSELL McDONNELL

APRIL 1969

Department of Metallurgy,
Imperial College of Science
and Technology,
University of London.

CONTENTS

1. SYNOPSIS

Single crystals and large polycrystals of the intermetallic compound NiAl have been grown by a modified Bridgman technique.

The self diffusion coefficient of nickel-63 has been measured in the stoichiometric and in ten non-stoichiometric compositions of the compound, in the temperature range 1000°C to 1350°C. The results have been interpreted in terms of both linear and non-linear Arrhenius dependences; the latter in recognition of the possibility of there being 'anomalous' diffusion behaviour in this compound.

A comparision has been made between the activation energies of self diffusion, as a function of composition, and previously reported activation energies for high temperature deformation.

The applicability of the six-jump cycle vacancy mechanism to diffusion in NiAl compounds has been discussed. An estimate of the activation energies of vacancy formation and of motion has been made from the self diffusion activation energies.

CHAPTER 2 INTRODUCTION & LITERATURE SURVEY

2.1 GENERAL INTRODUCTION

Intermetallic compounds have, during the last decade, been the subject of renewed interest due to the demand for new materials, especially for applications in high temperature environments. In such applications these compounds are of considerable importance in their capacities as second phases, which are precipitated in order to provide strengthening mechanisms. These compounds, and alloys based on them, have not found extensive industrial applications since, although their mechanical properties may be good, they are not sufficiently superior to those of existing alloys to warrant serious consideration. In some cases this lack of exploitations has been due to the technical problems of fabrication and handling, which arise from their low temperature brittleness. Other intermetallic compounds have found applications as superconductors and semiconductors.

The intermetallic compound NiAl has a relatively high melting temperature (1638°C), good resistance to oxidation at all temperatures below 1000°C, comparatively good high temperature strength and ductility, but low temperature brittleness. It is used as an oxidation resistant coating on turbine blades (Sheppard 1963). Harlo & Otto Gamba (1964) have produced a layer of NiAl, between a uranium fuel element and its aluminium can, which acts as a diffusion barrier, since diffusion rates in NiAl are relatively slow. The layer, produced by annealing the aluminium can with a layer of nickel on its inside surface, then provides protection to the can against attack from the element.

An understanding of intermetallic compounds generally

has been achieved by the extensive studies of compounds such as CuZn and AgMg, for example. NiAl, although it is isomorphous with AgMg, has a different defect structure on either side of the stoichiometric composition, whereas AgMg has the same defect structure throughout the non-stoichiometric alloys. Much of the fundamental interest in NiAl arises from this variation of defect structure and its role in determining the mechanical and physical properties of the material. A study of the variation in the activation energy of diffusion in NiAl, and a comparison with those found in AgMg, would give some indication of the atomic mechanisms involved in diffusion. A comparison between these activation energies and those obtained from high temperature deformation studies could establish a greater understanding of diffusion controlled deformation processes in this compound.

Interest in metallic diffusion is relatively recent and the greater bulk of experimental results have been presented this century. All the earlier studies employed chemical analytical techniques (Cyril Wells 1951), which, compared to modern radio-isotope methods, were crude and inaccurate, although the results of Roberts-Austin's measurements of gold diffusivities in lead in 1896 were reasonable, even by today's standards. It was not until 1920 that Groh & Von Hevesy introduced the use of radioactive tracers to diffusion studies, which have made the accuracies of modern techniques possible. There followed a period of intense activity in the field, which has been attributed to the need to understand diffusion controlled processes such as creep, phase transformations, precipitation, grain growth and sintering.

The results, at this stage of development, have been summarised in review articles by Mehl (1936 and 1937), Barrer (1941), Smithells (1949), Jost (1952) and Seith (1955).

Because of the greater accuracies achieved in subsequent studies, the greater bulk of this work is now only of qualitative interest. This is due to the availability of a wide variety of radioisotopes of high quality, which has lead to the development of a number of new and more precise techniques. This greater accuracy encouraged a growing emphasis on the elucidation of the atomic mechanisms of diffusion processes.

The object of the present study is to measure the self diffusion coefficients of nickel in NiAl as a function of composition and temperature. It is hoped that the activation energies will provide an insight into the mechanisms that are responsible for diffusion on either side of the stoichiometric composition, and that the results will aid the interpretation of the high temperature deformation behaviour of NiAl which has been studied in detail.

2.2 ATOMIC MECHANISMS OF DIFFUSION

Each of the mechanisms of volume diffusion involves the movement of atoms in relation to each other, which, when considered in large numbers, constitutes net transport of a species. In the majority of metallic systems these mechanisms are closely associated with crystal defects. For the purpose of considering these mechanisms in more detail they are shown schematically in Fig. 2:1 (after Lazarus 1960).

2.2.1. The Interchange Mechanism

In the direct interchange mechanism atoms undergo a correlated rotation about a common centre. As the number of atoms involved in the interchange ring increases, the theoretical activation energy first decreases rapidly and then

increases slowly (Zener 1950). The minimum theoretical activation energy occurs with either 4 or 6 atom rings, depending on the system and crystal structure. Because of the high distortion involved, it is energetically unfavourable in most systems, especially in close packed crystal structures. However, it has been invoked to explain certain apparent anomalies of diffusion behaviour in some transition metals with b.c.c. structures (Pound et al 1961). This seems a plausible suggestion in the light of the more open nature of b.c.c. lattices.

2.2.2. The Interstitial Mechanism

The interstitial mechanism can only occur in alloys in which the diffusing constituent occupies the interstitial sites in the lattice of the solvent constituent. An atom is said to diffuse by an interstitial mechanism when it passes from one such site to one of its nearest-neighbour sites without permanently displacing any of the matrix atoms. The mechanism is known to operate in the diffusion of carbon and nitrogen in iron (Birchenall & Mehl 1947; Fisher et al 1948). It is not likely to be important in highly ordered compounds like NiAl, nor are the 'interstitialcy' or 'crowdion' mechanisms (Paneth 1950), which are both modified interstitial mechanisms.

2.2.3. The Vacancy Mechanism

An atom is said to have diffused by a vacancy mechanism if it executes a jump into an adjacent unoccupied site or vacancy. The distance that the restraining atoms must move apart, in order for the diffusing atom to pass between them, represents the distortion involved in this mechanism. The mechanism has been established for most f.c.c. metals and alloys and in some b.c.c. and c.p.h. systems. The greatest

evidence of diffusion by a vacancy mechanism is the Kirkendall shift of an inert marker, placed initially at the interface of the two metals, and subsequently interdiffused (Kirkendall 1942: Smigelskas & Kirkendall 1947). The original explanation of the Kirkendall effect was given by Darken (1948) and was later amplified by Seitz (1948) and by Bardeen (1949). Further clear evidence of a vacancy mechanism has been provided by Bonzel (1965) by his reported enhancement of diffusivities following the production of excess vacancies by irradiation damage.

In ordered compounds and alloys the simple vacancy mechanism is unlikely because of the disorder that it would create. In ionic compounds like CsCl and NaCl atomic jumps to next-nearest-neighbour vacant sites are more likely because they would not leave atoms on 'wrong' sites. Such a mechanism would not occur in pure metals, which do not require the maintenance of order, so diffusion would be by the energetically more favourable nearest-neighbour jumps. (See also Chapter 6).

A second extension of the vacancy mechanism for ordered alloys has been postulated by Elcock & McCombie (1958) and Elcock (1959), which would allow diffusion, by motion round certain cyclic vacancy tracks, without creating disorder (Fig. 2:2, after Domian & Aaronson 1964). Each jump of the six jumps in the cycle is a jump to a vacancy at a nearest-neighbour site. Thus the first three jumps all create disorder by placing atoms on wrong sites, but the last three all recreate order on these sites. The first three jumps therefore require relatively high energy to overcome the disorder they create, but once completed, the probability of the remaining three jumps is high, due to the driving force provided by the ordering energy. The net result is that an atom of one species has changed position with a vacancy on a

diagonally opposite position (see Fig. 2:2), and two atoms of the second species have exchanged diagonally opposite positions. The mechanism makes two assumptions:

a) that the nearest-neighbour sites of one atom species are occupied exclusively by atoms of the second species, and

b) that the only unit mechanism for atom movements is by jumps to nearest-neighbour vacancies.

This mechanism is discussed in greater detail in Chapter 6 since there appears to be evidence to support the postulation that it is responsible for diffusion in ordered alloys, such as intermetallic compounds with a CsCl structure.

2.3 DIFFUSION THEORY

Studies of volume diffusion necessitate divorce from the effects of both grain boundary and volume diffusion, because it is otherwise difficult to differentiate between the contributions made by each type of diffusion. Many of the early diffusion studies were inaccurate because they were presented without sufficient understanding of this discrimination. The theory of diffusion developed in this chapter is related to volume diffusion only since the present study is concerned with its measurement. Surface and grain-boundary diffusion are dealt with only briefly.

2.3.1. Grain Boundary Diffusion

The fact that grain boundary diffusivities are greater than volume diffusivities is not difficult to understand if a grain boundary is visualised as a region in which there is a high concentration of defects compared to that of the bulk crystal, and assuming that the mechanism in both cases

involves defects. The first serious attempt to interpret grain boundary diffusion was made by Langmuir in 1934. More recently Fisher (1951) has mathematically analysed his analogy of heat conduction along copper wires embedded in cork, and has successfully predicted grain boundary diffusivities in silver. Since then renewed interest has developed due to the importance of grain boundary diffusion in grain growth, sintering and corrosion.

Modern radioisotope techniques have made it possible to differentiate between the diffusivity in one grain boundary to that in another within the same material. Acher & Smoluchowski (1951) have subsequently related boundary diffusivities to the misorientation angle of the boundary. It has been shown that only in the limit of zero misorientation does the boundary diffusivity approach the volume diffusivity (Yukawa & Sinnott 1955). These conclusions are important in so far as they justify the steps that are generally taken to eliminate grain boundary contributions to volume diffusion measurements. Although Turnbull (1951) has suggested that large grain sizes of 1 - 3 mm are necessary to eliminate such contributions, the only certain method of establishing whether grain boundary diffusion is contributing appreciably is to examine the isotope penetration macroscopically by autoradiography (see Section 3.2.4).

2.3.2. Surface Diffusion

Although it is obvious that the rates at which atoms migrate across free surfaces are going to be considerably greater than the rates of volume diffusion, surface diffusion still remains the least investigated and understood type of diffusion. The experimental difficulty of preparing chemically perfect surfaces, and of maintaining this perfection at high temperatures, are responsible for this. Surface

diffusion has been reviewed by Blakely (1963) and its mechanisms discussed by Birchenall (1959). It is of interest that Fisher's analysis (1951), which was developed in connection with grain boundary diffusion, has predicted surface diffusivities in some systems.

Surface diffusion interferes with volume diffusion measurements. For example, with techniques which follow the penetration of a radioisotope from one end of a cylindrical specimen, surface diffusion can cause contamination of the sides of the cylinder, so that subsequent penetration is not solely from the end of the cylinder. This can cause exaggerated estimates of isotope penetration, which introduce errors in the volume diffusion coefficient. The ways in which these errors are reduced or eliminated are discussed in greater detail in Chapter 3.

2.3.3. Other Forms of Preferential Diffusion

The dependence of volume diffusion on the crystal defect has been demonstrated by the pronounced diffusivity enhancement caused by the production of excess defects as a result of irradiation damage (Bonzel 1965). Williams & Slifkin (1958) have shown that a similar dependence exists with increasing dislocation densities. Enhancement of nickel self diffusion by mechanical deformation described by Dorn & Wazzen (1965) has given support to this dependence. Relatively small diffusivities in systems with low solid solubilities encourage short circuiting paths within a crystal as has been shown, for example by Hirano, Agarwala & Cohen (1962). Lazarus (1955) has suggested that diffusion enhancement in some systems is due to the valency difference between solute and solvent constituents.

2.3.4. Fick's Laws of Volume Diffusion

It is well-known that for the transport of heat in solids the thermal flux is proportional to the temperature gradient through a constant which is called the thermal diffusivity. Using this analogy Fick (1855) developed a similar relationship to describe mass flow in solids.

Fick's first law was developed from a consideration of unidirectional mass flow in a solid, assuming that the concentration (c) at a point is independent of time (t). The flux (J) of material passing through unit area of a plane, in unit time, is given by:

$$J = -D \frac{\partial c}{\partial x} \qquad (2.1)$$

where x is distance in the diffusion direction, and the proportionality constant D is known as the diffusivity or diffusion coefficient, which has dimensions of $(\text{length})^2/\text{time}$, usually cm^2/sec.

Fick's second law, derived from the first, was developed to describe diffusion under non-steady state conditions, in which the concentration changes with time, and is given by:

$$\frac{\partial c}{\partial t} = \frac{\partial}{\partial x} \left(D \frac{\partial c}{\partial x}\right) \qquad (2.2)$$

In the special case in which the diffusion coefficient is independent of the concentration this law becomes:

$$\frac{\partial c}{\partial t} = D \frac{\partial^2 c}{\partial x^2} \qquad (2.3)$$

Fick's laws preceded any quantitative experimental work and can be regarded as only a phenomenological or descriptive basis of diffusion theory. The laws do not describe adequately the majority of diffusion behaviour; in fact the

simple direct proportionality suggested by the first law is only found in exceptional circumstances.

2.3.5. The first Objection to Fick's Laws; and Self Diffusion

In practice the diffusion coefficient is found to be a function of the instantaneous composition, the composition gradient, temperature, pressure and other external fields. By careful control of experimentation these latter influences can be controlled, so that diffusivities can then be considered as functions of only composition and composition gradients. In the limiting case of vanishingly small gradients, diffusion is called self diffusion. Thus any flux of atoms in such a system must originate solely from random atomic motions through the lattice.

By the theory of random movements Chandrasekhar (1943) derived an expression for the self diffusion flux:

$$J = -\frac{1}{2}\alpha^2 \Gamma \frac{\partial c}{\partial x}$$

which is identical to Fick's first law providing:

$$D = \frac{1}{2}\alpha^2 \Gamma$$

where α is the mean jump distance and Γ is the average number of atom jumps/sec. Extending to three dimensions:

$$D = \frac{1}{6}\alpha^2 \Gamma \qquad (2.4)$$

The random jump frequency is given by:

$$\Gamma = n \nu f$$

in which n is the total number of independent jumps, each of

which has a jump probability of ν, and f is the probability that any jump is statistically independent of the previous jump and is called the correlation factor. Equation 2.4 now becomes:

$$D = \frac{1}{6}\alpha^2 n \nu f \qquad (2.5)$$

If a specific mechanism is now considered, for example substitution between nearest-neighbours in a simple cubic lattice, then the jump distance can be related to the lattice spacing (a) by: (Lazarus 1962)

$$a^2 = (n/6)\alpha^2$$

Substituting for α^2, equation 2.5 becomes:

$$D = a^2 \nu f \qquad (2.6)$$

By a more detailed study of diffusion by the random walk theory it can be shown that the correlation factor (after Bardeen & Herring 1951) is given by:

$$f = (1 + \overline{\cos\theta})/(1 - \overline{\cos\theta})$$

where $\overline{\cos\theta}$ is the average value of the cosine of the angle (θ) between successive jumps. Thus for purely random jumps which are statistically independent $\overline{\cos\theta}$ approaches zero, and f approaches unity. For the opposite extreme, in which all jumps are followed by one in the reverse direction, then $\overline{\cos\theta} = -1$ and $f = o$ and there is no atomic displacement.

In reality the correlation factors for the mechanisms

responsible for diffusion generally fall between the two extremes. A relatively simple model developed by Lidiard (1955) and Lidiard & Le Claire (1956), and extended by Manning (1959), has been used to calculate approximate values for correlation factors in specific systems. Manning (1958) has shown that for either an interstitial or interchange mechanism in a pure crystal $\cos\phi$ vanishes and f = 1. However, for a vacancy mechanism, f = 0.78 in b.c.c. lattices and 0.80 in f.c.c. lattices, although Compaan & Haven (1956) have calculated a value of 0.721 in b.c.c. lattices.

2.3.6. The Second Objection to Fick's Laws; and the Phenomenological Equations of Diffusion

Fick's laws indicate that the driving force for diffusion is the chemical concentration gradient of the diffusing species. However, it has now been established that it is the gradients in chemical potential which provide the driving force. Furthermore the chemical potential gradients of constituents, other than that of the diffusing constituent, also contribute a driving force for the diffusing species. The phenomenological equations were developed by Onsager (1931 & 1932) and Onsager & Fuoss (1932) to describe observed conditions of equilibrium and have since been discussed in detail by de Groot (1952).

The equations led Darken (1948) to relate the intrinsic or partial diffusion coefficient (D_p) to the self diffusion coefficient (D) by:

$$D_{pl} = D_l \left[1 + (\partial \ln \gamma_1 / \partial \ln N_1)\right] \qquad (2.7)$$

in which γ_1 is the thermodynamic activity coefficient of the first constituent which has an atom fraction of N_1 in the system. It can be seen that in the special case of Einstein's

ideal and dilute solution ($\gamma_1 = 1$) the two diffusion coefficients become equal.

The chemical diffusion coefficient ($\bar{D}$), as described by Fick's second law, and measured by the now classical method of Matano (1933), can be related to the other two coefficients. If, in an interdiffusion experiment to measure a chemical diffusion coefficient in a binary system, the two intrinsic diffusion coefficients are unequal, a displacement of the original interface between the two constituents occurs, as was first shown by Smigelskas & Kirkendall (1947). Darken (1951) then related the chemical coefficient to the two intrinsic coefficients in terms of the two atom fractions (N_1 & N_2) of the constituents:

$$\bar{D} = N_2 D_{p1} + N_1 D_{p2}$$

From this equation and equation 2.7 Darken finally related the chemical coefficient to the two self diffusion coefficients:

$$\bar{D} = (N_2 D_1 + N_1 D_2)\left[1 + (\partial \ln \gamma_1 / \partial \ln N_1)\right]$$

These equations have been verified experimentally in a number of systems, see for example Reynolds et al (1957). However, they contribute little towards a better understanding of diffusion on an atomic scale, which is of greater importance for establishing diffusion mechanisms.

2.3.7. Theoretical Calculations of the Diffusion Coefficient

It is now established that in the majority of metal systems the mechanism of diffusion involves crystal defects. Thus it is possible to derive a theoretical expression for the diffusion coefficient, which is similar to equation 2.6, in terms of the fraction of vacancies and the probability of

a jump to a neighbouring vacancy (W):

$$D = \gamma a^2 f \, w \, N_v \qquad (2.8)$$

in which in this case γ is a geometical factor. From this equation it can be seen that a theoretical calculation of D has been resolved essentially into one of calculating theoretical values of:

a) the vacancy concentration, and

b) the jump frequency.

These two calculations will now be considered in detail.

2.3.8. The Vacancy Concentration

The equilibrium concentration of vacancies (N_{ve}) can be derived from the entropy of mixing arising from vacancy additions (see, for example, Shewmon 1963), and is given by:

$$N_{ve} = \exp(-\Delta G_f/RT) \qquad (2.9)$$

where the Gibbs Free energy of vacancy formation is related to the changes in enthalpy (ΔH_f) and entropy (ΔS_f) at temperature T by:

$$\Delta G_f = \Delta H_f - T\Delta S_f$$

The equilibrium vacancy concentration therefore increases with temperature (see equation 2.9). The entropy of vacancy formation is difficult to estimate; if, however, it is assumed to be negligibly small then equation 2.9 reduces to:

$$N_{ve} = \exp(-\Delta H_f/RT) \qquad (2.10)$$

2.3.9. The Jump Frequency

Because of the limitations in present knowledge of interatomic bonding, theoretical calculations of the jump frequency can only be approximate. The most significant aspect of such calculations is the insight they provide to the factors which influence the frequency and therefore the diffusion coefficient.

Consider Fig. 2:3, which indicates schematically, in two dimensions, how an atom jumping from one equilibrium state (a) to another (c) passes through a saddle point or activated complex (b). The work done (W) in moving an atom from an equilibrium state to an activated complex is equal to the change in Gibbs Free energy required to form the complex:

$$W = \Delta G_m = \Delta H_m - T\Delta S_m$$

For an atom to jump two conditions must first be fulfilled:

a) the amplitude of vibration of an atom towards the vacant site must be sufficiently large, and

b) the two restraining atoms in the activated complex must simultaneously move apart enough to allow the jumping atom to pass between them.

It is reasonable to assume that the frequency of successful jumps (w) in a system is proportional to the concentration of activated complexes (N_m). The equilibrium concentration of activated complexes (N_{me}) has been related to the change in Gibbs Free energy of a complex formation (Zener 1952) and the jump frequency is given by:

$$w = \nu N_{me} = \nu \exp(\Delta G_m/RT) \qquad (2.11)$$

where ν is in this instance the frequency with which an atom

jumps from an activated complex to an equilibrium site, and as an approximation is generally taken as the Debye frequency.

The problem of calculating the jump frequency has been treated more rigorously by Vinyard (1957) using a statistical mechanical method. He expresses the mean jump frequency in terms of products of frequencies in equilibrium states and in activated states. The similarity between this result and that from Zener's simple statistical model is not surprising since both approaches rely on similar assumptions. The assumption, made in both cases, that a system containing activated complexes is in thermal equilibrium is doubtful, because it is unlikely that an atom has time enough to reach a state of equilibrium in the short time in which it is in an activated configuration. However, both theories are justified by their ability to predict experimental results.

Quantum considerations, which were ignored in both these models, might effect their results in two ways:

a) because atoms, which attain the barrier energy (W), do not all execute a jump, reduces the frequency term (ν) by (1-R), where R is the reflection coefficient, and

b) a second factor is introduced as a measure of the finite probability that atoms which do not quite attain the barrier energy do execute a jump.

These two quantum phenomena have been treated by the perturbation theory of Wigner (1932) who concluded that no serious errors are incurred by ignoring them, because they both have opposite effects and therefore tend to cancel each other out.

A dynamical model developed by Rice et al (1958 & 1959) avoided the doubtful assumption that atoms in an activated complex configuration are in equilibrium with the surrounding lattice, but produced an equation for the jump frequency

which was similar to Zener's. Manley (1960), by generalising this whole theory and simplifying the complex mathematical solutions, showed that Zener's theory (equation 2.11) was an approximation of Rice's theory.

2.3.10. The Temperature Dependence of D for 'Normal' Diffusion

Consideration of equations 2.8, 2.9 and 2.11 indicate that D should be temperature dependent. This dependence was originally described by Arrhenius (1889), and can be intimated by an equation of the form:

$$D = D_o \exp(-Q/RT) \qquad (2.12)$$

in which the frequency factor (D_o) and the activation energy for diffusion (Q) may be dependent on composition but are independent of temperature.

There are three essential features which may be said to characterise 'normal' diffusion behaviour:

a) the temperature dependence of D is described accurately by the Arrhenius law,

b) the activation energy Q is proportional to the melting point (T_m), or solidus temperature in the case of alloys. For self diffusion this empirical correlation is generally found to be, to within $\pm$ 20%, $Q = 34T_m$, and

c) the frequency factor (D_o) is usually in the range 0.1 to 10.0 cm^2/sec.

With reference to Section 2.3.8, a theoretical equation for D can be computed from equations 2.8, 2.9 and 2.11, i.e:

$$D = \gamma a^2 f \nu \exp(-\Delta G_f/RT) \exp(-\Delta G_m/RT) \qquad (2.13)$$

which, substituting enthalpies and entropies for free

energies, becomes:

$$D = \gamma a^2 f \nu \exp((\Delta S_f + \Delta S_m)/R) \exp((-\Delta H_f - \Delta H_m)/RT)$$

where ΔS_f and ΔH_f represent the entropy and enthalpy of vacancy formation; and ΔS_m and ΔH_m represent the entropy and enthalpy of vacancy motion. Comparing equations 2.12 and 2.13 D_o can be identified by:

$$D_o = \gamma a^2 f \nu \exp((\Delta S_f + \Delta S_m)/R) \qquad (2.14)$$

assuming that the activation energy of diffusion (Q) is equal to the sum of the enthalpy terms ΔH_m and ΔH_f.

Thus, from an experimental determination of D_o and the lattice parameter and approximate values of ν f and γ, it is possible to obtain a value of the entropy of activation of diffusion. However, this calculation can rarely be carried out with any precision.

2.3.11. Zener's Theory of D_o

Zener has derived a semi-empirical expression for ΔS_m (Wert & Zener 1949: Wert 1950: Zener 1952). The treatment is applicable to an interstitial mechanism, which would dictate that the ΔS_f term in equation 2.14 should vanish. ΔS_m, by definition, is given by:

$$\Delta S_m = (\partial \Delta G_m/\partial T) = -\Delta G_o (\partial(\Delta G/\Delta G_o)/\partial T)$$

where $\Delta G_o = \Delta Gm$ at absolute zero. By integration of the force required to move an atom into a saddle point, Zener showed that:

$$\Delta G \cong \varepsilon_o^2 \mu$$

where ε_o is a measure of the lattice strain and μ is the tensile elastic modulus. By substitution, and since $\Delta G \cong \Delta H_o$:

$$\Delta S_m \cong -\beta\eta \Delta H_o/T_m \qquad (2.15)$$

where the parameter β is defined by Zener as:

$$\beta = -\partial(\mu/\mu_o)/\partial(T/T_m)$$

and η is a constant, which is less than unity, to account for the fact that not all the work done in moving an atom into an activated complex configuration goes into straining the lattice. It is generally assumed to be 0.55 for f.c.c. and unity for b.c.c. solvent lattices. Because β, T_m and η are constants of any one solvent, then Zener's theory (equation 2.15) dictates that ΔS_m is proportional to ΔH_m, since $\Delta H_m = \Delta H_o$ is a reasonable approximation, and that negative values of ΔS_m are therefore not allowed.

Zener (1951) extended his theory to diffusion by a vacancy mechanism with a result very similar to equation 2.15. The modification involved the difficult evaluation of ΔS_f, which Zener simply rationalised in terms of two vibrational frequencies; that of an atom in a perfect crystal and that of an atom after a vacancy had been placed next to it. Since the lattice would be less rigid in the direction of the vacancy, the latter frequency would be smaller than the former and ΔS_f would be positive. For simplicity therefore ΔS_f can be assumed proportional to ΔS_m so that:

$$\Delta S = \Delta S_f + \Delta S_m \cong -\beta\eta \Delta H/T_m$$

where $\Delta H = \Delta H_f + \Delta H_m$.

The assumptions made for the extension of Zener's theory to a vacancy mechanism lead to less agreement with experimental data than in the case of interstitial diffusion.

Zener's theory, although it was in agreement with much of the experimental diffusion data available at the time, was instrumental in casting doubts on the validity of data which contradicted the predictions of the theory. In connection with more recent and accurate data, the theory, or extensions of it, have predicted diffusion behaviour (Le Clair 1953: Buffington & Cohen 1954). However, the positive value of ΔS stipulated by the theory is in direct disagreement with some diffusion results which consistently indicate negative activation entropies. This behaviour is discussed in detail in the next sub-section.

2.3.12. 'Anomalous' Diffusion Behaviour

'Anomalous' diffusion behaviour does not exhibit the features characteristic of 'normal' diffusion, (see Section 2.3.11). Curvature is found on the log D vs 1/T plots, which can either be interpreted in terms of a sum of two exponential terms or in terms of two separate Arrhenius dependences which are each applicable over a restricted temperature range.(see Chapter 5 for details). Activation energies and frequency factors in such systems are far below the values predicted from the empirical rules which govern 'normal' diffusion. Furthermore negative entropies are common in such systems.

In an attempt to refine Zener's theory in order to allow negative entropies Dienes (1953) suggested that the entropy was in fact the sum of two terms:

$$\Delta S = \Delta S_1 + \Delta S_2$$

where ΔS_1 arose from the reduction in vibrational frequencies

in the region of a vacancy, and ΔS_2, which is negative, from the increase in vibrational frequencies in the region of an activated complex. Thus it can be seen that should $\Delta S_2 > \Delta S_1$ then ΔS will be negative. Huntington et al (1955) developed a similar theory and, by simplifying an otherwise complex statistical mechanical analysis, were in full agreement with Dienes (1953).

2.4 THE INTERMETALLIC COMPOUND NiAl

2.4.1. The Nickel-Aluminium Phase Diagram

The first reliable phase diagram for the nickel-aluminium system was determined by Bradley & Taylor (1937). The generally accepted diagram, shown in Fig. 2:4, is that due to Hansen (1958).

NiAl is stable over a wide range of composition on either side of the equiatomic, or stoichiometric, composition of 31.5 wt % Al; at room temperature this stability extends from 41.5 to 55.0 at. % Al (24.5 to 36.0 wt % Al). The stoichiometric compound has a congruent melting point of 1638°C, which drops with increasing departure from stoichiometry. The fall of the solidus is sharper than that of the liquidus which means that the alloys, especially those near the limit of the phase field, solidify over a wide temperature range.

2.4.2. The Crystal Structure of NiAl

The stoichiometric alloy has an ordered CsCl (B.2) crystal structure which consists of interpenetrating nickel and aluminium simple cubic lattices, such that the atoms of one occupy the body centred positions of the other (Fig. 2:5). The non-stoichiometric alloys cannot therefore be strictly

fully ordered.

Bradley & Taylor (1937) found that the density increased with nickel content (Fig. 5:1) but that the lattice parameter exhibited a maximum near the stoichiometric composition. They explained their results in terms of a different defect structure on either side of stoichiometry. The nickel-rich alloys were considered to be substitutional solid solutions of nickel in NiAl, in which the smaller and heavier nickel atoms gave rise to an increased density and lower lattice parameter. In the aluminium-rich alloys vacancies were thought to occupy some nickel atom sites causing a decrease in both the density and lattice parameter.

Cooper (1963 A) found that the maximum lattice parameter occurred at approximately 51 at. % Al and not at the equi-atomic composition. This result was interpreted as being due to the limited substitution of aluminium for nickel up to between 51.0 and 51.5 at. % Al, beyond which constitutional vacancies were incorporated on nickel sites. A theoretical calculation of densities as a function of composition, assuming Bradley & Taylor's lattice parameters, gives a closer agreement to Bradley & Taylor's density curve if Cooper's substitutional limit of 1.5 at. % Al is also assumed.

This unusual defect structure of the aluminium-rich compositions can be explained by the electron theory (Lipson & Taylor 1939: Hume Rothery & Raynor 1962). The true electron compound is one which has an electron concentration of 1.5, which is governed by the Brillouin zones; and their phase field terminates when this critical ratio is exceeded. NiAl is an example of a defect electron compound because the incorporation of vacancies on nickel sites, which are allotted a zero vacancy, allows an extension of the phase field in aluminium-rich compositions without exceeding the critical electron concentration of 1.5. In practice electron

concentrations greater than 1.5 are found which substantiates Cooper's hypothesis of limited aluminium substitution in these alloys.

It is not clear whether the constitutional and thermal vacancies in NiAl are clustered or not. Nuclear magnetic resonance measurements in NiAl (West 1964) have indicated clustering, whereas Cooper's (1963 A) x-ray measurements did not. But Cooper (1964) has argued that, since nuclear magnetic resonance is sensitive to changes in nearest neighbours, small aggregates of vacancies, which are smaller than clusters, would be consistent with both observations.

2.4.3. The Stability of the CsCl Structure

The effect of an order-disorder transformation upon the rates of diffusion are important and most marked, see for example Kikuchi (1961) and Kuper et al (1956) who found that ordering reduced diffusivities in β-brass, CuZn. It is therefore important to establish whether or not such a transformation exists in NiAl within the temperature range in which it is intended to measure diffusivities. There is now considerable experimental evidence which shows that the order, which is known to exist at room temperature, persists to high temperatures. The conclusion that NiAl is ordered to its melting point is supported by the absence of changes in resistivity up to 1200°C (Guseva 1951) and of diffusivities up to 1350°C (Berkowitz et al 1954). Further support arises from the covalent nature of the bond between unlike atoms, which arises from a transfer of charge to this short bond position with no associated electron transfer (Cooper 1963 B), and the strong room temperature order.

An approximation of the ordering energy of NiAl can be obtained from the theory of Bragg & Williams (1935) which considers this energy to be proportional to the critical

ordering temperature. If, for NiAl, this critical temperature is taken as the melting temperature of the stoichiometric alloy, then the theory predicts an ordering energy of 0.082 eV/atom.

Instability at low temperatures in NiAl is indicated by a martensitic transformation which has been observed in nickel-rich NiAl by Alexander & Vaughn (1937) and in a stoichiometric alloy by Pascoe (1966). Similar transformations have been observed in other intermetallic compounds, for example in AuCd and CuZn by Westbrook (1960).

2.5 REVIEW OF PREVIOUS WORK

2.5.1. The General Properties of Intermetallic Compounds

Most of the significant studies on intermetallic compounds have been made during the last two decades. The structural aspects of these intermetallic compounds and of ordered alloys has been reviewed by Muto & Takagi (1955), and by Guttman (1956). Collongnes (1956) has discussed typical phase diagrams of intermetallic compounds, and the consequences of deviations from stoichiometry.

The mechanical properties of intermetallic compounds was the subject of an international symposium in 1959, and the literature before this date was reviewed by Westbrook (1960). Many early studies, involving simple hardness and corrosion resistance measurements, have been reviewed by Paine et al (1960).

During the last decade, the results from more sophisticated tensile and compression tests, on single and polycrystalline intermetallics, have been related to the dislocation and atomic structures. Westbrook (1965) has reviewed the more recent mechanical properties, and Stoloff &

Davies (1966) the effect of order on these properties.

The mechanical properties of the intermetallic compound NiAl have been studied recently by Lautenslager et al (1965), Vandervoort et al (1966), Ball & Smallman (1966), Wasilewski (1966) and by Pascoe & Newey (1968).

Many intermetallic compounds are susceptible to intergranular failure by what has become known as the pest (Westbrook & Wood 1963 B). The pest, which can lead to the complete disintegration of a material, is particularly common in silicides, beryllides and aluminides, including aluminium-rich NiAl. Westbrook & Wood (1963 A) showed that the conditions which encouraged the pest also caused anomalous hardening at grain boundaries. It has been shown that these conditions amount to oxygen absorption along grain boundaries (Seybolt & Westbrook 1964). Turner et al (1966) detected precipitates of aluminium suboxide (Al_2O) at grain boundaries in aluminium-rich NiAl. They suggested that the volume expansion associated with the oxidation of this highly unstable phase to the stable oxide α-Al_2O_3, on exposure to the atmosphere for several days, was responsible for the disintegration.

2.5.2. Diffusion in CuZn and AgZn

The most familiar compound amongst the intermetallic compounds which have a CsCl crystal structure is CuZn. Inman (1954) made a detailed diffusion study of copper-64 and zinc-65, both produced in situ by neutron irradiation, in polycrystalline CuZn. In 1956 Landergren measured a chemical interdiffusion coefficient in the same system, and found that the inert tungsten markers moved towards the zinc-rich side of the couple by distances which were consistent with Inman's self diffusion data substituted in Darken's

(1948) relationships (see Section 2.3.6). This study indicated that a ring-type or direct interchange mechanism were improbable since neither would provide the observed marker displacements.

Kuper et al (1956) measured self diffusivities of copper-64 and zinc-65, and the impurity diffusivity of antimony-124; the latter so that the effect of a change from nearly completely ordered CsCl structure to complete randomness could be followed. Curvature in the Arrhenius plots was attributed to the decrease in D as ordering increased. The investigation sought to distinguish between the interchange, vacancy and interstitialcy mechanism; the latter was thought to be most likely. In contradiction Slifkin & Tomizuka (1956), having previously also postulated the interstitialcy mechanism (1955), suggested a vacancy mechanism by nearest neighbour jumps. This conclusion, according to Lidiard (1957), was inconsistent with thermodynamic equilibrium and the maintenance of local order within the lattice (see also Chapter 6).

From the limited data available for AgZn it would appear that the situation is very similar to that of the CuZn compound, save that as much as an order of magnitude difference was found between the self diffusivities of zinc-65 and silver-110, (Gertstriken et al 1961), although the difference was observed to decrease with temperature.

2.5.3. Diffusion in NiAl, CoAl and FeAl

Diffusion studies in these intermetallic compounds are of particular interest because of the different defect structures which are exhibited on either side of stoichiometry (see for example Section 2.4.2). The role of the excess constitutional vacancies in aluminium-rich compositions should give some indication as to which mechanism operates in

these ordered CsCl-type structures.

The effect of the large concentrations of vacancies on diffusivities in NiAl was first studied by Smoluchowski & Burgess (1949), who measured the impurity diffusivities of cobalt-60 in seven compositions of NiAl at 1150°C. They found that the diffusivity increased with increasing excess nickel concentrations on the substitutional side of stoichiometry, but remained essentially constant with increasing excess aluminium on the defect side. They suggested that their results for the aluminium-rich compositions indicated that the excess nickel vacancies were unable to exchange with cobalt-60 atoms, because such a step would necessitate the intermediate exchange between a nickel vacancy and a nearest-neighbour aluminium atom. They argued that this intermediate exchange was unlikely because not only was the vacancy smaller than the aluminium atom but also that such an exchange would create disorder in an ordered system.

A study of cobalt-60 diffusion in CoAl, whose similar defect structure had been established by Bradley & Seeger (1939), was carried out by Nix & Jaumot (1951), to determine whether a similar effect existed in this compound. At all the three temperatures at which they measured diffusivities, in contrast to the behaviour found in NiAl by Smoluchowski & Burgess (1949), they found a minimum diffusivity at the stoichiometric composition but with an indisputable increase for the aluminium-rich compositions. The activation energies showed a marked decrease in the aluminium-rich compositions from a maximum at the stoichiometric composition. They concluded that the cobalt vacancies did in fact contribute significantly to diffusion. In order to justify this conclusion they suggested that, in the light of the disordering effect of a nearest-neighbour vacancy mechanism,

the increase in diffusivities could be due to the probable existence of an appreciable degree of disorder, at the relatively high diffusion temperatures (Tret'yakov & Khomyakov 1959), which would permit some of the excess cobalt vacancies to be distributed over the lattice in a more random fashion. The results of Gertstriken & Dekhtyar (1956), who also studied diffusivities in this compound, supported the majority of Nix & Jaumot's data.

Berkowitz et al (1954) re-examined cobalt diffusivities in NiAl in more detail (see Fig. 5:20 & Section 5.7) than Smoluchowski & Burgess (1949). Their results, which disagreed with the constancy found in aluminium-rich diffusivities by Smoluchowski & Burgess, indicated a pattern similar to that found in CoAl by Nix & Jaumot (1951). They suggested that the difference between the constant activation energy, which they postulated for aluminium-rich compositions and which represented the enthalpy of vacancy motion only, and the energy at the stoichiometric composition was equal to the enthalpy of vacancy formation. For this to be true a vacancy mechanism must have been operative and there must have been no contribution from vacancy formation in the activation enthalpy of diffusion in these aluminium-rich alloys. From their results they then obtained a value of approximately 25 Kcals/mole for this energy of vacancy formation (see also Chapter 6), which they thought reasonable, and concluded that a vacancy mechanism was strongly indicated, especially in aluminium-rich compositions.

The cobalt tracer atoms which were used in the self diffusion studies discussed above substitute for nickel atoms in NiAl. The results therefore represent nickel self diffusion only. A determination of aluminium self diffusivities in NiAl has not as yet been carried out. Such a study has so far been precluded by procedural difficulties owing

to the low specific activities, high expense and short half lives of the aluminium isotopes available.

The present knowledge of the variation of the self diffusion activation energies with composition, especially in aluminium-rich compositions, remains inconclusive and unsatisfactory (see Fig. 5:20). No activation energy measurements have yet been made in these alloys of sufficient accuracy to establish the true form of their variation with composition, from which confident suggestions as to a diffusion mechanism could be made. From the point of view of establishing a mechanism it is unfortunate that a simultaneous self diffusion study of both nickel and aluminium is not possible, since it is likely that the ratio of these diffusivities would fall within certain limits (see Chapter 6) if a six-jump cycle mechanism is operative. This project was envisaged in anticipation that an accurate self diffusion study of nickel-63 would establish a pattern for the activation energy variation with composition.

Vandervoort et al (1966) concluded that high temperature deformation in NiAl was by a diffusion-controlled viscous creep mechanism (Weertman 1957), and found that the activation energies for the mechanism (see Fig. 5:20) were higher but of the same order as those determined for cobalt-60 self diffusion by Berkowitz et al (1954). They also re-examined the data of Berkowitz et al at 55.5 at. % Ni and suggested that the activation energy for that composition should have been higher than that postulated by Berkowitz et al. The suggestion reduced the difference between their deformation activation energy and the value originally postulated by Berkowitz et al. It also indicated a less marked, but still linear, decrease in the activation energies with increasing excess nickel content.

Ball & Smallman (1966), as part of their deformation

studies in NiAl alloys, measured the rate at which dislocation loops annealed out at temperatures above 700°C using electron microscopy. By comparison with annealing rates in systems with known self diffusion activation energies, and assuming that dislocation annealing out was by a diffusion-controlled climb process, they were able to estimate self diffusion activation energies in three compositions. The only value obtained for a nickel-rich composition was in close agreement with those of Berkowitz et al (1954 and Fig. 5:20). Ball & Smallman suggested that their two results for aluminium-rich compositions, although showing similar agreement, did not confirm the activation energy constancy postulated by Berkowitz et al. Instead they suggested that the increasing percentage of constitution vacancies with departure from stoichiometry tend to decrease the activation energies.

Diffusion in FeAl compounds, which have a similar defect structure to NiAl, has been investigated by Gertstriken et al (1958). Their activation energies also show a sharp decrease with increasing excess aluminium content beyond the stoichiometric composition.

2.5.4. Diffusion in AgMg and AuCd

The intermetallic compound AgMg has received much attention as a model ordered b.c.c. structure, of the CsCl-type. Its relatively low melting temperature of 960°C and fair workability have both made more accurate experimental data possible. Initially the hardness (Westbrook 1957) and tensile behaviour (Wood & Westbrook 1962) suggested the possibility that the greater strengthening and lower activation energies for flow stress observed in magnesium-rich alloys, when compared to those in silver-rich alloys, resulted from concentrations of constitutional vacancies

similar to those found in aluminium-rich NiAl alloys. Although a part of this effect was later found to result from grain-boundary hardening (Westbrook & Wood 1963), Hagel & Westbrook (1961) concluded, from lattice parameter and density measurements, that only substitutional defects exist on both sides of stoichiometry. In three compositions only they also investigated the self diffusion of silver-110 and found no marked differences in the activation energies. Domian & Aaronson (1964) next provided diffusion data for silver-110 in six compositions of AgMg. Their activation energies showed a linear relationship with composition on both sides of stoichiometry, rising to a maximum value of 41 Kcals/mole at the stoichiometric composition. They assumed that an extension of the vacancy mechanism, namely the six-jump cycle (see Section 2.2.3), was the mechanism of diffusion in this compound, and calculated theoretical values of the activation energies which showed fair agreement with their experimental values (see also Chapter 6). Hagel & Westbrook (1965) and Westbrook & Hagel (1963), doubting the variation of the activation energies with composition in silver-rich alloys as postulated by Domian & Aaronson (1964), re-examined diffusion of silver-110 in three alloys on that side of stoichiometry. They found, in contrast to their previous investigation (Hagel & Westbrook 1961), that the activation energies do decrease with increasing excess silver content but do not to the extent reported by Domian & Aaronson (1964). The decrease was found to be proportional to the liquidus temperatures of the alloys. To account for the discrepancy between the two sets of data, Hagel & Westbrook (1963) have suggested that the low values reported by Domian & Aaronson were due to their specimen grain sizes, which were slightly smaller than is customarily acceptable for accurate volume diffusion

determinations (see also Section 2.3.1). On the magnesium-rich side of stoichiometry, however, both investigations are in agreement as to the compositional dependence of the activation energies, although both found that the energies decreased at a rate slightly faster than that predicted by the empirical melting temperature rule (see Section 2.3.10). Domian & Aaronson (1965) have measured the simultaneous diffusion of silver-110 and magnesium-28 in the stoichiometric composition of AgMg. The outer limits of their theoretically determined ratio of D_{Mg}/D_{Ag} are consistent with their experimental data. Their analysis has provided basic support for their prediction that a six-jump cycle could be the dominant mechanism in stoichiometric AgMg (see also Chapter 6).

A similar study has been carried out on the self diffusion of gold-198 and cadmium-115 in single crystals of stoichiometric AuCd (Huntington et al 1961), which also has an ordered b.c.c. CsCl structure. The cadmium-rich alloys have a defect structure of excess vacancies, similar to that found in aluminium-rich NiAl, although no evidence for such a defect structure was found for the gold-rich alloys from Gupta's (1961) density measurements. A discrepancy between the activation energies of Huntington et al (1961) and those predicted from Wechsler's (1957) resistivity measurements arose as a result of quenched in vacancies and short range order, giving anomalously low activation energies from the resistivity experiments. The ratio of D_{Cd}/D_{Au} was found by Huntington et al (1961) to be consistently 1.35. This value bore good agreement with a theoretical ratio, which provided evidence in support of a six-jump cycle mechanism. Gupta (1961) conducted the simultaneous self diffusion of gold-195 and cadmium-109 in three single crystals of AuCd, two of which contained excess gold. The ratio of the diffusivities for the cadmium-rich alloy varied between 0.6 and 1.6 so the

results were analysed assuming a six-jump cycle mechanism (see Chapter 6). A discrepancy, which exists between the data of Huntington et al (1961) and Gupta (1961), can be eliminated if the composition of the former's stoichiometric composition was in fact 50.2 at. % Cd. This illustrates one of the main difficulties of conducting diffusion measurements on intermetallic compounds - the problem of maintaining constant composition during diffusion anneals.

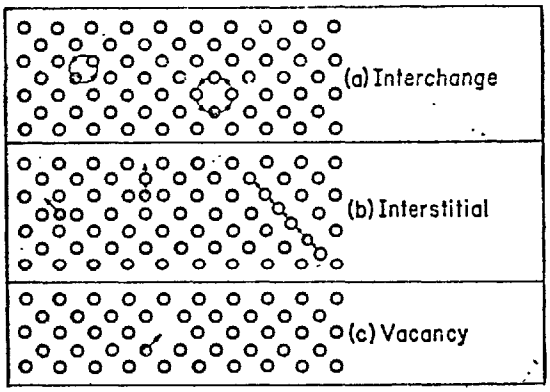

FIG. 2:1 MECHANISMS OF DIFFUSION

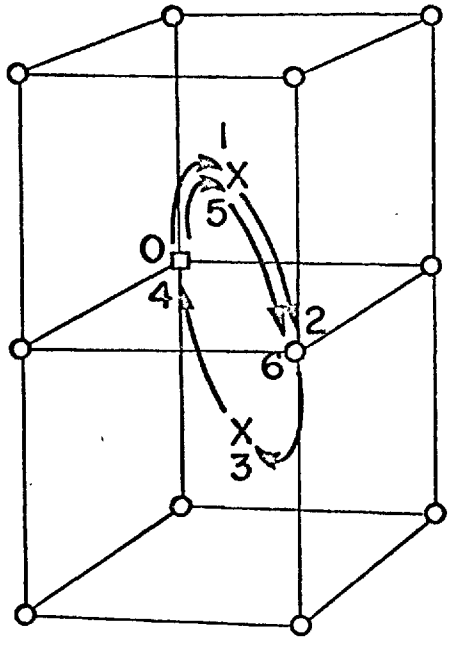

FIG. 2:2 THE SIX-JUMP CYCLE MECHANISM

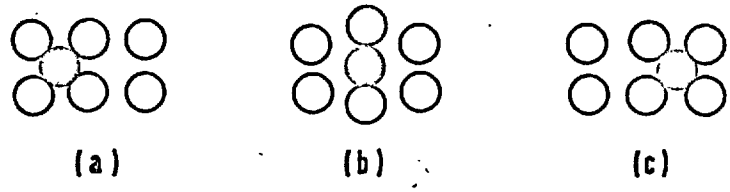

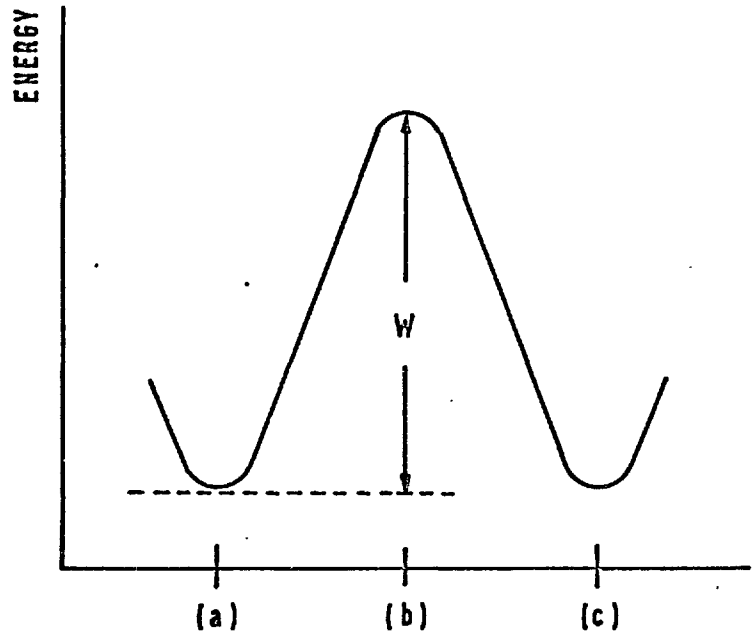

FIG. 2:3

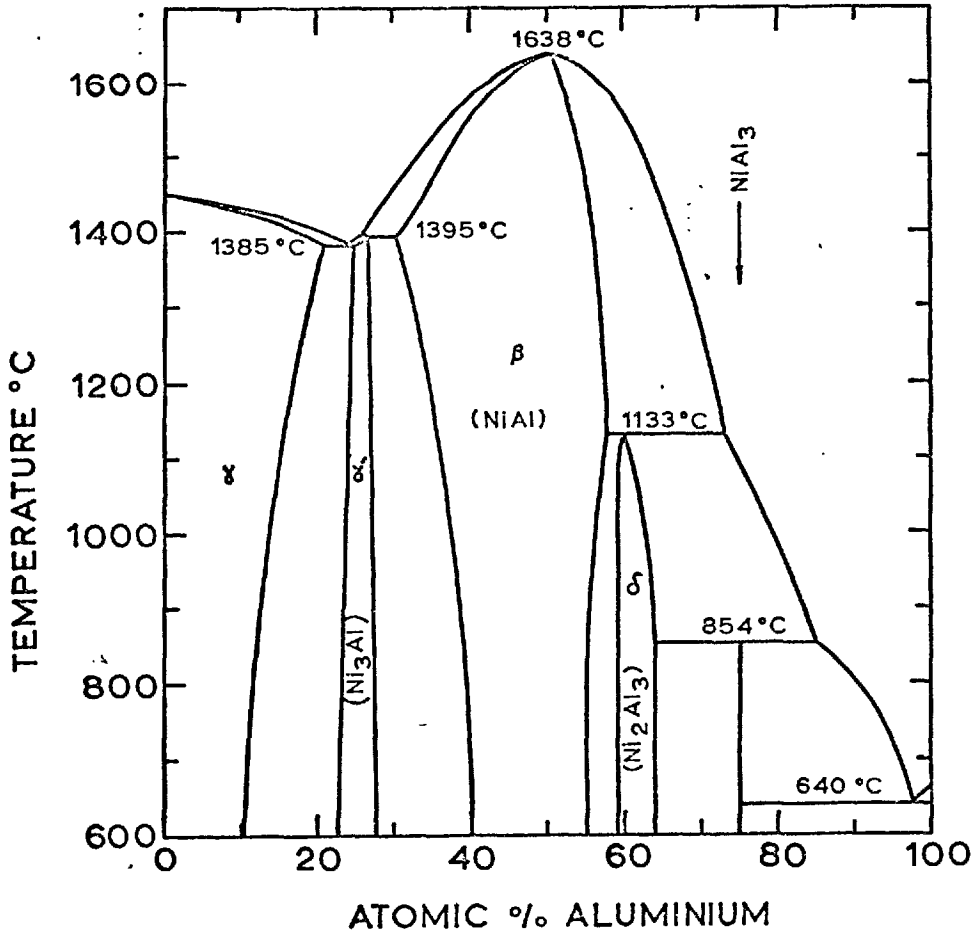
1638°C
1600
1400
1385°C
1395°C
NiAl3
β
(NiAl)
1200
1133°C
γ
α2
1000
854°C
(Ni3Al)
σ
(Ni2Al3)
800
640°C
600
0
20
40
60
80
100
TEMPERATURE °C
ATOMIC °/o ALUMINIUM

FIG. 2:4

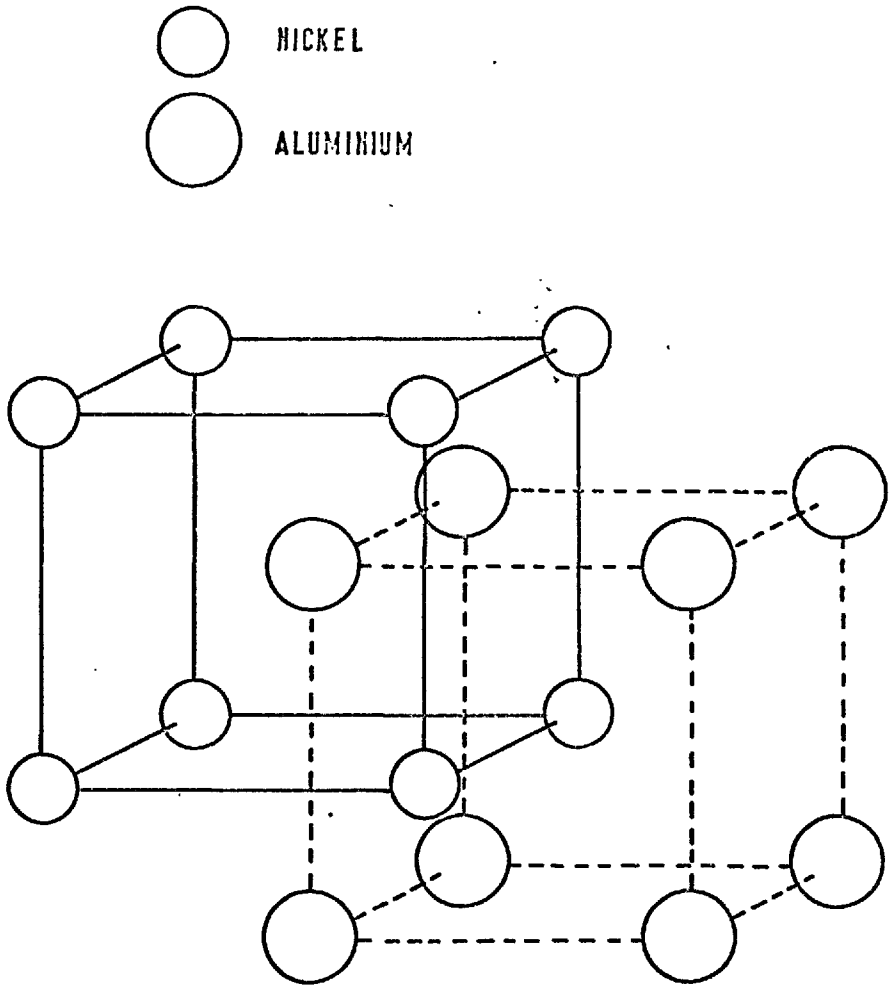

FIG. 2:5 THE CsCl B2 STRUCTURE

CHAPTER 3 INTRODUCTION TO EXPERIMENTAL TECHNIQUES

3.1 SOLUTIONS TO FICK'S EQUATIONS

Mathematical solutions to Fick's laws of diffusion (see Section 2.3.4), subject to sets of boundary conditions, still form the basis of most experimental determinations of the diffusion coefficient (Jost 1952: Crank 1956: Carslaw & Jaegar 1959).

Solutions to Fick's 2nd law of diffusion (see equation 2.2) for chemical interdiffusion, in which the diffusion coefficient varies with the concentration of the diffusing species, cannot be obtained by integration. Boltzman (1894) showed that the two variables (time (t) and the distance of diffusion in the x direction (x)) can be replaced by a single variable $\lambda = x/(t)^{\frac{1}{2}}$. A solution of Fick's 2nd law was then provided by Matano (1933) which yielded the chemical diffusion coefficient ($\overline{D}$). Experimentally the concentration of the diffusing species was determined as a function of distance from the Matano interface, and $\overline{D}$ is obtained from the determination of a slope and an area of a curve representing interpenetration. More recently Kass & O'Keeffe (1966) have provided numerical solutions of Fick's equations for chemical diffusion and concentration dependent diffusion coefficients. Chemical diffusion, because it represents transport under the driving force of chemical concentration and potential gradients, is of limited value to present theoretical work, which is attempting to understand self diffusion, or diffusion by random atom movements only. In order to calculate diffusion coefficients in the absence of chemical concentration gradients, it is necessary to use only very small quantities of the diffusing tracer, so that the small

concentration gradient may be safely neglected. The relevant solution to Fick's 2nd law (see equation 2.3), for diffusion which is independent of concentration, is called the 'thin film' solution. The diffusing species is initially present in a small concentration (C_o) at one end of a cylindrical shaped specimen. The concentration (C) at a parallel plane a distance x from the initial plane after a time t is given by the solution as:

$$C = \frac{C_o}{(\pi Dt)^{\frac{1}{2}}} \exp(-x^2/4Dt)$$

which satisfies the boundary conditions since:

$|x| > o$ for $C \rightarrow o$ as $t \rightarrow o$
and $x = o$ for $C \rightarrow \infty$ as $t \rightarrow o$

The solution is applicable only under isothermal and isobaric experimental conditions, and when the specimen can be considered infinite in the diffusion direction (i.e: $x > 4(Dt)^{\frac{1}{2}}$, see Shewmon 1963). In practice the diffusion coefficient is obtained from the slope (1/4Dt) of the linear plot of log C against x^2.

3.2 EXPERIMENTAL METHODS FOR DETERMINATION OF D

Diffusion coefficients can be measured experimentally by a variety of methods (Hoffman 1951: Cyril Wells 1951). By far the most accurate methods now available are those which employ radioactive tracers (Le Claire 1949: Leymonie 1963: Slifkin et al 1952: Tomizuka 1959). A readily available radioactive isotope of nickel (nickel-63) has made such techniques possible in the present study. The five most commonly employed methods all require that a thin layer of

the isotope is deposited on a specimen's reference face, so that 'thin film' solutions to Fick's laws are applicable (see previous Section). The methods all involve an analysis of the isotope penetration into the specimen as a result of diffusion anneals carried out under isothermal and isobaric conditions.

3.2.1. The Sectioning Technique

This technique, which is most commonly used, entails the successive removal of layers, parallel to the original specimen's reference face, and the estimation of the activity within each layer. These activities are proportional to the isotope concentrations. The activities are generally measured from a solution of the material, which renders the method unsuitable for isotopes with low radiation energies, because absorption will interfere with the activity counting. The method is also unsuitable for small diffusion coefficients since the layers removed would have to be correspondingly small.

The method has the advantage of simplicity providing the layers removed by lathing (Makin et al 1957), or other techniques (Liu & Drickamer 1954: Neiman & Chinear 1954), are carried out with sufficient care and precision. The method of removing layers can introduce an error if the new face is not exactly parallel to the specimen's original face (Shirn et al 1953). The diffusion coefficient is calculated from the slope of a penetration curve (log (activity) vs x^2).

3.2.2. The Surface Decrease Method

This method involves the measurement of the specimen's surface activity after each of a succession of diffusion anneals (Zhukhovitsky 1956). The diffusion coefficient is calculated from the rate at which this surface activity

decreases (Steigman et al 1939). The method is rendered inaccurate by the experimental difficulties of reducing the heating and cooling times for each anneal to a minimum, and by surface diffusion, which will contribute a decrease in the surface activity. The method demands a knowledge of the absorption behaviour of the radiation (Ruder & Birchenall 1951), since not all the activity measured can be attributed to the surface atoms. The method therefore is more applicable to systems in which the absorption is large. A measurement of the absorption coefficient is often rendered experimentally impossible because of difficulties in producing thin layers of the solvent. The main advantage of the method is that it does not necessitate the removal of a succession of layers from the specimen's active face.

3.2.3. The Residual Activity Technique

This method is similar to the sectioning technique, in so far as it also involves the removal of successive layers, but a measure of the isotope penetration is obtained from activity counts taken from the newly exposed faces. The diffusion coefficient is calculated, in the same way, from the slope of the penetration curve (Gruzin 1952). By removing the layers by precision grinding techniques (Portnoy et al 1954: Einsen & Birchenall 1957), instead of by lathing, it is possible to attain high accuracy with this method, and to measure small diffusion coefficients. The most important advantage of this technique over the sectioning technique is that it does not depend upon the collection of 100% of the material removed from the specimen, and which therefore avoids the errors incurred by such operations. The greatest disadvantage of this method arises when the energy of the isotope's radiation is such that a residual activity count will include a contribution from buried atoms. The error

involved cannot be accurately compensated for when this contribution originates from depths greater than those removed by grinding (Birchenall & Bourg 1960). The method is therefore most suitable when the isotope radiation is strongly absorbed.

3.2.4. Autoradiography

The activation of photographic emulsions by radiation allows a macroscopical image of isotope penetration to be made by autoradiographical methods (Gatos & Kurtz 1954). The penetration distances are generally amplified by photographing faces which have been cut at an oblique angle to the diffusion face. A penetration curve is obtained from intensity measurements on the exposed film. With these methods errors arise from the radiation contributions from buried atoms for which an approximate correction has been suggested by Kurtz et al (1955).

The technique has found its greatest application in the estimation of the extent of grain boundary and surface diffusion in self diffusion studies. For self diffusivity measurements the method is not generally considered as accurate as those already discussed, although Renouf (1964) and Mortlock & Tomlin (1959) have claimed to have attained comparable accuracies.

3.2.5. Kriukov's and Joukhovitzky's Method

This method involves the fabrication of very thin slices ($\sim 100\mu$) of the solvent which are plated and annealed in the same way as before. The activities of both the original plated surface and the opposite face are measured and the diffusion coefficient determined from their ratio (Kriukov & Joukhovitsky 1953). It is often experimentally difficult to produce these thin slices with sufficient precision, which

renders the method impractical in many cases.

3.2.6. Other Less Common Methods

Both Kuczynski (1948) and Le Claire (1949) describe a method involving activity measurements of various fractions of an exposed face of the specimen, perpendicular to the originally plated face, and parallel to the diffusion direction. The specimen is shielded in a lead box and a lead shield is employed to cover that part of the cut face not being counted. Kuczynski (1948) also describes a method based on sintering rates. Savitskiy (1964) has described a method of measuring self diffusion coefficients from measurements made on the redistribution rates of isotopes when the parent metal is immersed in one of its fused salts. Hudson & Hoffman (1961) used the sectioning technique but removed layers by electrolysis.

The diffusivities of asymmetrical solute atoms, e.g. carbon in α-iron, can be determined by internal friction methods (Zener 1948: Ke 1947: Nowick 1952 and 1953).

The measurement of diffusion coefficients by Nuclear Magnetic Resonance techniques (Holcomb & Norberg 1955), although reputedly not as accurate as tracer methods, make studies possible where other techniques are not applicable. Notable examples are systems in which suitable isotopes are not available. The main disadvantage to the method is the necessity of working with either very fine powders or very thin foils.

3.2.7. The Selection of a Method for the Present Study

The sectioning technique is not practical in the present study because of the very low energy of the radiation from nickel-63 (0.063 mev) being heavily absorbed by the solution during counting. The method is also impractical because of

the unmachinable nature of the compounds. Hirano et al (1963), on their work with iron cobalt & nickel diffusion in gold, found the surface decrease method less accurate than the residual activity method. The low energy of nickel-63 makes the isotope most suitable for the residual activity method, the validity of which has been discussed by Mackliet (1958) in connection with his study of nickel diffusion in copper. Although MacEwan et al (1959) employed the surface decrease method with nickel-63 they showed that the radiation from the surface of the Fe-Ni alloys originated from depths no greater than $\frac{1}{2}\mu$. This figure lends weight to the suggestion of Leymonie (1963) that no corrections are necessary for absorption if the layers removed are greater than 2μ.

If I_n is the activity measured from a surface, a distance x_n from the specimen's originally plated face, and μ is the absorption coefficient, then according to Gruzin (1952):

$$\mu I_n + \frac{\partial I_n}{\partial x_n} = \frac{\text{constant}}{(\pi Dt)^{\frac{1}{2}}} \exp\ (-x_n^2/4Dt)$$

The very low energy of nickel-63 radiation implies that the absorption will be high and that (I_n/x_n) will be very small compared to μI_n and can therefore be ignored.

Hoffman et al (1956) have employed both the surface decrease technique and the residual activity technique for their study of nickel self diffusion. A comparison of the results has lead them to suggest that, although good agreement is evident, the surface decrease method is less accurate. Jaumot & Smith (1956) have made a similar comparison in their study of zinc self diffusion, and reached the same conclusion.

3.3 THE SELECTION OF A METHOD OF DEPOSITING THE ISOTOPE

Irradiation, to produce an isotope in situ (Le Claire 1948), is not only impractical but is well known to produce excess defects as a result of radiation damage. The two most common methods of producing an isotope layer are by evaporation and electrodeposition (Hagel 1962). Jaumot & Smith (1956) compared the two methods for zinc with the result that both produced satisfactory deposits. In the present study it was considered more convenient to electrodeposit nickel from a solution. Amongst others Mackliet (1958) and Hirano et al (1961) have described nickel electrodeposition from solutions of nickel sulphate.

CHAPTER 4 EXPERIMENTAL PROCEDURE

4.1 ALLOY FABRICATION

4.1.1. Melting and Casting in a Molybdenum Furnace

Initial attempts to produce NiAl were carried out in an existing molybdenum tape-wound furnace using an argon atmosphere. These experiments were unsuccessful because the temperature of 1638°C, required to melt the stoichiometric alloy (Fig. 2:4), was not obtainable with sufficient superheat to provide a reasonable cast ingot. The oxidised state of the ingots which were produced indicated that the atmosphere control in the alumina work-tube was far from adequate.

4.1.2. Radio Frequency Induction Melting and Casting Techniques

First attempts to produce NiAl alloys by rf induction heating were carried out using a single stage coil in conjunction with a 15 KW rf generator. Melts were carried out in a graphite susceptor/crucible, contained in a silica tube and under an argon atmosphere (Wilkinson 1965). Wetting of the crucible by the melt, and consequent contamination, rendered the system unsatisfactory. Water-cooled copper crucibles of various designs, as first described by Stirling & Warren (1963) were tried with a similar system of atmosphere control (Fig. 4:1 and Fig. 3 of Appendix III). Although these crucibles offered a possible solution to contamination problems, due to the low coupling efficiency of the system there was insufficient power available to reach melting temperatures.

A more powerful (25 KW) rf generator was subsequently

purchased with a Stanelco cold-crucible (silver-boat) rig. The experimental arrangement then used was similar in design to that which has been used with the smaller generator, but with a number of modifications. A three-stage coil (Fig. 3 of Appendix III) was substituted in order to concentrate the output power into a smaller length of ingot. The coupling efficiency was increased by reducing the diameter of the silica tube so as to just clear the cold-crucible. To prevent overheating of the tube a concentric pyrex tube was incorporated and cooling water passed between the two. The experimental details of the alloy production carried out with this apparatus have been published and are included in Appendix III.

At an early stage in the development of the procedure, the Stanelco multitube silver-boat was replaced by a boat of simpler design and large capacity, which was formed from a single copper tube (Fig. 4:2). A depression or trough was formed in this tube by pushing a mandrel into it in successive stages, and annealing after each stage, until a perfect 'U' shape had been achieved with approximately a mm gap between the two inner walls. The tube, or copper-boat was prevented from collapsing during this forming process by enclosing it in a mild steel tube, which contained a slot to accommodate the mandrel. The ends of the tube were prevented from collapsing by the insertion of two plugs with shoulders which fitted against the ends of the boat. The copper-boat remained in this tube throughout the entire forming and annealing stages. The boat was carefully removed from the tube using a hammer and punch against one of the two plugs.

Alloys of various compositions within the NiAl phase field were produced in this apparatus (Fig. 4:3) from crushed mixtures of two master alloys (of compositions 54 and 42 at. % Al.). The master alloys were cast by International

Nickel Ltd. from 99.99 wt % Al and 99.999 wt % Ni. Early ingots produced in the copper-boat were made directly from charges made up of small (approximately $\frac{1}{2}$ cc) chunks of 99.99 wt % Al and 99.999 wt % Ni. The tenacious oxide coating formed during the ingot production was removed by grinding. The ingots were then remelted.

4.1.3. Single and Polycrystal Growth by a rf Technique

The ingots produced in the copper-boat were found to be unsuitable for specimen preparation for diffusion studies, because of inhomogeneity and small grain sizes. They were also oval in section, which, since it is impossible to machine NiAl by conventional methods, would have resulted in severe problems of specimen preparation.

Single and large polycrystal ingots of constant cross section were produced in the apparatus illustrated in Fig. 4:4, from those ingots produced in the copper-boat. For this purpose a round-bottomed, cylindrical alumina crucible was substituted for the pointed-bottomed, tapered crucible, referred to in Appendix III, which was used specifically for single crystal growth. The ingots produced were, on average, between 7 - 8 cm in length and 13 mm in diameter (Fig. 4:3).

4.1.4. Homogenisation

The well-known colour change that occurs in alloys over the composition range of NiAl (Bradley & Taylor 1937) afforded a visual indication of alloy composition and homogenuity. It was apparent that most ingots were richer in aluminium towards their top, which rendered a homogenisation treatment necessary. A knowledge of the diffusion coefficient (Berkowitz et al. 1954) indicated that a homogenisation anneal lasting of the order of a week at 1400°C would be required. Early results established the inadequacy

of anneals of this length so all subsequent ingots were annealed for minimum periods of two weeks at 1400 ± 25°C. These anneals were carried out in an alumina work tube, with provision for both prior evacuations to 10^{-3}torr and a continuous feed (of 300-400 cc/hr) of a purified and dried hydrogen atmosphere for the duration of the anneal. The work tube was contained in a crucilite element furnace insulated with M.I.28 bricks. The temperature was controlled to within ± 2°C by a Pt/Pt-Rh thermocouple situated between the work tube and the element, used in conjunction with a 1600°C anticipatory controller. The oxidation of these ingots during the homogenisation anneals was subsequently attributed to the slight porosity of the alumina work-tube to oxygen at the annealing temperatures.

A microscopical examination of the ingots revealed no evidence of oxygen absorption or of oxide contamination except in regions close to the ingots surface. There was no evidence of the 'pest' in any of the ingots (see Figs. 4:5, 4:6, 4:7 and 4:8). Since the ingots' surfaces were eventually removed, it was assumed that no serious effects would result from the surface oxidation observed.

4.1.5. Estimation of Specimen Composition

The composition of every specimen was estimated from a measurement of the specimen's density and the use of a density vs. composition calibration curve published by Bradley & Taylor (1937). The curve has been reproduced in Fig. 5:1. The validity of this calibration has been confirmed by several density and chemical analyses measurements (see Sections 5.1 and 5.2). The use of this method of estimating the specimen's composition in the present study was particularly apt for two reasons:

a) it was a non-destructive method and
b) a measure of the specimen density was also required

for the estimation of isotope penetration distances during the penetration analysis.

Density measurements were carried out under isothermal conditions ($23 \pm \frac{1}{2}^{o}C$) on a semi-micro balance by the displacement technique using dibromoethane. The density of the dibromoethane was measured at $23^{o}C$ using a highly polished rod of high purity nickel as a standard. It was assumed that the nickel had the theoretical density of 8.900 g/cc.

A metal bridge across the pan of a Mettler balance supported a glass dish of dibromoethane, the temperature of which was recorded between every density measurement. A platinum wire cage was used to suspend the specimen in the dibromoethane. The true density of a specimen was taken as the average of three individual determinations. Repeated determinations on the same specimen established their high reproducibility and accuracy (see Section 5.1). Using Bradley & Taylor's (1937) curve, the compositions could be estimated to within $\pm$ 0.2 at. % Al (see Section 5.2).

A variation of between 0.5 and 1.0 at. % Al was generally found to exist over an ingot's whole length. This means that there was a variation of approximately 0.1 at. % Al between neighbouring diffusion specimens cut from the ingot. Composition variations were more pronounced toward the top of an ingot, of which some 2 - 3 cm were consequently discarded. Those ingots which had undergone the longest homogenisation anneals showed much smaller composition variations.

4.2 SPECIMEN PREPARATION

4.2.1. Machining of Ingots Prior to Specimen Preparation

The method employed for the estimation of the thicknesses

removed from the specimen during the penetration analysis (see Section 4.5.2) required specimens of constant cross section. Several attempts were made to machine the NiAl ingots by conventional lathe methods, using various types of tool, but were all unsuccessful. However, most of the nickel-rich alloys, were eventually machined on a lathe that was modified to carry a high-speed grinding wheel in the place of the machine tool; diamond-impregnated and 'green-grit' grinding wheels could be used.

At best, the ingots were ground with a variation in diameter of only 0.0025 cm along their length. However, some of the ingots proved to be unmachinable, The grinding wheels removed small chunks from their surfaces and others, especially aluminium-rich alloys, fractured even when using low lathe speeds with high grinding wheel speeds.

Diffusion specimens were produced from these ingots by cutting at 3 mm intervals, producing disc-shaped specimens (see next Section).

4.2.2. Cutting of Diffusion Specimens

Diffusion specimen cutting was carried out using high-speed, rubber-bonded, carborundum slitting wheels, 10 thou in thickness. The ingot was set firmly in a wax ('Tanwax') and cooled by a constant jet of a dilute solution of soluble machine oil.

The ingots which proved unmachinable and which therefore had non-uniform cross sections, were cut into slices which were then cut again to reduce the section to a square. These specimens were very difficult to handle, due to their brittleness, and were often rendered useless for the diffusion study by the loss of material from specimen edges and corners. Cutting of these alloys often heated the ingot beyond the capacity of the cooling, causing the ingot to move in the softened wax. When the ingot was not held rigidly, non-

parallel specimen faces resulted.

4.2.3. Polishing, Etching and Microscopical Examinations

All specimens were polished mechanically on successively finer grades of silicon carbide papers down to 600 prior to electrodepositing the radioactive isotope of nickel. Specimens for microscopical examinations were further polished on diamond pastes down to 1 μ.

Grain boundary etchants recommended for NiAl alloys, which include Vilella's reagent (Grala 1960) and chromium trioxide in hydrochloric acid (Wood & Westbrook 1960) etched satisfactorily but rather slowly. A quicker etchant was found in a strong solution of alcoholic ferric chloride (5 g $FeCl_3$, 2 ml HCl and 95 ml ethanol).

Figs. 4:5, 4:6, 4:7 and 4:8 show that the grain size of the ingots varied from approximately 1 mm (Fig. 4:5) to 5 mm (Fig. 4:8); several ingots were single crystals. The grain size of the polycrystalline ingots did not vary significantly along their length. It was possible to record the grain sizes of almost every specimen because light oxidation clearly revealed the granular structure (Fig. 4:5).

Compared to the master alloys, from which the ingots were made, the ingots exhibited far fewer microscopically visible inclusions and impurities. This was attributed to the refining effect which probably occured during the re-melting procedure, and the removal by grinding of oxide and of those inclusions which had floated to the ingot's surface during the initial production stage.

4.3 ELECTRODEPOSITION

Nickel-63, which decays by the emission of β particles with an energy of 0.063 mev, was chosen as a suitable

isotope for use as the diffusing species, and was supplied by Radiochemical Centre (Amersham) as a solution of nickel chloride. As discussed previously, in Section 3.3, electrodeposition was chosen as the most suitable technique for producing a thin even layer of the isotope on a specimen's diffusion face. Nickel is more readily electrodeposited from a solution of its sulphate than its chloride (Hirano, Cohen & Averbach 1961). The conversion was achieved by evaporating to dryness and dissolving the resulting crystals in Sulphuric acid. The hydrogen chloride was boiled off, and the solution neutralised with ammonium hydroxide. The precipitate of nickel sulphate crystals was washed and dissolved in distilled water ready for use.

The most satisfactory electrodeposited layer was made using a current density of between 1 and 2 amps/cm^2, supplied from a 6v battery charger. The main glass container of the electrodeposition apparatus (Fig. 4:9) held the plating solution of nickel sulphate and a small amount of ammonium chloride (as buffer agent). A platinum anode was sealed into the glass at the base of the container. One of the branching tapped reservoirs of the apparatus contained Boric acid as buffer solution (the most effective buffer in the pH range from 4.5 to 5.5) and the other a strong solution of ammonium hydroxide which was used to neutralise the sulphuric acid produced during electrodeposition. A pH value of between 4.5 and 5.5 was maintained using pH papers as indicators. A deposition temperature of 40 $\pm$ 10°C was achieved by means of a water bath. The electrolyte was stirred during electrodeposition.

An appropriate measure of the thickness of the deposited layers was obtained from the specimen's increase in weight, as a function of deposition time, using a semi-micro balance. Any isotope which was deposited on the specimen's sides

during plating was removed by light grinding on 500 Å silicon carbide papers.

4.4 DIFFUSION ANNEALS

4.4.1. The Diffusion Annealing Furnace

It was decided, in the light of the high affinity which NiAl alloys have for oxygen at temperatures above 1200°C, and to subsequent catastrophic disintegration resulting from oxygen and/or nitrogen absorption (Westbrook & Wood 1963), that the diffusion anneals should be carried out in either an inert or a reducing atmosphere. The use of vacuum was ruled out because of the high vapour pressure of aluminium which would lead to significant composition changes during the anneals.

An annealing furnace (Fig. 4:10) was designed and built specifically for the annealing treatments. In the event of crystal growth in the rf apparatus proving unsuccessful, design features were incorporated which provided facilities for crystal growth by the Bridgeman technique.

The furnace was contained in a water-cooled, brass shell. Access to the inside of the furnace was achieved via brass plates which were screwed against 'O' ring sealed flanges, situated at both top and bottom of the furnace can.

A furnace element of molybdenum wire (0.8 mm dia.) was wound onto an alumina tube. This tube was completely contained within the furnace can, thus precluding the necessity of providing seals which would accommodate furnace tube expansion. Protection from oxidation, for both the specimens and the element, was provided by the same atmosphere. Although argon had proved successful in the rf

apparatus, to provide added protection to the molybdenum element, a reducing atmosphere of purified and dried hydrogen was used in this furnace.

The furnace windings were efficiently insulated from the furnace can by four concentric, cylindrical radiation shields, with tops and bottoms which fitted against the furnace tube. Each radiation shield was formed from bright finish molybdenum sheet (0.02 cm thick) and held together by stitches of molybdenum wire. A molybdenum wire frame held a series of molybdenum discs just inside the top of the furnace tube to minimise heat losses along the tube and to encourage furnace temperature stability. Facilities for vacuum were provided by 2.5 cm dia. tube soldered through the sides of the two furnace cans. Smaller diameter tubes were used for admitting the atmosphere and a control thermocouple. The latter was placed between the furnace windings and the first radiation shield. The power for the windings was applied via two modified sparking plugs (K.L.G., F.75) which screwed against two 'O' ring seals in the furnace can, and whose central electrodes extended through the furnace cans allowing the windings to be attached to them with insulated fittings.

A specimen thermocouple was encased in an alumina tube which extended from the furnace hot spot to the bottom of the furnace. A molybdenum tray, which held the diffusion specimens, was attached to the upper closed end of the specimen thermocouple tube (Fig. 4:11). A sliding 'O' ring seal between this thermocouple tube and the bottom furnace plate enabled the specimens to be introduced to or removed from the furnace hot spot very rapidly.

This facility eliminated the necessity of applying corrections to the time of the diffusion anneal, which became necessary when the heating and cooling times

constitute a significant percentage of the total annealing times (see Section 5.4.2.).

Early anneals in the furnace yielded specimens which were oxidised. This was attributed to a small leak, into the furnace from the surrounding water jacket, which was successfully sealed with 'Araldite'. The persistent, but reduced oxidation of specimens during subsequent anneals, continued despite rigorous prior evacuation of the furnace to pressures of 10^{-4} torr. Out gassing was carried out at a furnace temperature of 600°C with the specimens and thermocouple tube in the lowered position in the water-cooled column. The purified atmosphere was then introduced and the furnace temperature increased to the annealing temperature before the specimens were introduced to the hot spot.

Later in the project oxidation was attributed to the slow diffusion of oxygen through the top of the alumina thermocouple tube, once it had been raised into the furnace hot spot. An iron thermocouple tube was substituted and significant improvements in the atmosphere purity achieved during all remaining anneals. Several small chunks of aluminium-rich NiAl were included in the specimen tray for these anneals - their greater affinity for oxygen made them effective preferential oxygen 'getters'. Many specimens annealed towards the end of the project appeared to be free of oxide, whereas others showed only a trace, which served to indicate the material's grain size. (Fig. 4:5).

4.4.2. Diffusion Anneals in Silica Capsules

Before the successful modifications were made to the diffusion annealing furnace, an alternative method of annealing the specimens was tried in an attempt to overcome the heavy specimen oxidation. A complete diffusion study

of the nickel-rich, non-stoichiometric alloys was carried out annealing the specimens in sealed silica capsules. This method has been employed by Mackliet (1958) and Ya Shinyayav (1964) amongst others. A crusilite element furnace with a recrystallised alumina work tube, was constructed for these anneals which were carried out in air.

The fused silica tubes were sealed at one end and between four and six specimens were introduced in pairs of the same composition and with their active faces in contact. To facilitate the eventual sealing, the other end of the tube was necked down to a bore of less than 1 mm dia. The tubes were then evacuated to a pressure of 10^{-6} torr, filled with pure argon and sealed. A pressure of 250 mm of mercury of high purity argon, sufficient to prevent the collapse of the tube at the higher annealing temperature of 1300°C was used. Specimen oxidation was still unsatisfactorily high so the tubes and the specimens were out gassed at 400°C, under high vacuum, before they were sealed. Helium atmospheres were tried as an alternative to argon. Specimens were wrapped in molybdenum or nickel in order to reduce the attack that previous specimens had suffered from direct contact with the silica tubes. The condition of the annealed specimens improved throughout these experiments but oxidation continued to provide a problem of paramount importance, the significance of which is discussed in Section 5.5.

It was not until the diffusion work on the nickel-rich alloys was complete for some seven annealing temperatures, using these specimens which had been annealed in silica tubes, that it became apparant that the results were highly unsatisfactory due to inaccuracies, and the possibility of specimen contamination by nickel, molybdenum or silica. Several trace impurity chemical analyses rejected the

possibility of contamination.

The severe attack or fracture of nearly all these nickel-rich specimens destroyed their constant cross-section and therefore precluded their re-use for diffusion studies. Because of this, and the unsatisfactory results obtained for these alloys, a second series of ingots were prepared in the rf apparatus in order to repeat the diffusion studies.

Silica capsule diffusion anneals were discontinued because of poor results and all subsequent anneals were carried out in the diffusion annealing furnace. The final modifications that were then made to this furnace have already been described.

4.4.3. Specimen Configuration During Diffusion Anneals

The conventional methods of annealing diffusion specimens, with their active faces either in contact or separated by a washer welded between the two active faces, were both eventually abandoned. In many cases it was found impossible to separate the two specimens without breaking them, because their active faces had become welded together during the anneal. In an attempt to overcome this problem, nickel and molybdenum annular washers were used as spacers, placed between the active faces of the two specimens, which were held together by a molybdenum wire harness. During the anneal these washers became partially welded to the specimens, which made them difficult to separate, and created a contamination problem. The specimens that were separated had the remains of an annular washer adhering to the active face. Before a penetration analysis could be contemplated, all traces of the washer had to be removed without removing any material from the specimen face. This operation proved difficult and extremely laborious. The

method most commonly adopted for the removal of a welded washer involved machining the specimen diameter to less than that of the hole in the centre of the washer. In this way all traces of the washer and that part of the specimen to which the washer had welded, were removed. The method was impractical with the unmachinable alloys in this study. The use of alumina discs as separators was eventually discarded because, although they did not weld to the specimens, they did not reduce the oxidation on the active faces below the level normally found on a specimen which had been annealed with its active face free. All the later anneals were therefore carried out with all the specimens' active faces uppermost in the specimen tray.

4.5 ANALYSIS OF ISOTOPE PENETRATION

4.5.1. Precision Grinding for Penetration Analysis

Layers of thickness varying between 4-15 μ were removed from the specimen's active face using a grinding block similar to that employed by Einsen & Birchenall (1957; and Figs. 4:12 and 4:13).

The grinding operations were carried out in a glove-box on silicon carbide papers of various grades, attached firmly along one edge to a flat sheet of plate glass. The specimen, which was held firmly to the base of a perspex grinding piston, was aligned parallel to the grinding paper by the tight fit between the grinding piston and the sleeve of the brass grinding block. The grinding operation involved turning the whole grinding assembly through 90°, every two pushes up the grinding paper in order to ensure that material was removed evenly from the specimens and block. The dust created on the papers during grinding was

collected in the concentric grooves in the base of the block to avoid the assembly being lifted from the papers. If the block was lifted from the papers then the critical geometry which held the specimen axis at right angles to the papers would have been destroyed and the ground face of the specimen would no longer have been parallel to the original specimen diffusion face.

The hard and brittle properties of these NiAl alloys precluded all mechanical methods of attaching a specimen firmly to the base of the gringing cylinder so the specimens were glued into place using the arrangement in Fig. 4:13. The active face of the specimen was held firmly against the upper face of a flat glass slide by pressing it down into a thin layer of viscous grease. The block was then placed over the specimen and aligned with the aid of a grid, situated underneath the glass slide, so that when the cylinder was lowered down the sleeve of the block, the specimen was glued onto it in a central position. The block served to hold the cylinder at right angles to the slide while the glue set ensuring that the specimen's active face was parallel to the base of the block.

The specimens, which were prepared in order to repeat the diffusion studies of nickel-rich alloys, were cut using a new machine, which had a tendency to produce measurably non-parallel faces. This promoted mounting difficulties with the existing method so an alternative was employed. A standard metallurgical mounting press was modified to enable a hot specimen (50-70^{o}C) to be pressed into a small bed of 'Tanwax', located on top of the inverted cylinder. The cylinder was held by the grinding block so that the specimen's active face was again parallel to the bottom face of the block. The specimen was held firmly in this position until the 'Tanwax' had solidified and fully

hardened. Since the alcohol, which had previously been used during the specimen washing procedure (see next Section), dissolves 'Tanwax', a protective coating of a stopping off medium (Cannings Lacomite) was applied (Fig. 4:14).

4.5.2. Estimation of Thicknesses Removed by Grinding

The quantity of material removed from a specimen face during the grinding operation was determined from a measure of the change in weight of the cylinder and attached specimen. For this purpose a semi-micro, single pan, balance (Mettler type B6), capable of giving reproducible weighings to $\pm$ 0.00001 g was used. The accuracy with which these weight changes were made was proportional to the ratio of the weight change to the total weight of the cylinder plus specimen. Light perspex cylinders of sufficient mechanical strength and rigidity were constructed with thin wall thicknesses and weighing less than 10 g. Because the weight of perspex is known to vary with changes in relative humidity and temperature, a rigorous procedure of washing in alcohol and then drying in a stream of air at room temperature, preceded weighings made under isothermal conditions. Three independent weighings were made; the average of which was taken to represent the true weight.

The penetration distance or thickness of material removed during grinding, was calculated from a knowledge of the specimen density, cross sectional area and the measured change in weight.

4.5.3. Counting Specimen Activity

The activity of the ground face of the specimen was counted with a scintillation counter consisting of a phosphor, sensitive to β particles, and a photomultiplier-tube, mounted in a lead shielding castle (Fig. 4:15). The count

was recorded on an I.D.L. scaler and calculated from the time taken for 10^4 counts. The apparatus was calibrated by the adjustment of the photomultiplier high tension voltage, and the disc bias voltage, to give the highest possible ratio of specimen counts to background counts.

The inside of the lead castle was modified to accommodate a brass jig (Fig. 4:16). This was designed to hold the perspex cylinder and attached specimen, and to expose the active face parallel to the phosphor's surface.

An important source of error in such diffusion experiments is the contribution to the count rate resulting from surface diffusion. Because surface diffusion rates are greater than those of volume diffusion, a percentage of the isotope is transported from the diffusion face onto the specimen's sides during the early stages of the diffusion anneal. This subsequently diffuses into the bulk of the specimen by volume diffusion and contributes an isotope concentration which is indistinguishable from that due to volume diffusion from the diffusion face.

Isotope can also be transported to the specimen's sides as a result of isotope evaporation from the diffusion face. This contribution has been estimated by Ya Shinyayav (1964), from his work on nickel self diffusion, to be less than 3% at annealing temperatures above 1200°C.

The errors invoked by these contributions are greatest near the sides of the specimen and, in conventional techniques, are generally eliminated by the removal of some 25-50% of the specimen's diameter prior to the penetration analysis. This practice was not possible in the present study on unmachinable alloys, and an alternative method was developed. Only the activity from an area in the centre of the specimen's face was counted by interposing a window between the specimen and the phosphor (Einsen & Birchenall

1957). The window used was a 99.99% pure lead sheet, which had been carefully rolled to a thickness of 1.5 thou, in the centre of which a sharp-edged hole (0.25 inch dia.) was produced with a precision punch. A thickness of 1.0 thou of lead had been estimated to reduce the activity arriving at the phosphor by more than 95% assuming Lambert's law, and assuming a value of the half-thickness for nickel-63 absorption by nickel of 0.5 mg/cm^2 (Brosi et al 1951). This theoretical estimation was verified by several simple specimen counts, taken with and without the interposition of a lead sheet. Great care was always taken to expose the specimen in exactly the same position, relative to the counting jig, for every count taken during any one penetration analysis.

The interposition of a lead foil window between the specimen and the phosphor, reduced the 2π counting geometry. The errors which can be introduced due to poor counting geometry, have been outlined by Buffington et al (1961). In the present study it was estimated that the geometry had been reduced to 1.984π, which was not considered great enough a reduction to contribute measurable inaccuracies in specimen counts.

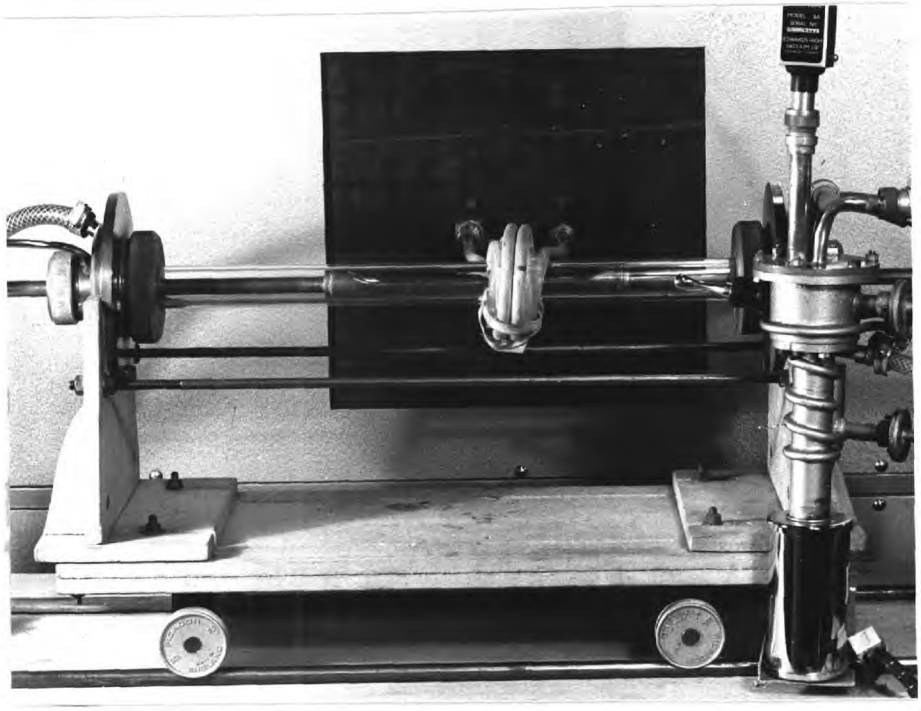

Fig. 4.1. The Horizontal rf Melting Apparatus in which Ingots were prepared for Consolidation in the Vertical Apparatus.

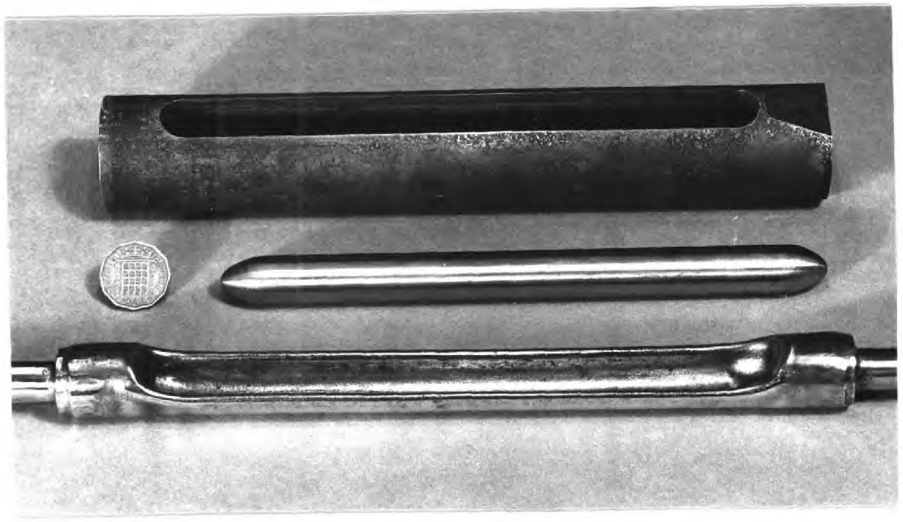

Fig. 4.2. The Copper Boat, as used in the Horizontal Apparatus. The Mandrel and Former from which it was made is also shown.

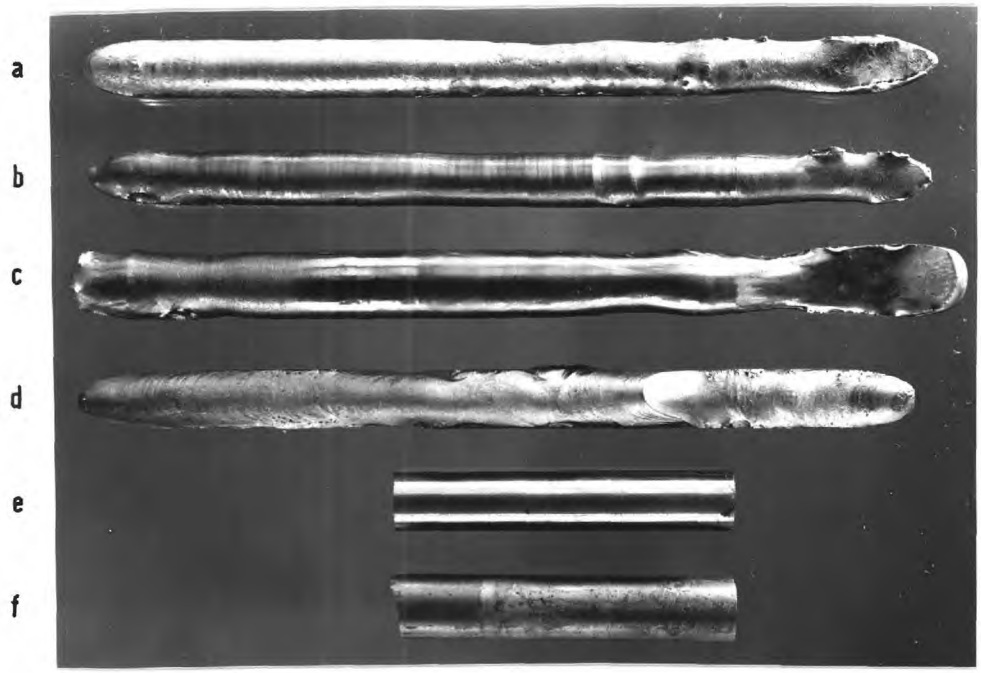

Fig. 4.3. NiAl Ingots. From left to right:-

(a) Ni Rich, from the Horizontal Apparatus
(b) Near Stoichiometry, from the Horizontal Apparatus
(c) Near Stoichiometry, from the Horizontal Apparatus
(d) Al-Rich, from the Horizontal Apparatus
(e) Surface ground, from the Vertical Apparatus
(f) As removed from the Vertical Apparatus Crucible.

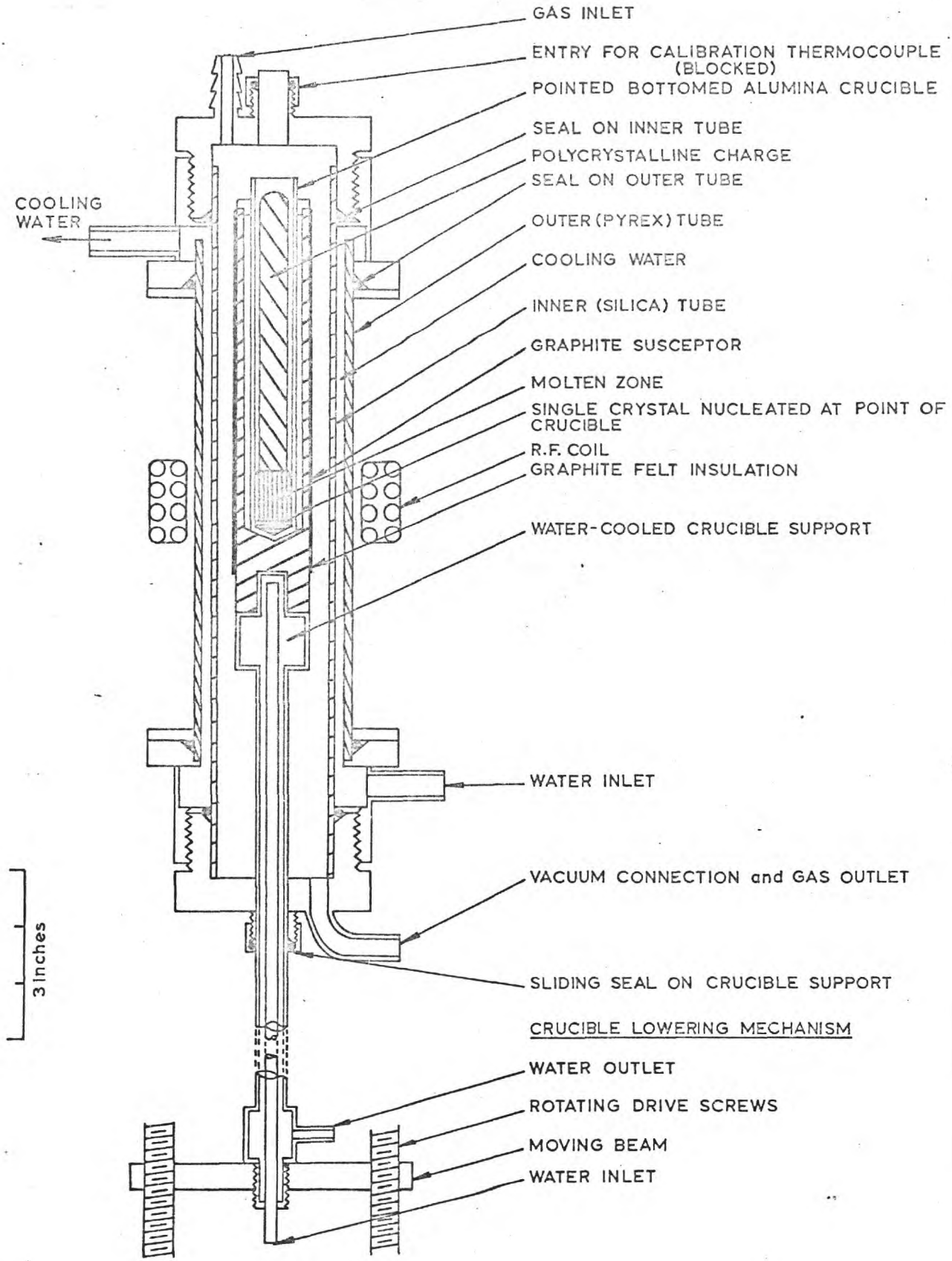

Fig 4:4 Schematic Diagram of the Vertical Casting Apparatus.

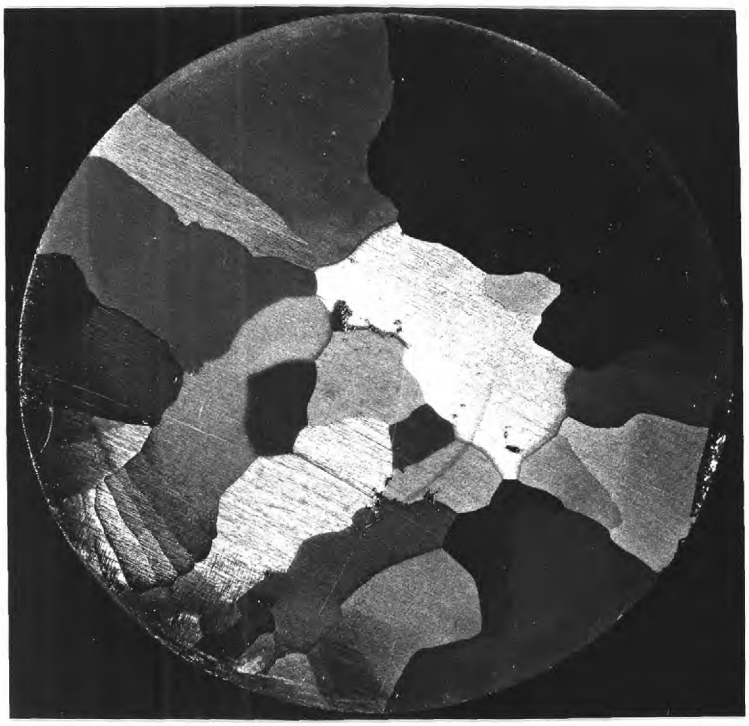

Fig. 4.5. The Grain Size (1 mm) indicated in 58 at. % Ni by a thin oxide coating formed during the Diffusion Anneal (x 8).

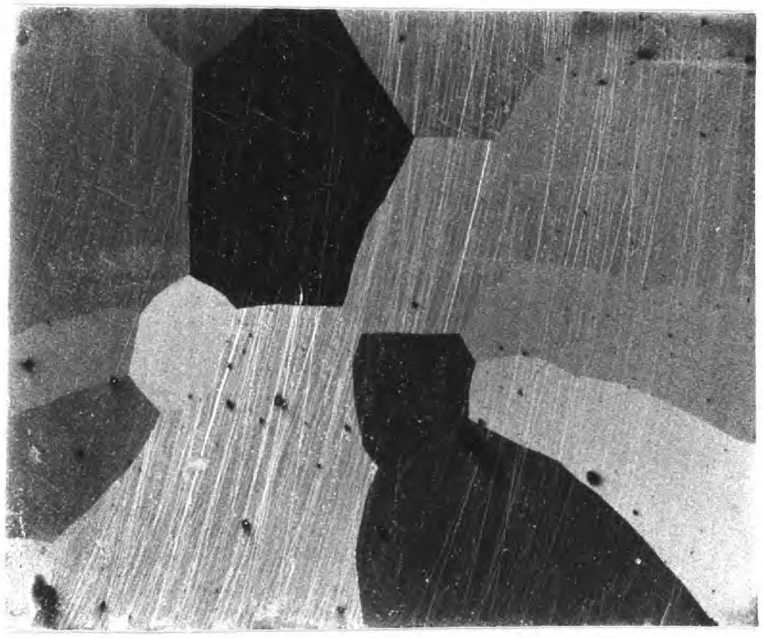

Fig. 4.6. 48.3 at. % Ni, showing 2 mm Grain Size and Inclusions. Etched in Alcoholic Ferric Chloride. (x 12)

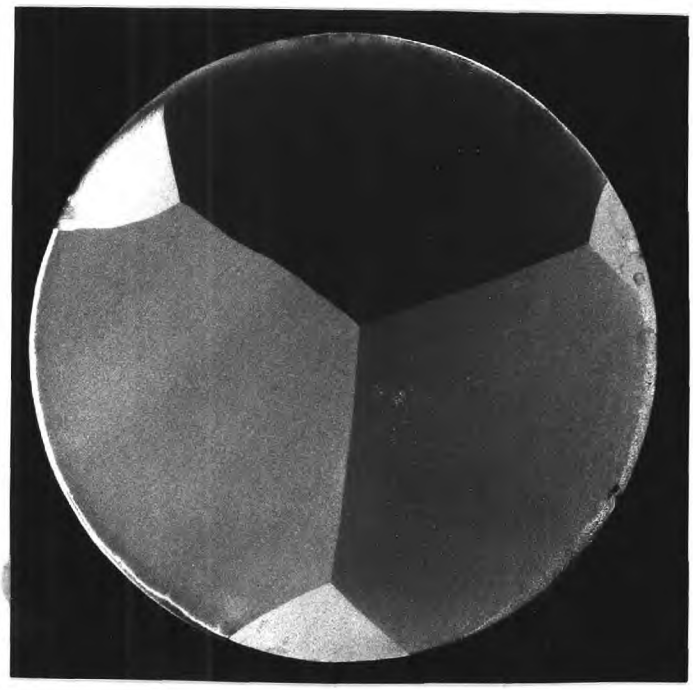

Fig. 4.7. Stoichiometric NiAl, showing 4 mm Grain Size. Etched in Alcoholic Ferric Chloride.
(x 8)

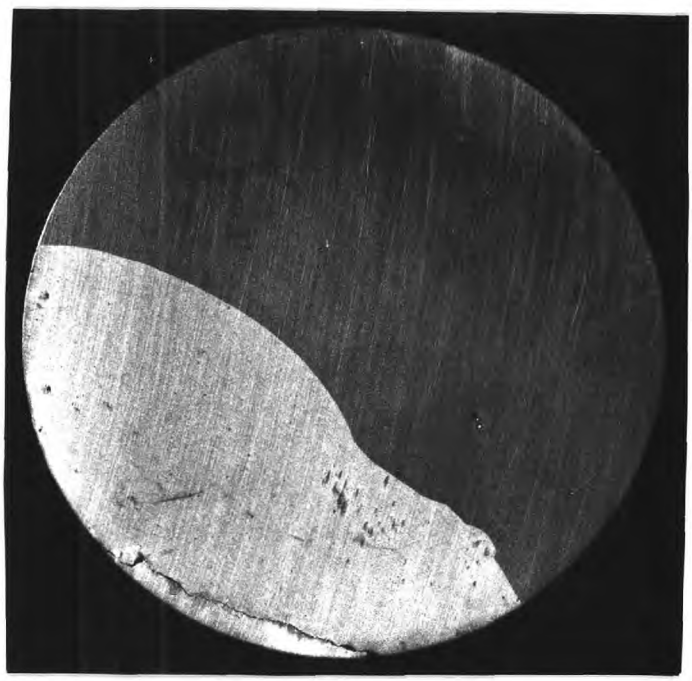

Fig. 4.8. 58.5 at. % Ni, showing 5 mm Grain Size. Etched in Alcoholic Ferric Chloride.
(x 8)

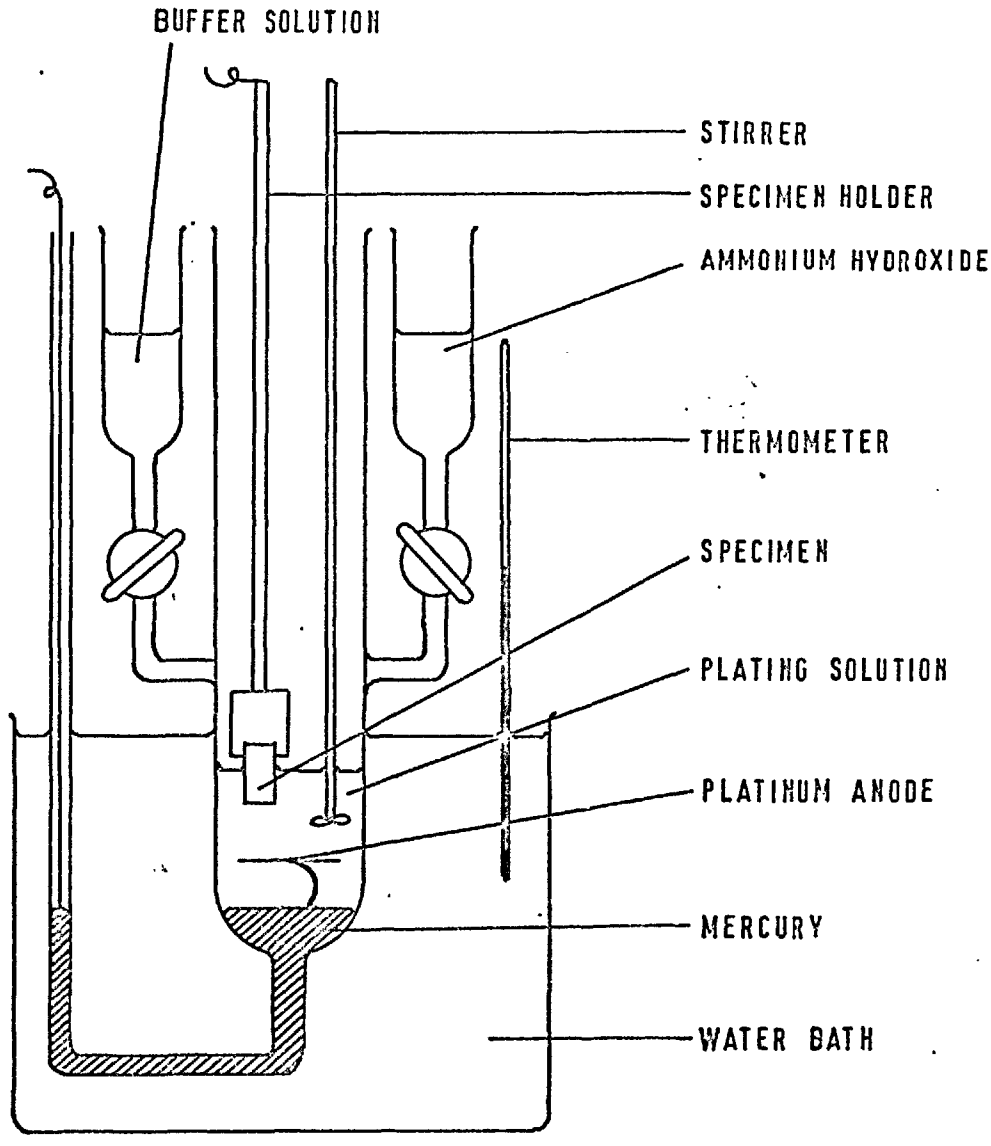

FIG. 4:9
ELECTRO DEPOSITION APPARATUS

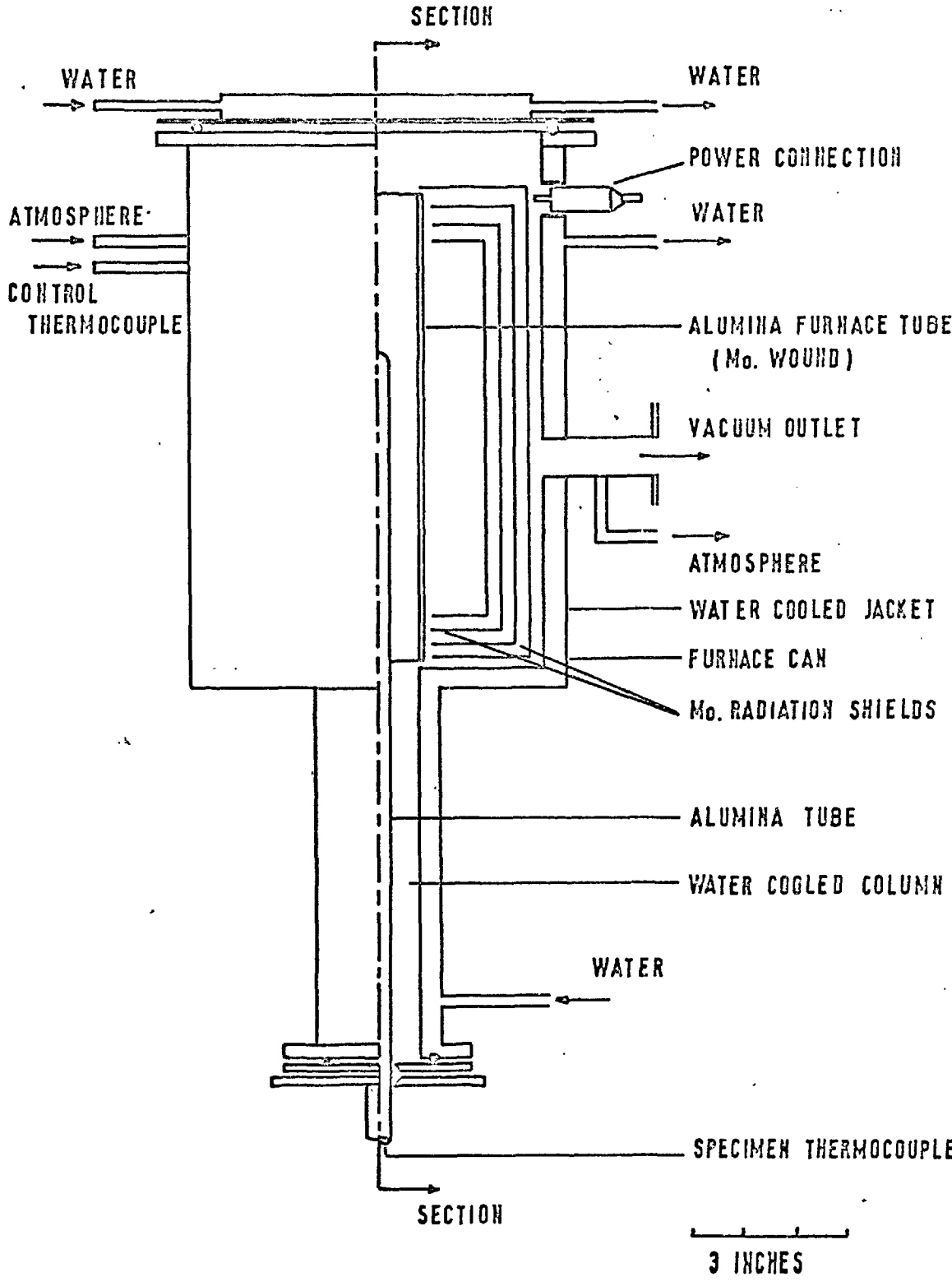

FIG. 4:10 1600°C DIFFUSION ANNEALING FURNACE

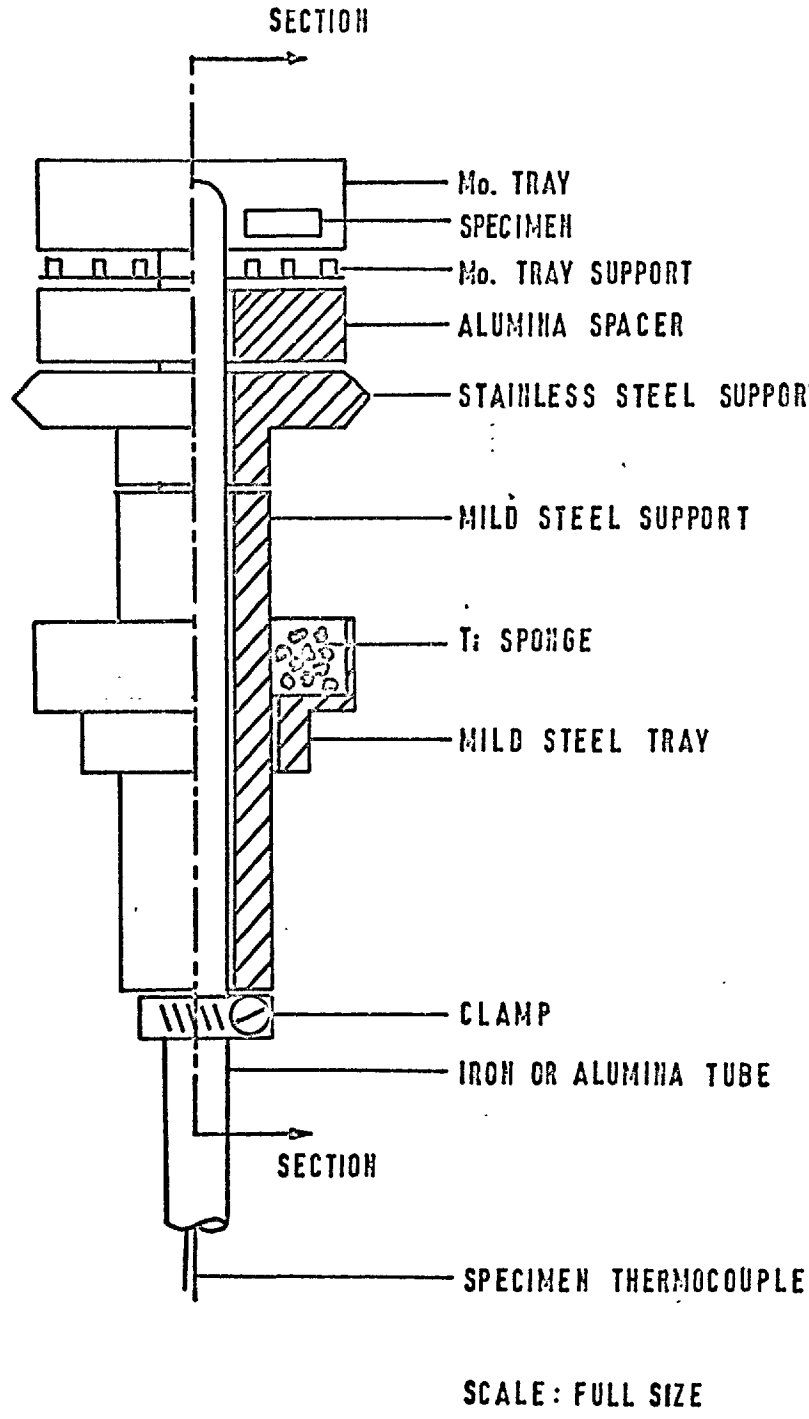

FIG. 4:11 SPECIMEN HOLDING ARRANGEMENT FOR THE DIFFUSION ANNEALING FURNACE

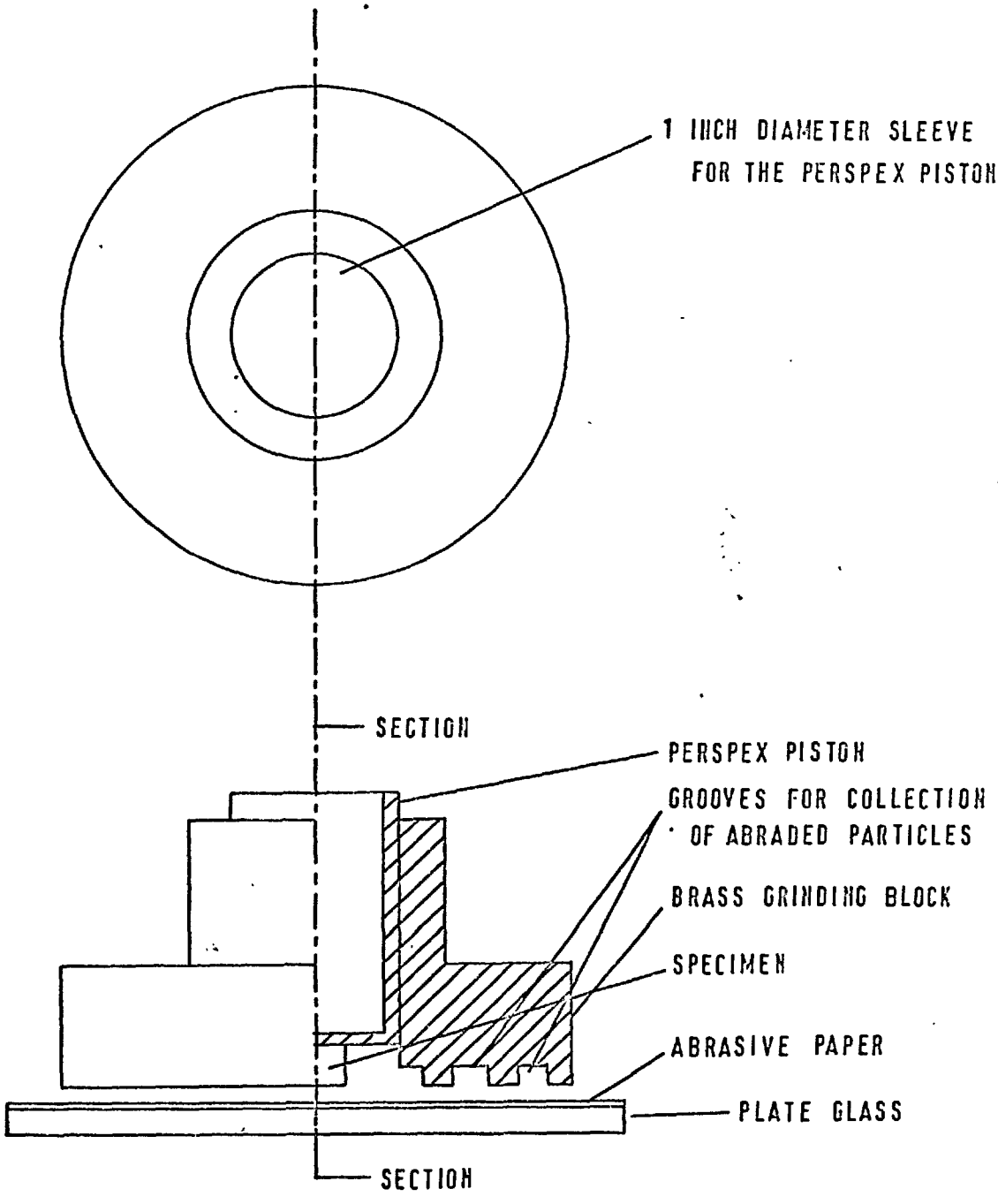

FIG. 4:12 GRINDING MACHINE

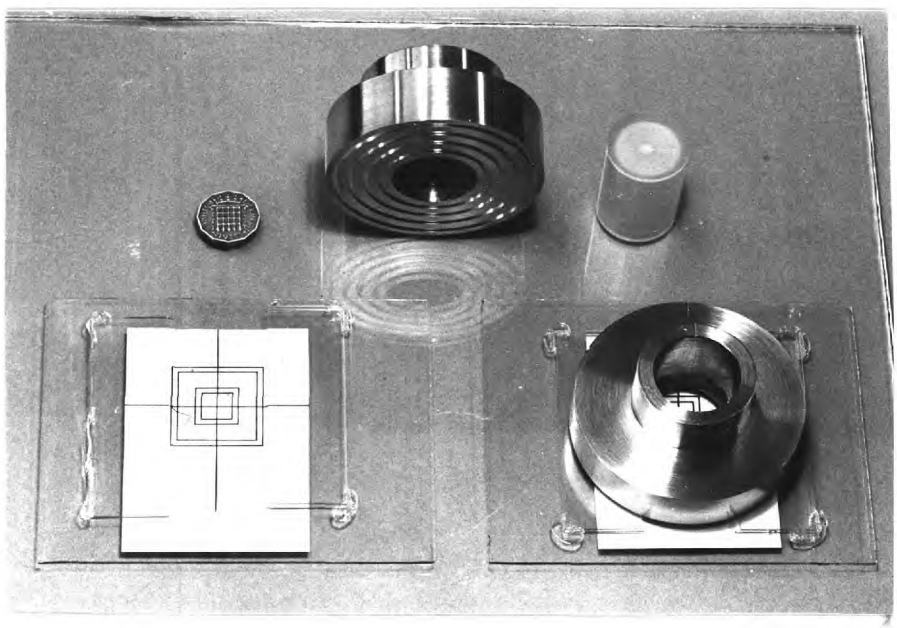

Fig. 4.13. Grinding Block and Perspex Cylinder, showing some details of the arrangement employed for mounting the specimens.

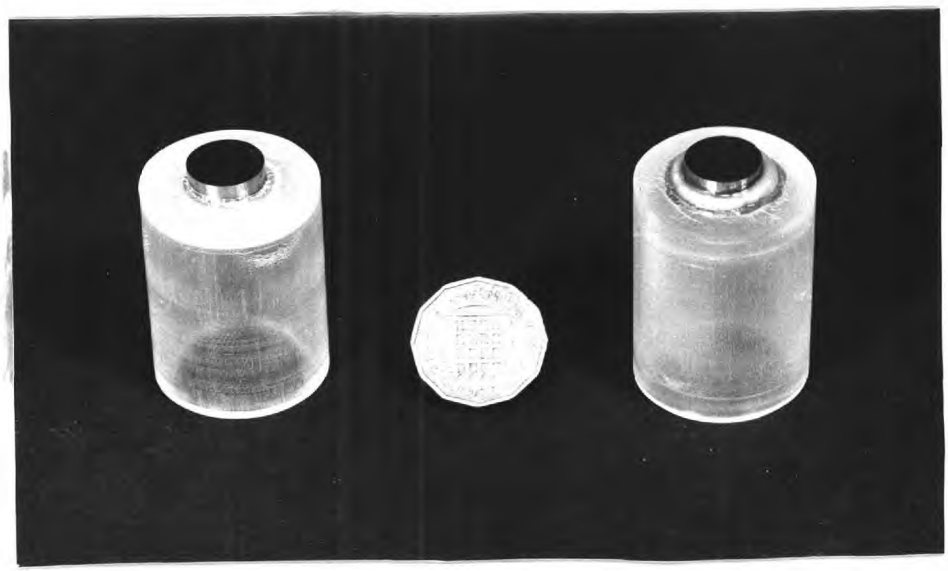

Fig. 4.14. The Perspex Cylinder, showing mounted specimens. From left to right:-
(a) Specimen mounted with glue
(b) Specimen mounted in wax, subsequently coated with Laconite.

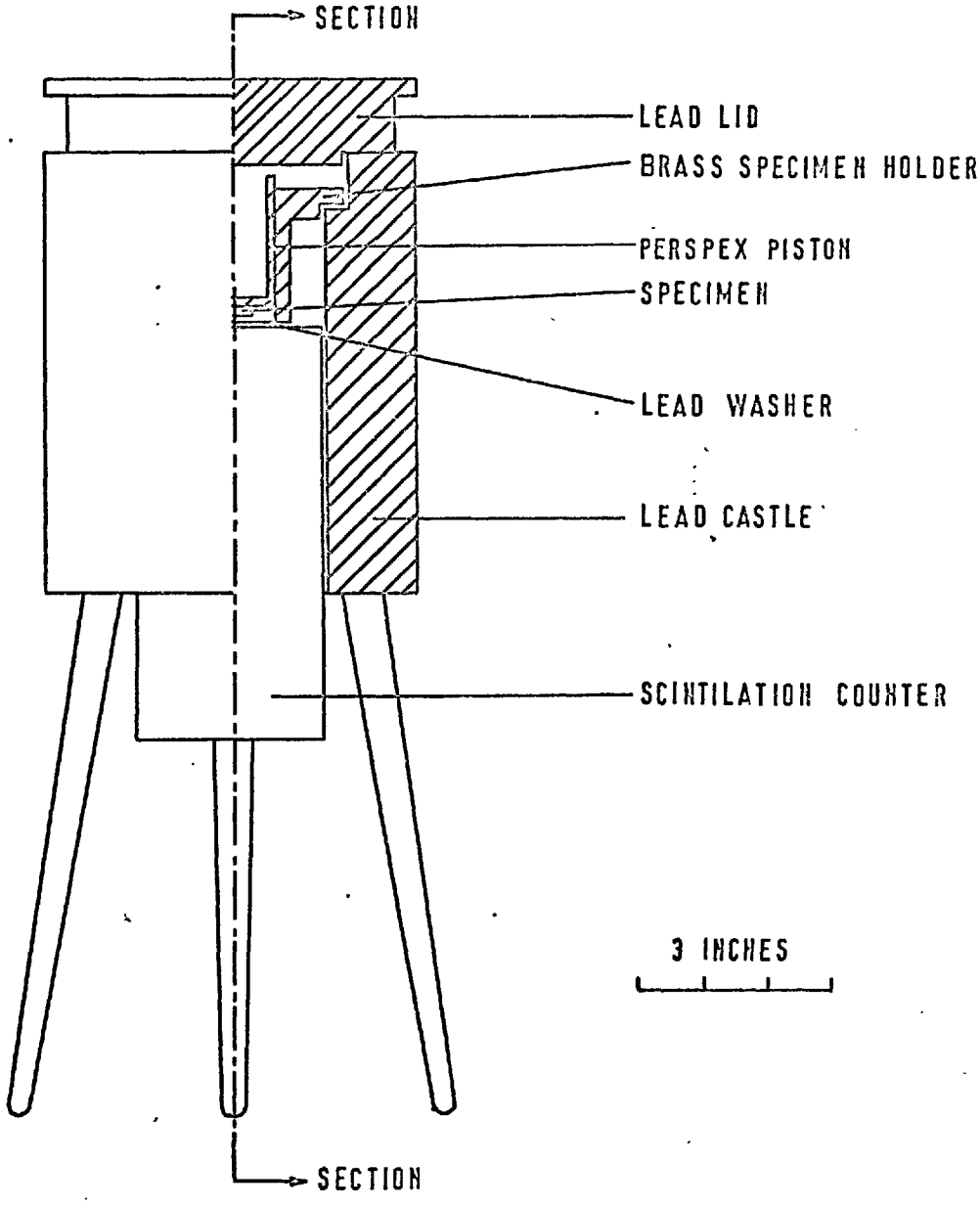

FIG. 4:15 SPECIMEN COUNTING APPARATUS

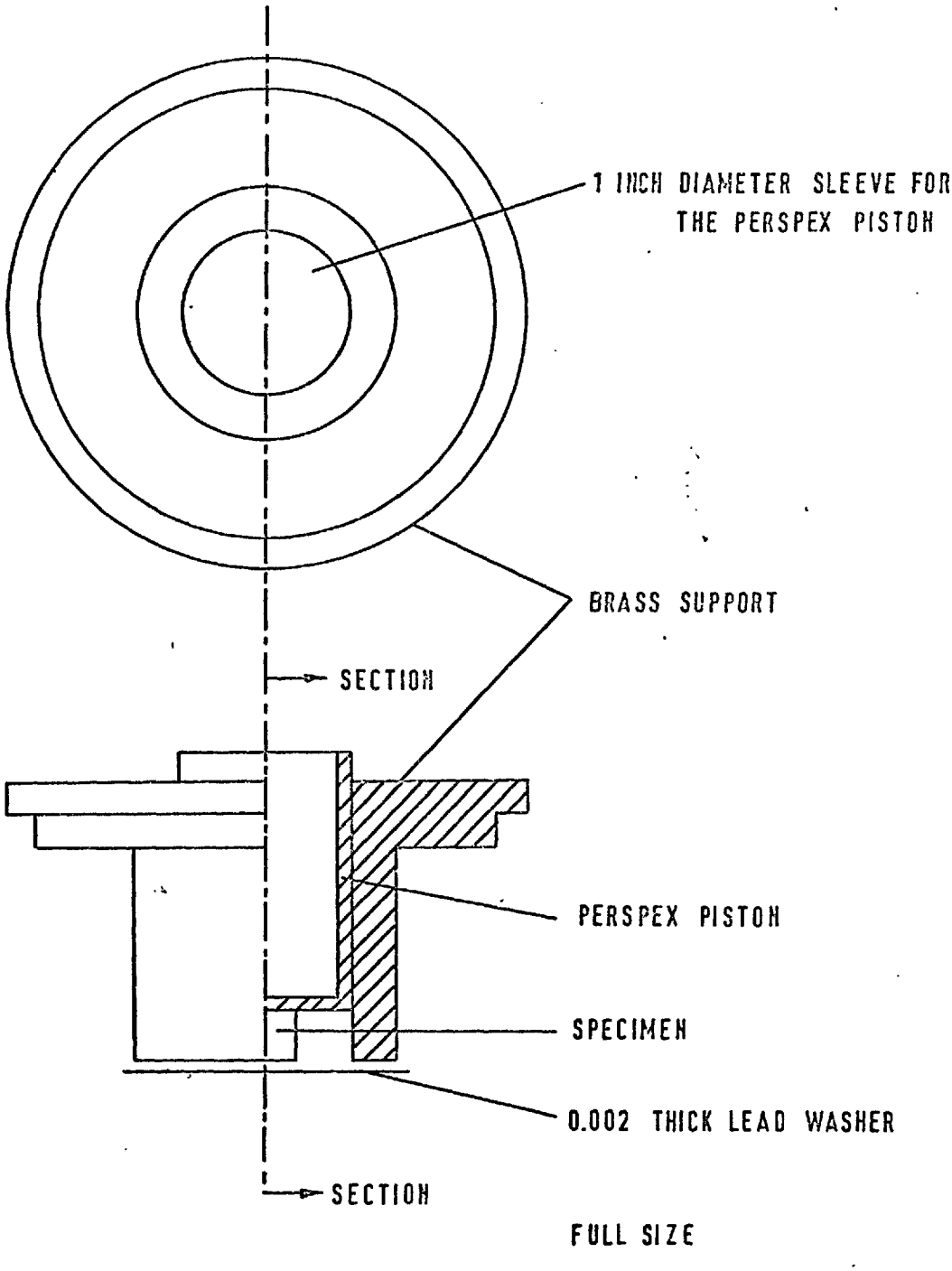

FIG.4:16 SPECIMEN COUNTING JIG.

CHAPTER 5 RESULTS

5.1 ERRORS IN THE DENSITY DETERMINATIONS

The accuracy with which the density measurements were made was estimated to be $\pm$ 0.11%, by calculating the total error from the absolute errors incurred in each experimental measurement (see Appendix I). Assuming an average specimen density of 6.0 g/cm^3, this fractional error represents an absolute error of $\pm$ 7 x 10^{-3} g/cm^3. Repeated density measurements on the same specimen differed by amounts smaller than those expected from the calculated errors. The average experimental error was found to be 4 x 10^{-3} g/cm^3.

5.2 ERRORS IN THE COMPOSITION DETERMINATIONS

The atomic composition of each specimen was estimated from density measurements using Bradley & Taylor's (1937) density vs composition data as a calibration curve (see also Section 4.1.5). Assuming the above calculated error in the density measurements, and that the errors in Bradley & Taylor's data were less than 0.01%, composition estimations could be made with an average absolute error of $\pm$ 0.2 and $\pm$ 0.08 at. % Al for nickel-rich and aluminium-rich compositions respectively.

The variation in the estimated composition of successive specimens cut from an ingot was generally within this error. The indication that the actual variation of composition along an ingot might have been less than that indicated from the density measurements, was confirmed in the majority of sample chemical analyses.

A series of specimens were chemically analysed as a check on the data of Bradley & Taylor (1937). The results, which are plotted along with Bradley & Taylor's data in Fig. 5:1, indicate that the densities of nickel-rich alloys are marginally higher and those of aluminium-rich alloys are lower than those of Bradley & Taylor. There was, however, insufficient experimental data in the present study to confirm these indications with any certainty, so all specimen compositions quoted hereafter have been estimated from the data of Bradley & Taylor rather than from this study's suggested calibration (see Fig. 5:1). The difference between the two calibrations, although small, would increase the absolute error of the estimated compositions to approximately $\pm$ 0.5 at. % Al, if the suggested calibration were the more accurate.

5.3 CALCULATION OF THE DIFFUSION COEFFICIENT AND THE ERRORS INVOLVED

Gruzin's (1952) 'thin film' solution to Fick's 2nd law, as described in Sections 3.1 and 3.2.7, allows D to be calculated from the slope of ln C vs x_n^2. In this study log I_n, which is proportional to ln C, was plotted against M^2, where M is the weight of material removed by grinding and is related to x_n by:

$$M = \rho A x_n$$

ρ and A are the specimen density and cross sectional area respectively. The slope of this graph (see Figs. 5:2, 5:3 and 5:4) is (1/4Dt.2.303), so that D, at any temperature T,

is given by:

$$D(T) = d(M^2)/d(\ln I_n).4.t.\rho^2.A^2.2.303 \qquad (5.1)$$

The 'thin film' solution only holds when the thickness of the isotope layer is small enough to be rapidly absorbed at the diffusion temperature. If this condition is not satisfied then a chemical diffusion coefficient would be measured. In order to ensure that this condition was satisfied isotope layers of thickness $0.5\mu \pm 40\%$ were used. The 'thin film' solution also dictates that the specimen should be in the form of a semi-infinite bar (i.e. of thickness much greater than $2(Dt)^{\frac{1}{2}}$) which was satisfied in all cases in this study.

Errors in D originated from errors incurred experimentally in the measurement of the variables from which it was calculated (i.e, from equation 5.1, these variables are I_n, t, M, ρ and A).

5.3.1. Errors in the Surface Activity (I_n)

In the present study it has been assumed that the surface activity measured was representative of the true tracer concentration at the specimen surface, and that it does not include a contribution from atoms below the surface. This assumption appears to be reasonable since the radiation from nickel-63 is relatively heavily absorbed. Brosi et al (1951) found the half thickness for the absorption of radiation from nickel-63 by nickel was 0.5 mg/cm^2. If similar absorption behaviour is assumed for NiAl then, assuming an NiAl density of 6.0 g/cm^3, a half thickness of 0.8μ can be assumed for these alloys. Since sections of thickness of the order of 8μ were removed by grinding (see Section 4.5.2) it seems reasonable to assume that

contributions to the count rate from buried atoms is negligible. This conclusion is consistent with the absence of corrections in published work on nickel-63 self diffusion, see for example Hoffman et al (1956), Mackliet (1958) and Hirano et al (1963).

Borg & Birchenall's (1960) correction to the activity counted from a surface calculates the activity within a section removed by grinding from the activities measured from the surfaces before and after the section removal. The correction is applicable to systems in which the thicknesses removed are small compared to the absorption half thickness. Furthermore the necessity of applying such a correction is generally indicated by non-linearity in the penetration plots, which again does not apply to the present study. The correction was consequently not applied.

The count rates were corrected for contributions from background radiation. Between each count the background count was recorded (an average of 80 counts/min was found) and subtracted from the next specimen count. Specimen counts were calculated from the time taken to record 10^4 counts. It was estimated experimentally that a fractional error of $\pm$ 1.5% was incurred.

5.3.2. Errors in the Annealing Time (t)

In diffusion studies in which the specimen undergoes heating and cooling cycles, before and after the diffusion anneal, a correction to the annealing time is generally applied in order to find the true annealing time (Makin et al 1957: Shewmon 1963). The practice employed in this study, of virtually instantaneous introduction and withdrawal of the specimen into and from the furnace hot zone (see Section 4.4.3), precludes the necessity of applying such a correction. Using this method, the error incurred is

reduced to the relatively short time that the specimen takes to heat up to and to cool down from the diffusion temperature. An absolute error of ± 3 mins. has been assumed for all annealing times. In some cases this is likely to be an over-estimation and gives a fractional error of ± 1.2% for 1350°C anneals, and ± 0.49% for 1000°C anneals; the largest error being associated with the shortest annealing time.

5.3.3. Errors in the Penetration Distances (x_n)

The penetration distances (x_n) were calculated from the weights of the layers removed by grinding (M), the measured specimen density (ρ) and the specimen cross-sectional area (A). The errors that arise in x_n, and which contribute to the error in the calculation of the slope of the penetration plot, therefore originate from errors in the measurement of M, ρ and A.

The fractional error in the square of M was estimated to vary from ± 0.1% to 1.0%. The errors in ρ have been outlined in Section 5.1. The fractional error in A, which was found to vary from 0.8% to 1.5%, originated from an estimated average absolute error of ± 5 x 10^{-3} cm in micrometer measurements.

5.3.4. Total Error in D

An average total fractional error in the calculated diffusion coefficient of ± 3% was calculated (see Appendix II), although a minimum error of ± 1% and a maximum error ± 5% was calculated. The variation in the calculated total fractional error in D originates from variations in the estimated fractional errors in I_n, t, M, ρ and A (see preceding Sections).

It was found that the experimental variation in D from independently repeated determinations was greater than the

calculated total fractional error. On average the fractional error indicated from the experimental reproducibility was in some cases found to be as large as ± 20%. This figure is slightly greater than the generally accepted standard of accuracy in diffusion studies, which is between ± 5% and ± 15%, see for example Ruder & Birchenall (1951) and Huntington et al (1961). The discrepancy between the calculated error and that found experimentally indicated that other sources of error were involved of which the following are examples:

a) The layers removed during grinding were removed in such a way that the newly exposed face was not parallel to the original diffusion interface.

b) Short circuiting effects from grain boundaries, sub-grain boundaries, dislocation pipes, cracks and holes, and possibly from a preferred diffusion orientation.

c) A variation in the vacancy concentration, in the same alloy and at the same temperature.

d) A variation in the extent of oxidation of a specimen from one diffusion anneal to another at the same temperature.

The first of these possibilities applied to only a minority of specimens which had been poorly mounted (see Section 4.5). The error arising from non-parallel sectioning was difficult to estimate and has therefore been ignored.

Since all specimens were prepared in an exactly similar way (see Sections 4.1 and 4.2) it is not thought likely that variations in the dislocation density, and/or vacancy concentrations could exist to an extent that would create any significant error in specimens of the same composition and annealed at the same temperature. Microscopical examinations (see Section 4.2.3) did not reveal any visible cracks

or holes. The grain sizes of the specimens were approximately the same (see Section 4.2.3), and the smallest grain size would not have contributed significantly to the measured volume diffusion (see Section 2.3.1). Furthermore it is difficult to imagine that sub grain boundaries could account alone for such inaccuracies in D, although this, and a preferred diffusion orientation, remain possible explanations.

A variation in the extent of specimen oxidation from one anneal to another at the same temperature could well have provided a source of error in this study. For this reason the effects of an oxide layer on the penetration plots has been fully investigated.

5.4 SPECIMEN OXIDATION AND ITS EFFECT ON D

If a specimen was removed from the annealing furnace without any trace of oxidation, then its surface was taken as the diffusion interface, and all penetration distances were measured from that surface. This procedure was not possible for specimens whose surfaces had become oxidised during the diffusion anneal, since the exact location of the original specimen surface had become obscured by the oxide film. Most specimens exhibited such an oxide film, and the penetration analyses were carried out with reference to the surface of the oxide film. This naturally introduced an error in all the penetration distances measured. If the volume of oxide was greater than the volume of metal from which it was formed, then the measured penetration distances would have been greater than the true penetration distances. The converse would have applied had the volume of oxide been less than that of the metal from which it was formed.

A definite maximum was exhibited at low penetrations in

all penetration plots of oxidised specimens, and it was therefore assumed that the former situation applied to this investigation. This maximum cannot be confused with the odd effects reported by Lundy et al (1965). Not only was the maximum exhibited at much greater penetration distances than these odd effects, but the technique used in this study would have been too insensitive to detect such effects. The penetration plots did not show any departure from linearity at large penetration distances. The 'tails' observed amongst others by Peart (1965) were not apparent in penetration plots of this study.

Fig 5:2 is the penetration of the most heavily oxidised specimen and shows a pronounced maximum at approximately 10μ from the specimen surface. Fig 5:3 is an example of a penetration plot from a specimen with a typical amount of oxidation and is representative of the plots from this study. Fig 5:4 is an example of a plot from an unoxidised specimen and is characteristic of those obtained towards the end of this study as a result of the improved atmosphere control in the annealing furnace (see Section 4.4.1).

Since the measured penetration distances were greater than the true values, the value of D calculated from the slope of the penetration plot, was greater than the true D. It was necessary therefore to apply a correction to the penetration plots from oxidised specimens, which involved the location of the true diffusion interface. The subsequent correction could then be achieved by subtracting the distance from the oxidised specimen surface to the calculated interface from all the measured penetration distances. The calculated interface should coincide with the maxima on the penetration plots.

The calculation primarily involved establishing that the

relationship between log I_n and x_n was in fact parabolic. This was achieved by carrying out a least squares analysis of the penetration data assuming that all powers of x_n up to and including 10 existed in the relationship. For this purpose a Library, Fortran IV, computer program was used on an IBM 7090 computer. The result was that all values of x_n, with powers higher than 2, were negligibly small, and that the data was best described by a parabola of the form:

$$\log I_n = a x_n^2 + b x_n + c$$

in which a, b and c were the parabolic constants. Differentiating the equation and equating to zero:

$$\frac{d \log I_n}{dx_n} = 2 a x_n + b = \text{zero}$$

gave the position of the maximum, or calculated diffusion interface, at $x_n = -b/2a$. The location of the interface therefore resolved itself into the calculation of the parabolic constants a and b.

A second Fortran IV program was written to carry out this calculation incorporating an existing minimisation subroutine from AERE Harwell, which performed least squares fits to a parabola by an iterative technique, and calculated the parabolic constants. Assuming that the value of the interface calculated from these constants represented the true diffusion interface the program corrected the penetration data. It also plotted the penetration parabolas so that the position of their maxima could be used as a rough check on the program result.

Corrected penetration plots were drawn from the program data (see dotted lines in Figs. 5:2 and 5:3) and a corrected value of D obtained from their slopes as before. The average

difference between the corrected D and that calculated from the original data represented an average error of approximately ± 2%. This indicated that the error arising from specimen oxidation was less than the calculated fractional error in D (see Section 5.3.4) and did not account for the larger error indicated by poor experimental reproducibility.

The computer program, although it gave perfect results with good data, was sensitive to data departures from a parabola in the region of the maximum at low penetrations. In many instances the data in this region was inaccurate. This could be attributed either to the effect on the diffusion coefficient of absorbed oxygen, or to the fact that the initial activity counts were taken from partially oxidised surfaces. This interference with the parabolic nature of the data created an unavoidable error in the corrected data yielded by the program.

5.5 THE TEMPERATURE DEPENDENCE OF D BETWEEN 1000°C AND 1350°C

In general D has been measured at 50°C intervals between 1000°C and 1350°C. In some alloys, where a shortage of specimens restricted a thorough study, specimens were used to repeat measurements rather than to make measurements at all the temperatures indicated above. This was particularly true in aluminium-rich compositions, where many specimens were rendered useless by fracture or cracking (see Chapter 4). Here D has been measured only at 100°C intervals in some instances.

An Arrhenius type linear dependence has been assumed to describe the data over the temperature range in which D was measured (see Section 2.3.10). A least squares analysis has been carried out on all data for each composition and the

values of Q and D_o calculated from the analysis. No experimental data was excluded in the analysis.

5.5.1. The Temperature Dependence of D in Aluminium-rich Alloys

The results for the four aluminium-rich compositions, and for a stoichiometric composition, are presented as a function of reciprocal temperature in Figs. 5:5 to 5:9 inclusive. In most cases each individual point on these graphs represents an average of three separate determinations; the error bars have been drawn to indicate the experimental reproducibility and not the calculated fractional error (see Section 5.3.4).

The results are shown collectively in Fig. 5:10 in which the temperature dependence for each composition has been represented by a straight line calculated from a least squares analysis (Fig. 5:5 to 5:9).

5.5.2. The Temperature Dependence of D in Nickel-rich Alloys

The results for six nickel-rich compositions are presented as a function of reciprocal temperature in Figs. 5:11 to 5:16 inclusive. The data represents the results of the second study in nickel-rich alloys described in Section 4.4. The limited data for the 55.5 at. % Ni composition (Fig. 5:13) are the only exceptions and are the only results from the first study to be presented here. All the data for all the nickel-rich compositions represent single determinations. There was therefore no experimental estimation of reproducibility in these alloys and no error bars have been drawn. The straight lines which have been drawn in Figs. 5:11 to 5:16 are the result of least squares analyses and are shown collectively in Fig. 5:17.

5.6 THE COMPOSITION DEPENDENCE OF D

The isothermal composition dependences of D, at 50°C intervals between 1000°C and 1350°C, are shown in Fig. 5:18. The error bars which are shown in Figs. 5:5 to 5:9 for the aluminium-rich data are not drawn in Fig. 5:18 in order to avoid confusion as a result of overlap. Curves have been drawn through the data to indicate a suggested composition dependence of D at each temperature.

5.7 THE COMPOSITION DEPENDENCE OF THE ACTIVATION ENERGY

Activation energies of diffusion (Q) were calculated as part of the least squares analysis of the linear log D vs 1/T relationships in Figs. 5:5 to 5:9 and Figs. 5:11 to 5:16, and are shown as a function of composition in Fig. 5:19. The error bars drawn on the activation energies were also calculated from the least squares analysis. Lines, which represent a suggested dependence, have been drawn through the data on either side of the stoichiometric composition.

The data from this study (Fig. 5:19) has been reproduced in Fig. 5:20 in which the values of Q, which have been determined or suggested by previous studies, are shown. The dependences which were suggested by these previous studies are also indicated. These previous studies include the cobalt-60 self diffusion studies of Berkowitz et al (1954), the study of the annealing out of dislocation loops (Ball & Smallman 1966) and the deformation studies of Vandervoort et al (1966).

5.8 THE FREQUENCY FACTORS OF DIFFUSION

Frequency factors (D_o) were calculated during the least squares analysis of the linear log D vs 1/T relations in Figs. 5:5 to 5:9 and 5:11 to 5:16 (see also Section 2.3.10). The calculated values of D_o and Q (see preceding Section) are listed in Table 5.1 together with the atomic compositions at which they were measured.

The majority of these D_o values fall within the fairly restricted range of 0.1 to 10.0 cm^2/sec within which D_o values from 'normal' diffusion (see Section 2.3.10) are expected to fall (see for example Le Claire 1965). The more obvious exceptions are the D_o values for the three most aluminium-rich compositions, which are all more than two orders of magnitude smaller than the lower limit of the empirical range, and are of the same order of magnitude as values associated with 'anomalous' diffusion behaviour (see Section 2.3.12). There are two other exceptions namely the values for 55.5 and for 58.0 at. % Ni. The first of these has been calculated from insufficient data and cannot therefore be considered accurate. The second is less than a factor of 10 outside the empirical range which cannot be considered significant in the light of the experimental reproducibility of the data.

5.9 ANOMALOUS DIFFUSION BEHAVIOUR

Although the results have been interpreted assuming an Arrhenius dependence characteristic of 'normal' diffusion behaviour (see Section 2.3.10), the possible existence of curvature amongst this data cannot be ignored. However, the

high experimental errors suspected in this study do not permit curvature to be established with any certainty. Nevertheless the deviations from the least squares linear lines (Figs. 5:11 to 5:16) in the data for nickel-rich compositions, in which curvature appears to be most prominent, serves to support a tendency towards curvature.

The curves that have been drawn through the data for the nickel-rich compositions in Fig. 5:21 indicate the general trend of curvature amongst these compositions. There is little evidence for curvature in the data for the stoichiometric composition so this is represented by a least squares straight line, as in Fig. 5:9.

Curvature of this kind, which has been found to be a typical feature of 'anomalous' diffusion behaviour (see Section 2.3.12) is generally interpreted in one of two ways:

a) as a sum of two exponential terms, i.e:

$$D = D_1 + D_2 = D_{o1} \exp(-Q_1/RT) + D_{o2} \exp(-Q_2/RT)$$

This analysis is generally applied to systems in which Q and D_o are temperature dependent. For example Kidson (1965) has used this analysis to explain two competing processes of vacancy diffusion by either 'intrinsic' or thermal vacancies, which predominate at higher temperatures, or by 'extrinsic' vacancies, which predominate at lower temperatures and are formed near impurity atoms in order to relieve lattice strains. The analysis is applicable to the temperature range between the two extremes in which both processes will contribute to the measured diffusion coefficient. Murdock (1965) has found that his data for titanium and vanadium diffusion in titanium is best described by this analysis.

b) as two separate relationships of the Arrhenius type,

which each describe the behaviour over temperature ranges which do not overlap, i.e:

$$D_1 \ (T_1 - T_2) = D_{o1} \exp (-Q_1/RT), \text{ and}$$

$$D_2 \ (T_2 - T_1) = D_{o2} \exp (-Q_2/RT)$$

where $T_3 > T_2 > T_1$, and where T_2 is the temperature at which the two linear relationships between log D and 1/T intersect. This analysis suggests two mechanisms but presumes that the high temperature mechanism does not contribute towards diffusion at low temperatures, and vice versa. Such an analysis, for example has been used to explain observed curvature in vanadium self diffusion (Lundy & McHargue 1965: Agarwala et al 1968).

The inaccuracy of the data in the present study does not permit a justifiable choice to be made between the two analyses. However, since in the limit of a small temperature range over which Q and D_o are temperature dependent the first analysis approximates to the second, the data from this study has been analysed in terms of two separate linear Arrhenius relationships. The log D vs 1/T data has therefore been interpreted in terms of two straight lines, which have been calculated by the least squares method, assuming an intersection between the two dependences in the region of 1150°C. This assumption is supported by the indication that an intersection exists at this temperature in the data of the 54.5 at. % Ni for example.

The least squares straight lines for the high temperature dependence (Fig. 5:22) have been calculated from the values of log D at the five highest temperatures (1350, 1300, 1250, 1200 and 1150°C). Similarly the low temperature lines have

been calculated from the data for the four lowest temperatures (1150, 1100, 1050 and 1000°C). Because the intersection of the two straight lines has been assumed to be close to 1150°C the data at this temperature was used in both the least squares analyses. The value of D for the 53.2 at. % Ni composition measured at 1100°C was rejected from the low temperature analysis because its large deviation from the least squares analysis in Fig. 5:11. Because of insufficient data for the 55.5 at. % Ni composition an analysis in terms of two linear dependences has not been carried out and the single linear dependence represented in Fig. 5:13 has been reproduced in Fig. 5:22.

In the aluminium-rich compositions there is increasing evidence of curvature with increasing aluminium content in excess of 50.8 at. % Al. There is however no such evidence in either the stoichiometric composition (Fig. 5:9) or the 49.2 at. % Ni composition (Fig. 5:8). There is insufficient data for the three most aluminium-rich compositions (Figs. 5:5 to 5:7) to allow an analysis in terms of two linear dependences.

Values of Q and D_o in nickel-rich compositions, for both the high and low temperature dependences, were calculated from the least squares analyses as before, and are indicated in Tables 5.2 & 5.3. The values of Q are shown as a function of composition in Fig. 5:23.

For diffusion in ordered alloys with a substitutional defect structure, as in these nickel-rich alloys (see Section 2.4.2), the absence of continuity between the relative positions of the linear dependences in Fig. 5:22 would not be expected. On closer examination of the data from which these linear dependences have been calculated, this lack of continuity is not surprising. The activation energy dependence on composition Fig. 5:23, serves to amplify these

doubts concerning the results of the least squares analysis of a high and a low temperature range.

The values of D_o for the high temperature dependence differ wildly with composition, although, within the accuracy limits, they all fall in the empirical range expected for 'normal' diffusion. The values for the low temperature range are all smaller than the minimum of this empirical range and are of the same order as values calculated from 'anomalous' diffusion behaviour.

In view of the high experimental errors suspected in these nickel-rich compositions, poor results must be expected from a least squares analysis on only four or five data points. The lack of continuity amongst the least square products could therefore be attributed to scatter in the data.

Assuming that some degree of continuity would exist between the data for one composition and that of another, and assuming that there are two separate temperature dependences, a series of straight lines have been drawn through the data and are shown collectively in Fig. 5:24. They are intended to represent suggested temperature dependences for each composition in which D has been measured, and have not been calculated by a least squares method.

The values of Q have been calculated from the slopes of these linear dependences and are shown as a function of composition in Fig. 5:25. Two straight lines, representing suggested high and low temperature composition dependences, have been drawn through the data. Values of D_o for both dependences were calculated from the intercept of the extrapolated lines at $1/T = 0$. The values for the high temperature dependence fall within the expected range for 'normal' diffusion (Table 5.3), in agreement with indications of the least squares analysis for two temperature dependences

(Table 5.2 and Fig. 5:22). Similar agreement exists for the low temperature dependences, namely that all values of D_o are smaller than those expected of 'normal' diffusion behaviour, and are typical of values expected of 'anomalous' behaviour.

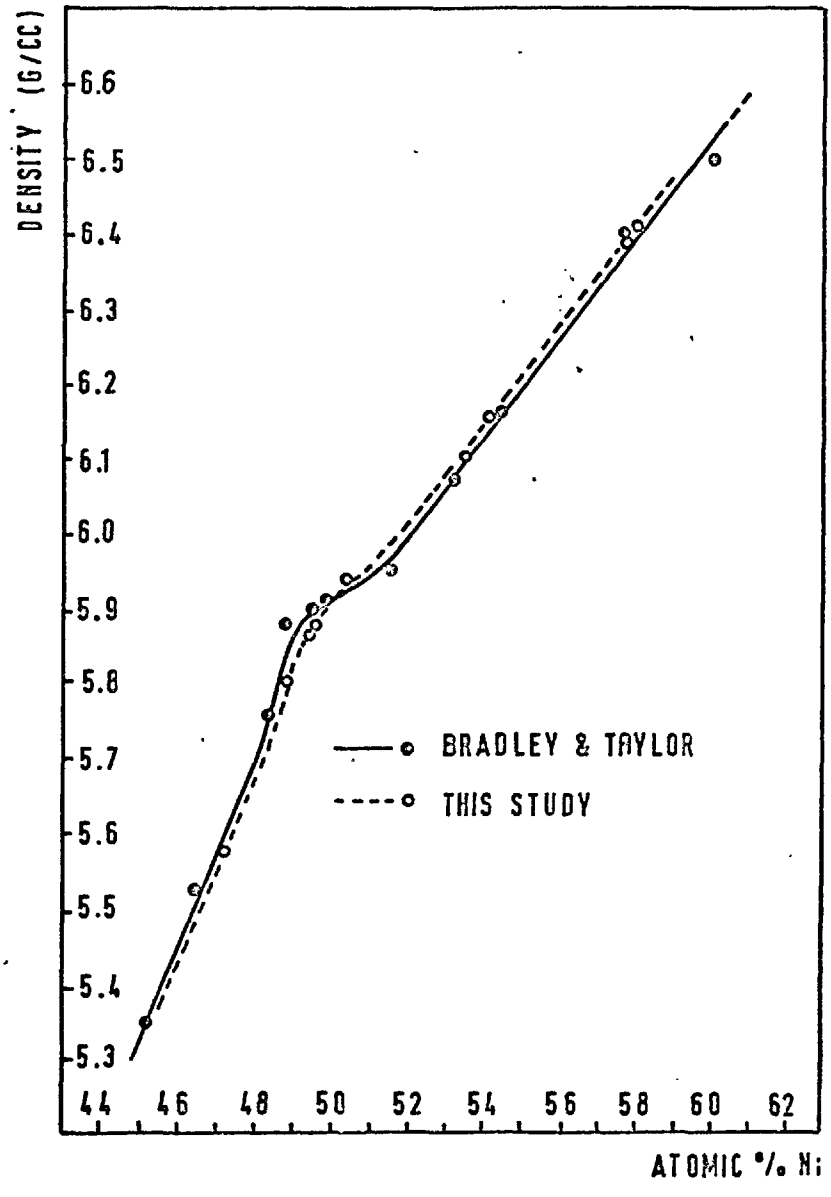

FIG. 5:1 DENSITY VS COMPOSITION

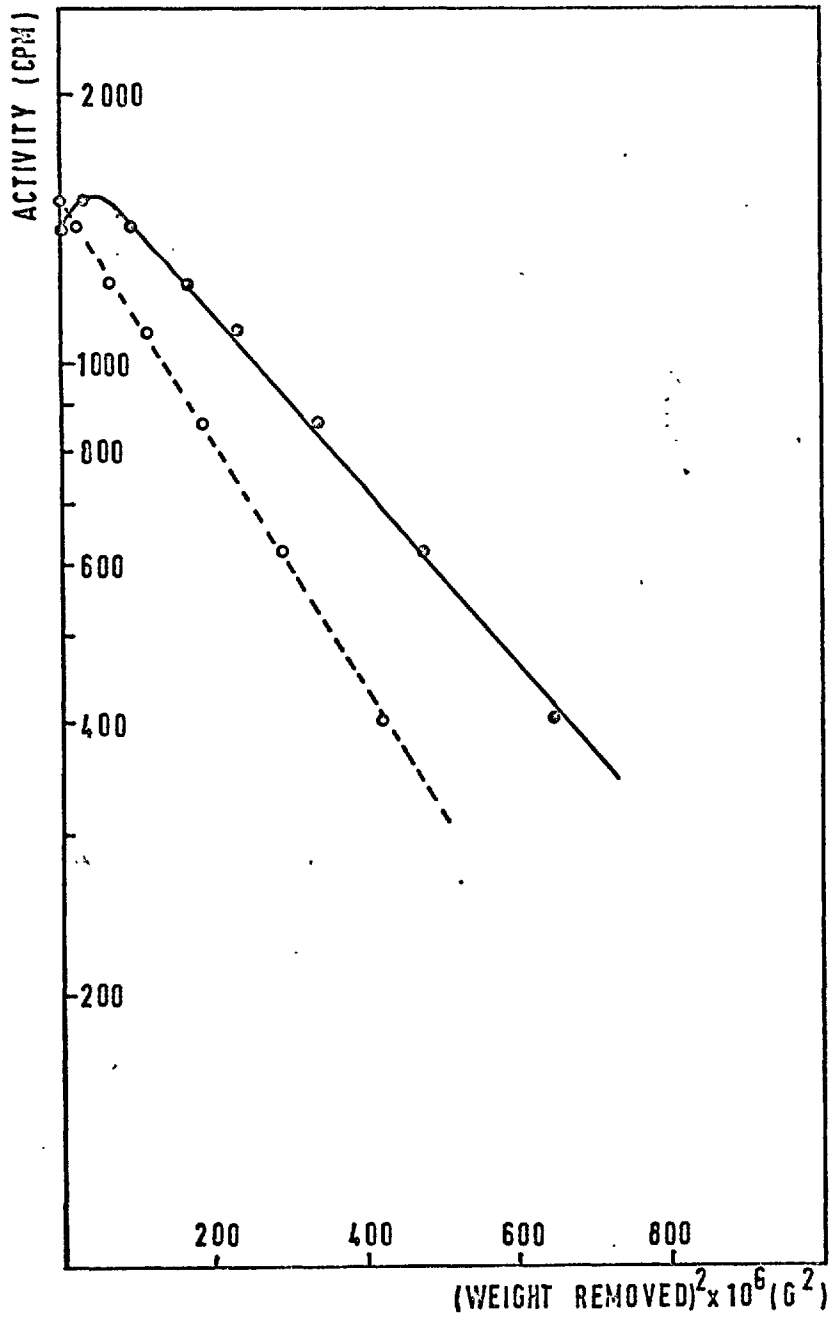
ACTIVITY (CPM)
2000
1000
800
600
400
200
200
400
600
800
(WEIGHT REMOVED)^2 x 10^6 (G^2)

FIG. 5:2

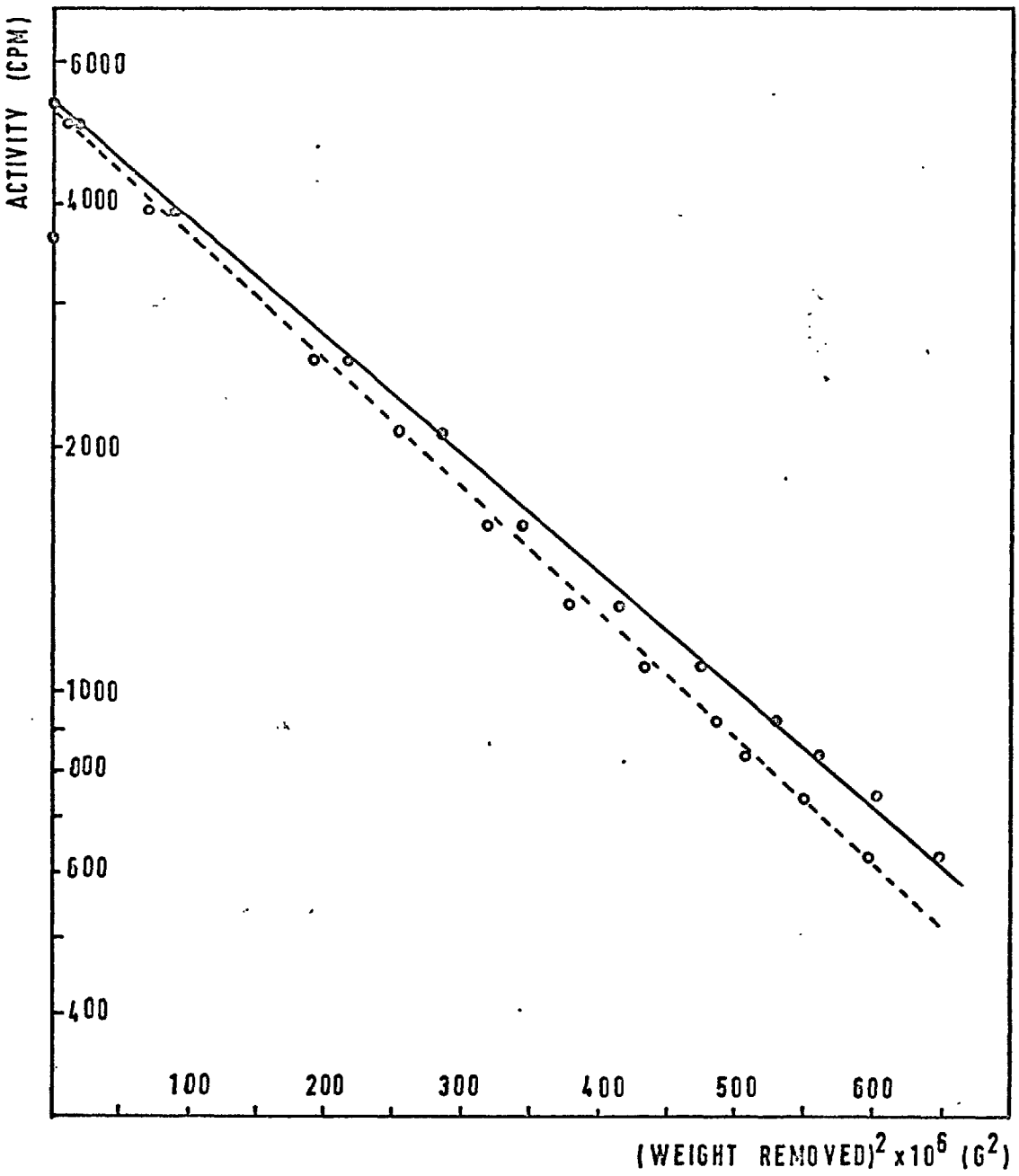
ACTIVITY (CPM)
6000
4000
2000
1000
800
600
400
100
200
300
400
500
600
(WEIGHT REMOVED)^2 x 10^6 (G^2)

FIG. 5:3

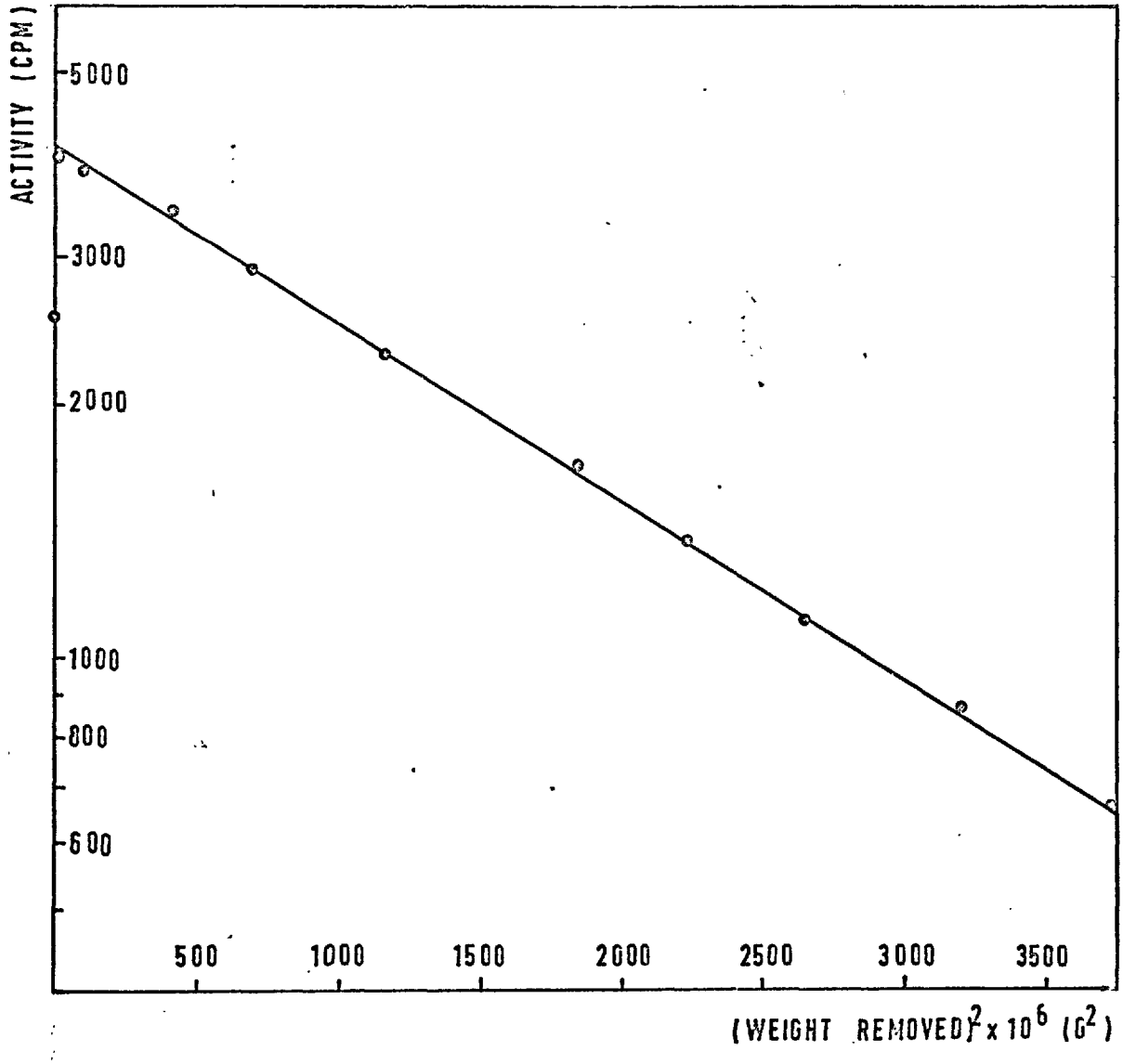
ACTIVITY (CPM)
5000
3000
2000
1000
800
600
500
1000
1500
2000
2500
3000
3500
(WEIGHT REMOVED)^2 x 10^6 (G^2)

FIG. 5:4

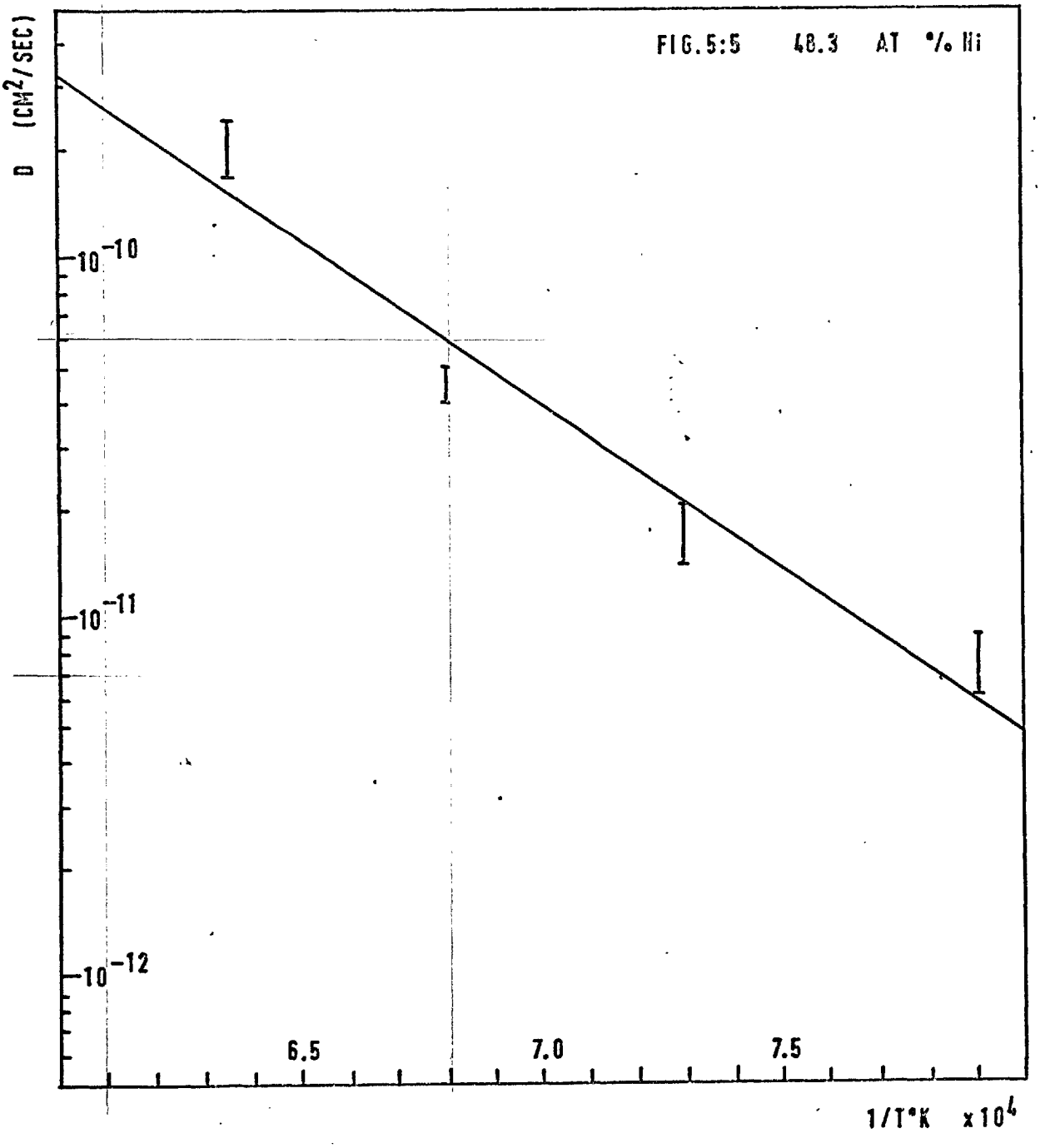
FIG.5:5 48.3 AT % Ni
D (CM²/SEC)
10⁻¹⁰
10⁻¹¹
10⁻¹²
6.5
7.0
7.5
1/T°K x10⁴

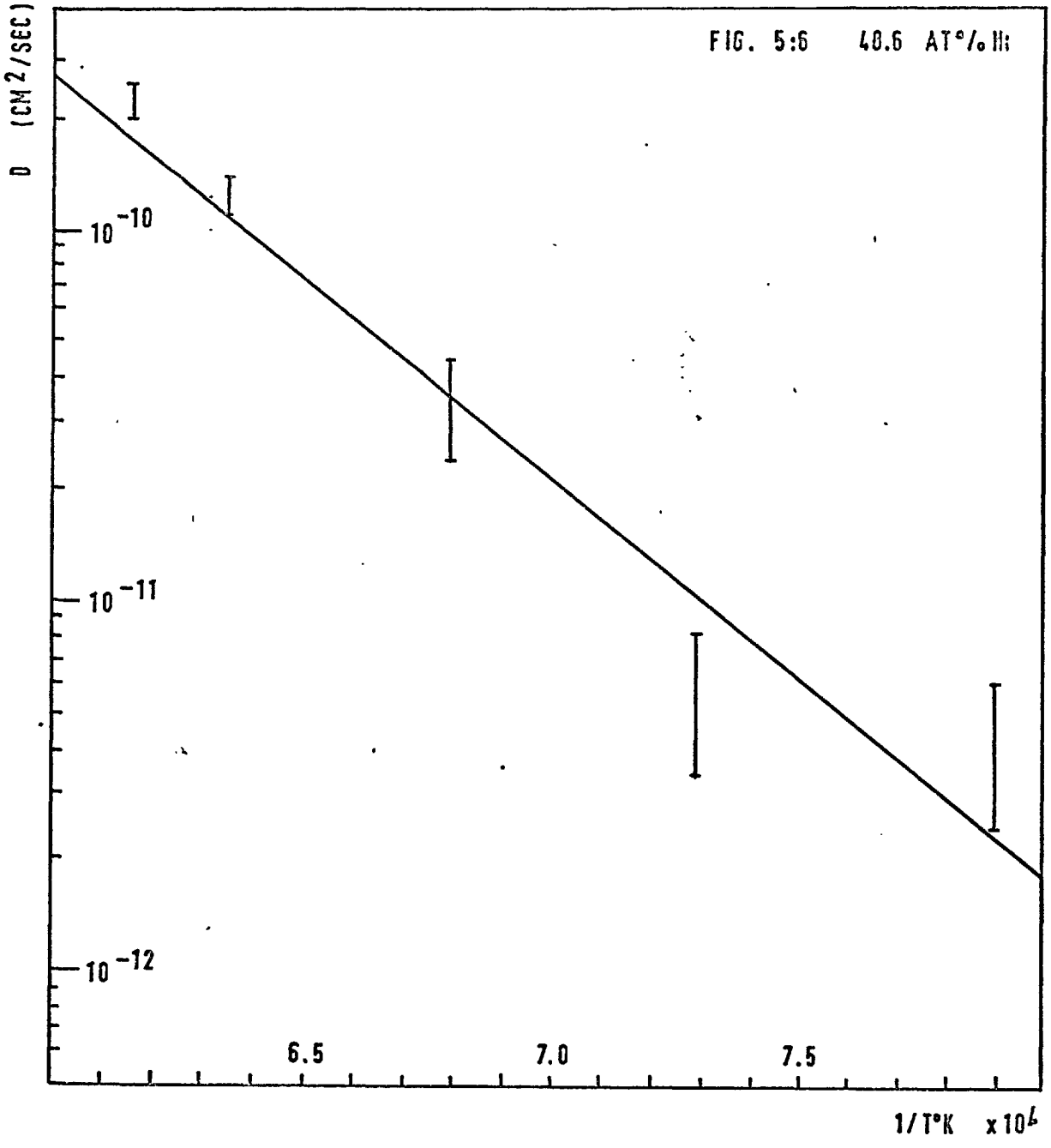
FIG. 5:6 48.6 AT°/o Ni
D (CM 2/SEC)
10 -10
10 -11
10 -12
6.5
7.0
7.5
1/T°K x10 4

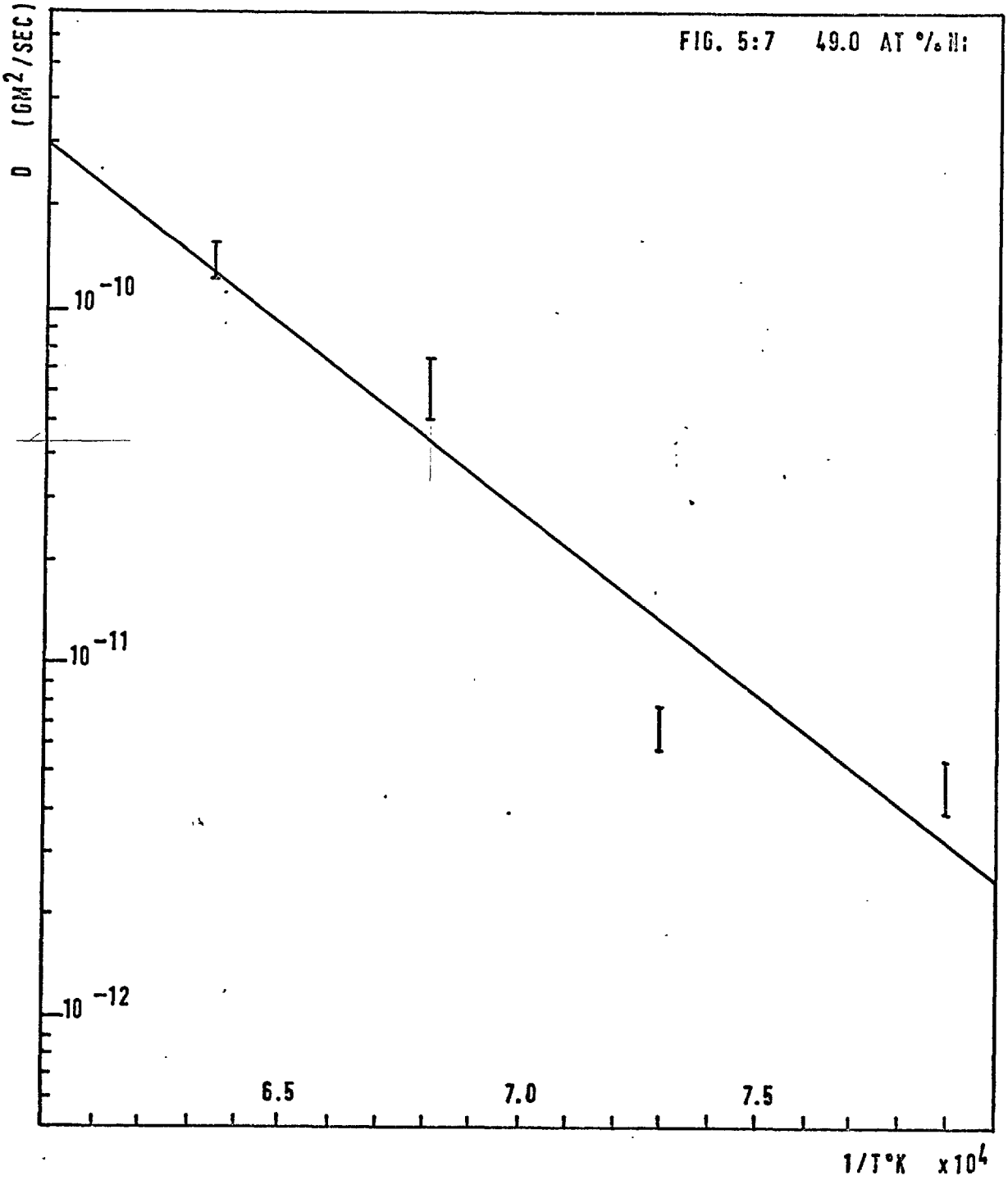
FIG. 5:7 49.0 AT %Ni
D (CM2/SEC)
10-10
10-11
10-12
6.5
7.0
7.5
1/T°K x10⁴

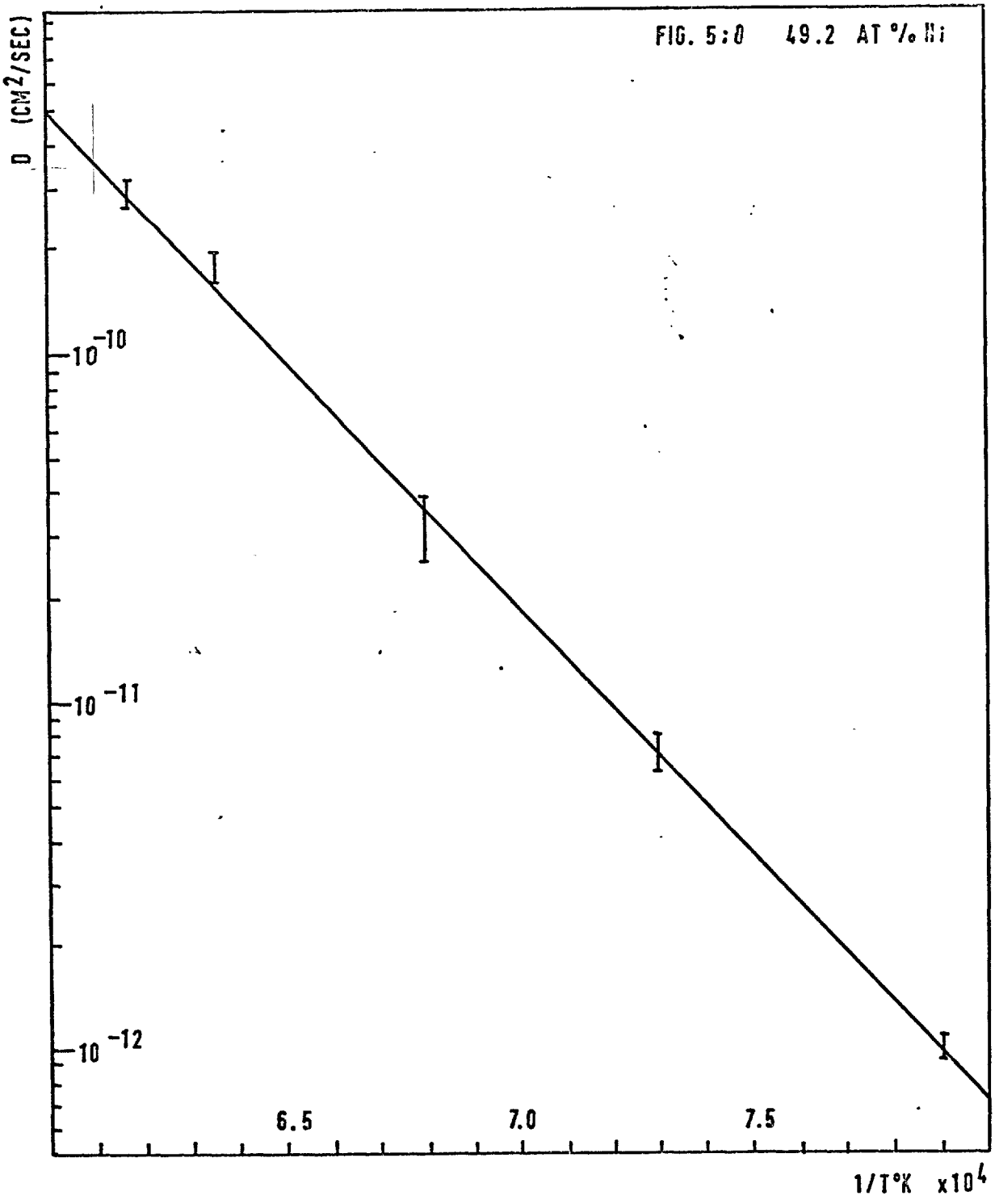
FIG. 5:0 49.2 AT % Ni
D (CM2/SEC)
10-10
10-11
10-12
6.5
7.0
7.5
1/T°K x10⁴

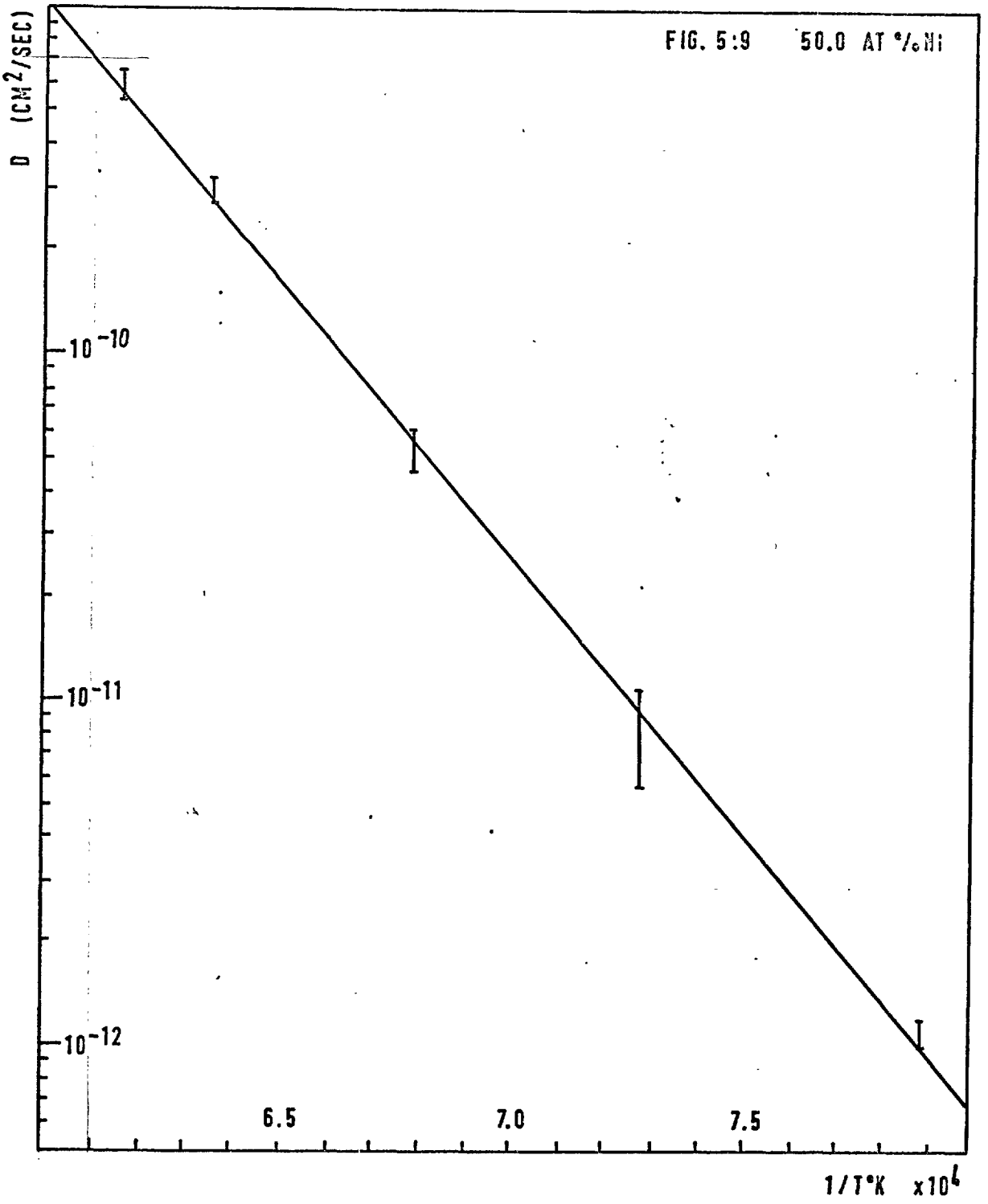
FIG. 5:9 50.0 AT %Ni
D (CM²/SEC)
10⁻¹⁰
10⁻¹¹
10⁻¹²
6.5
7.0
7.5
1/T°K x10⁴

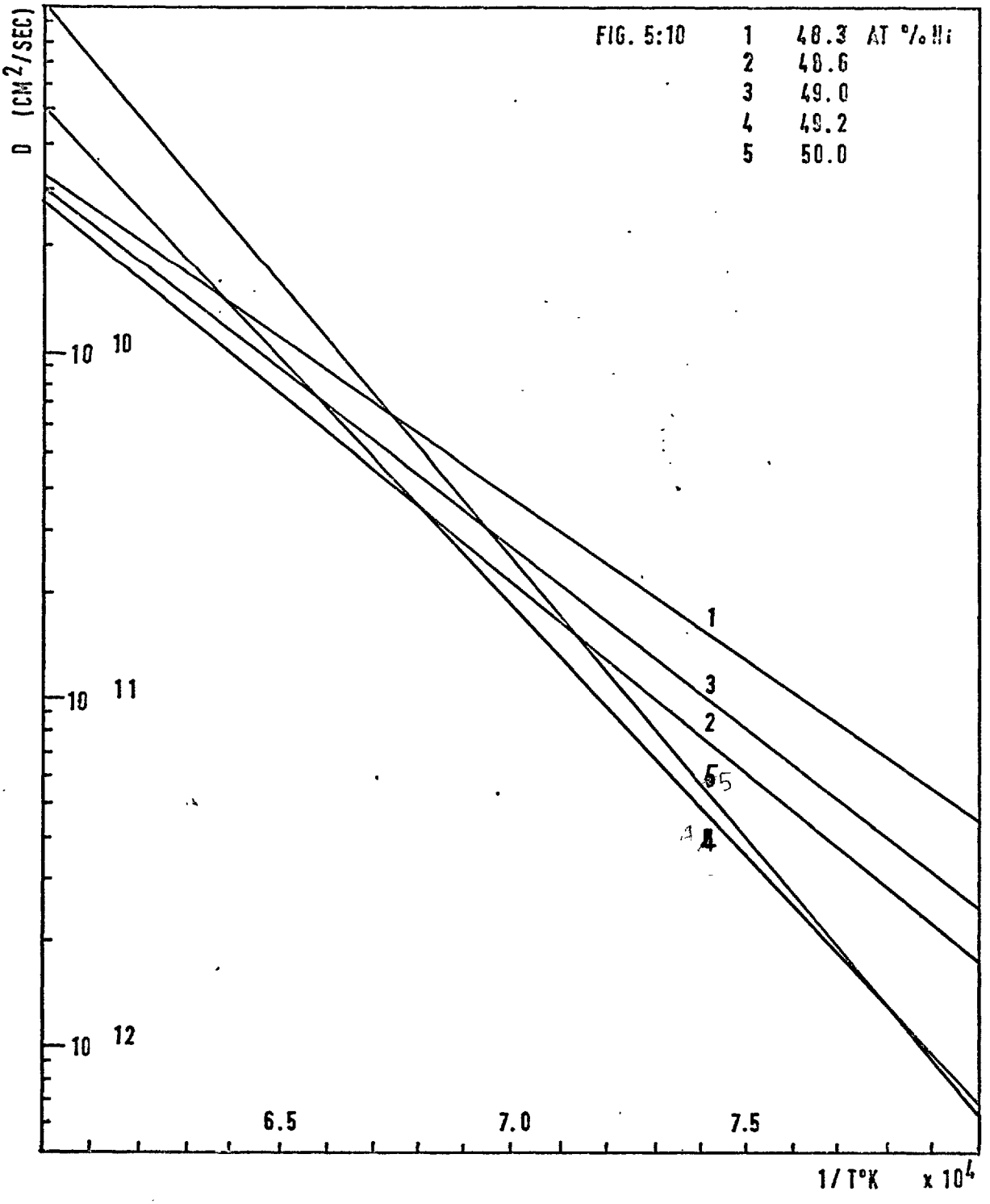
FIG. 5:10
1 48.3 AT % Ni
2 48.6
3 49.0
4 49.2
5 50.0
D (CM²/SEC)
10 10
10 11
10 12
6.5
7.0
7.5
1/T°K x 10⁴
1
3
2
5
4

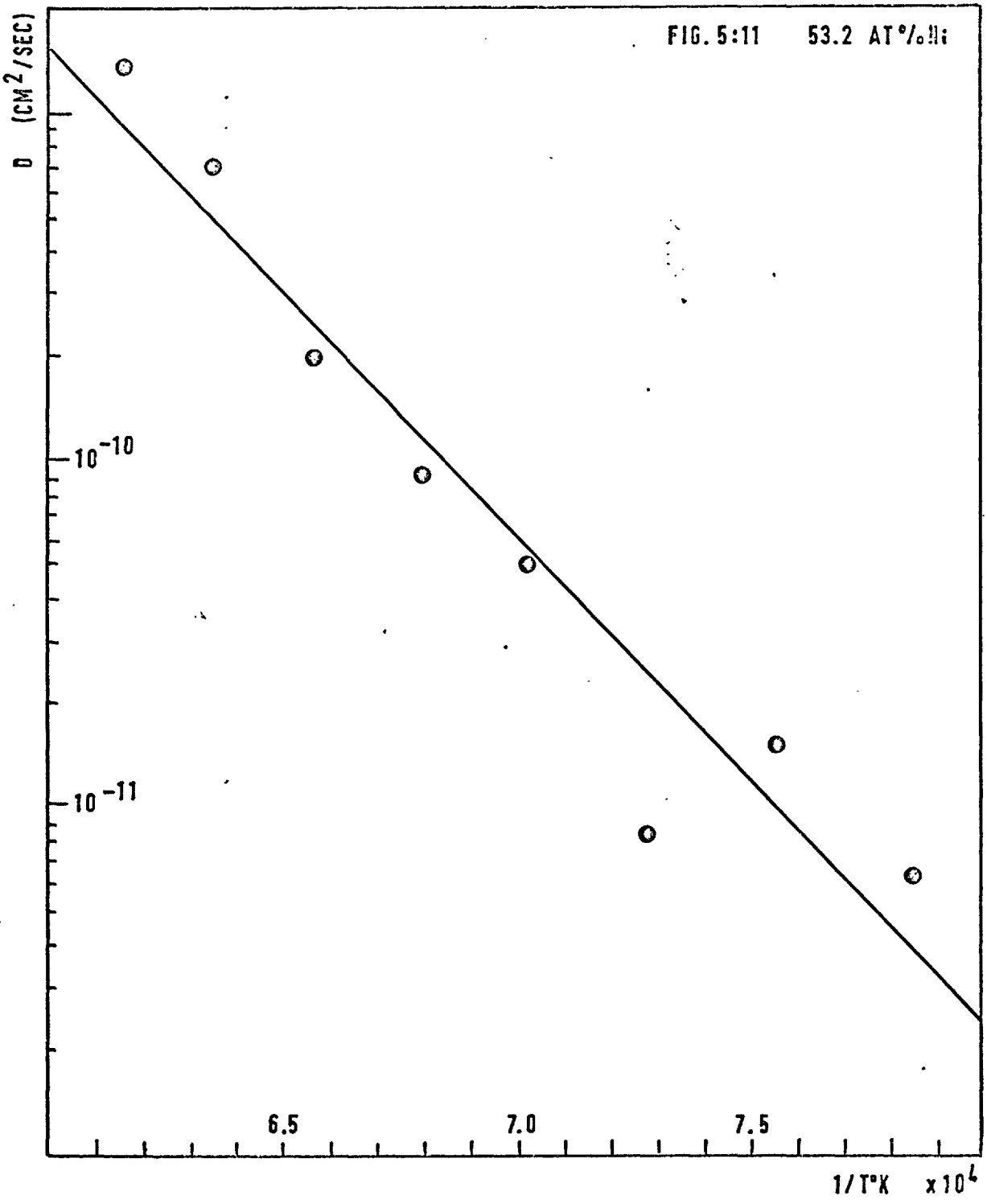
FIG. 5:11 53.2 AT%Ni
D (CM²/SEC)
10⁻¹⁰
10⁻¹¹
6.5
7.0
7.5
1/T°K x10⁴

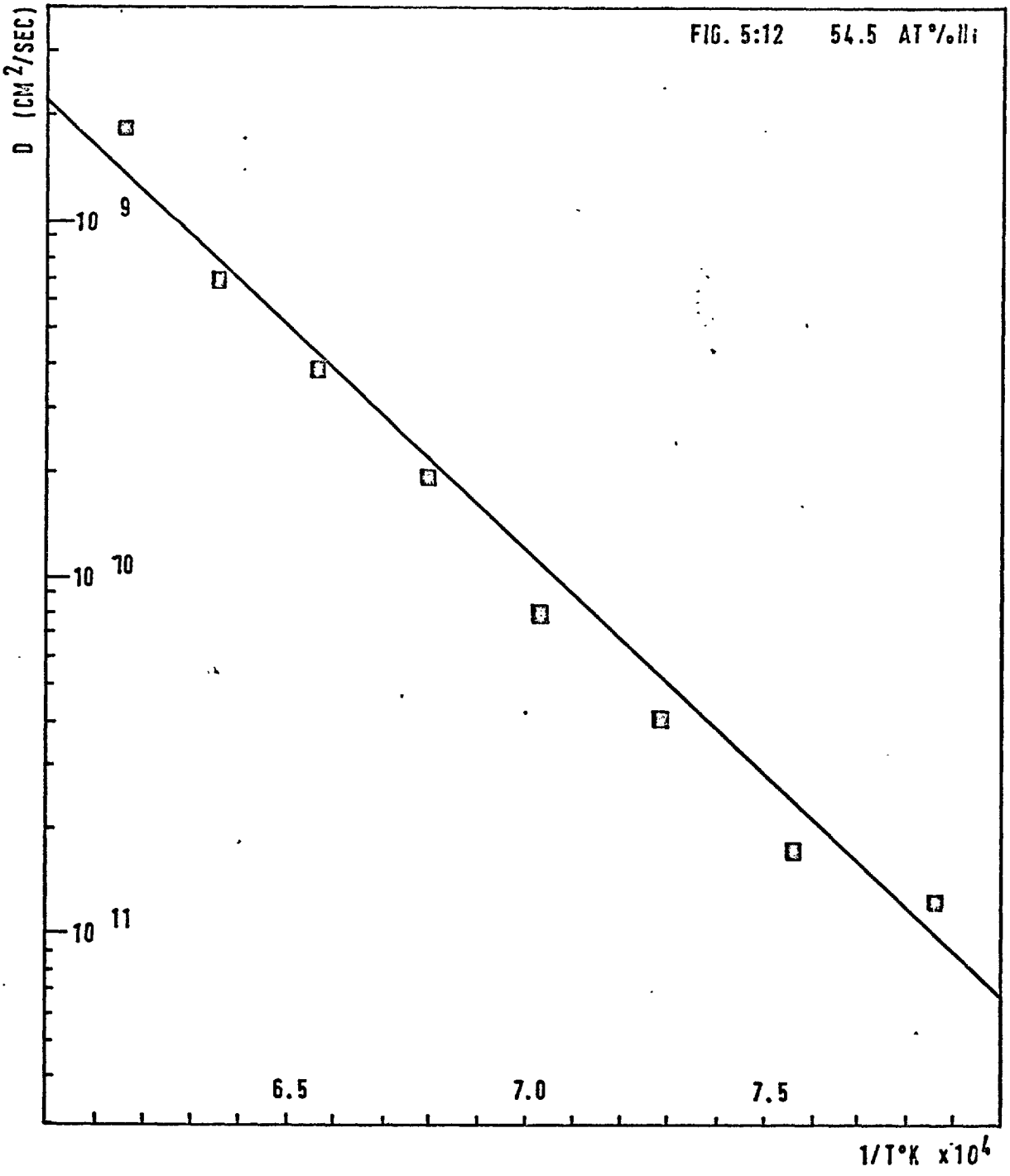
FIG. 5:12 54.5 AT%Ni
D (CM²/SEC)
10 9
10 10
10 11
6.5
7.0
7.5
1/T°K x10⁴

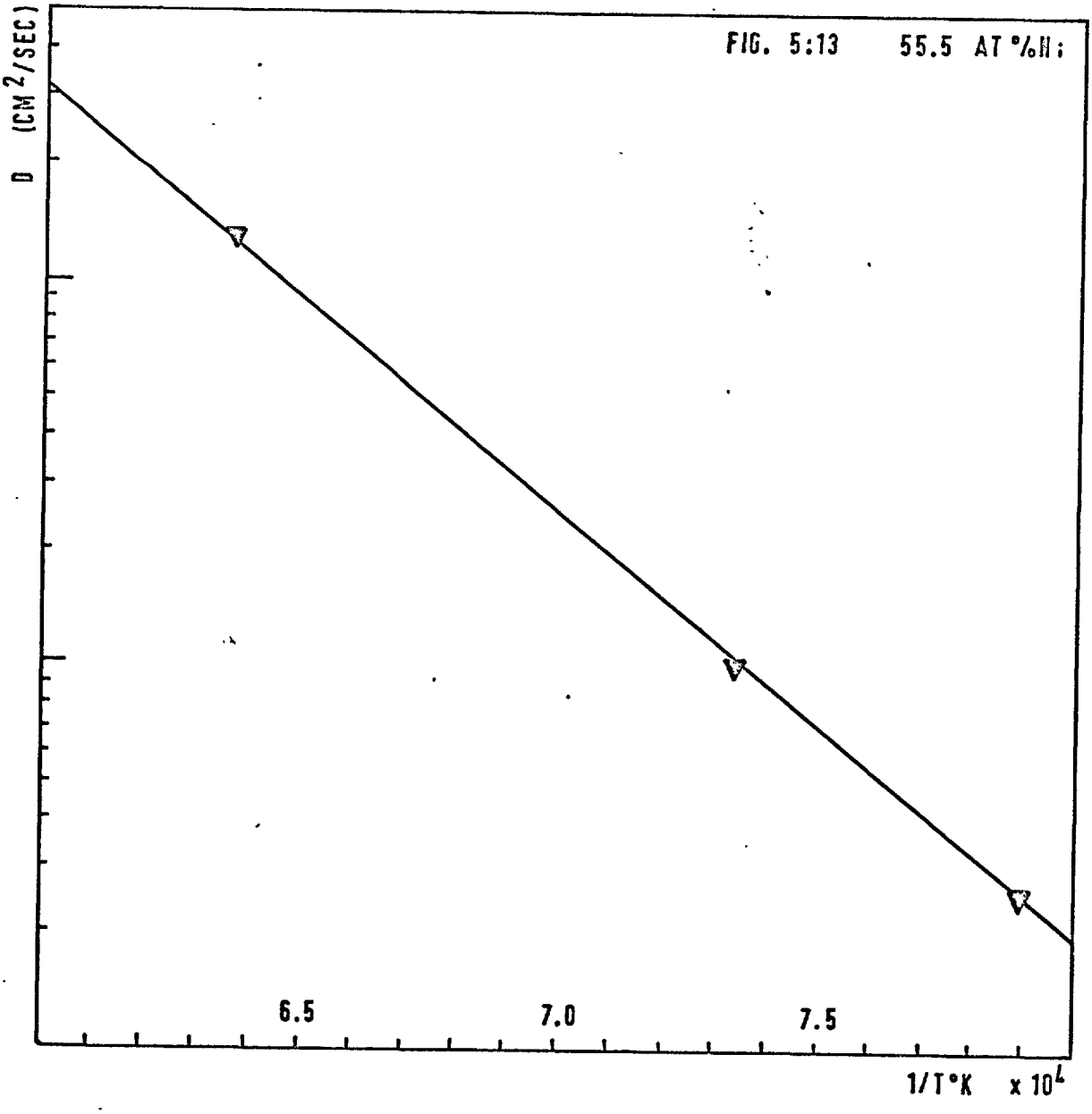
FIG. 5:13 55.5 AT %H;
D (CM 2/SEC)
6.5
7.0
7.5
1/T°K x 10 4

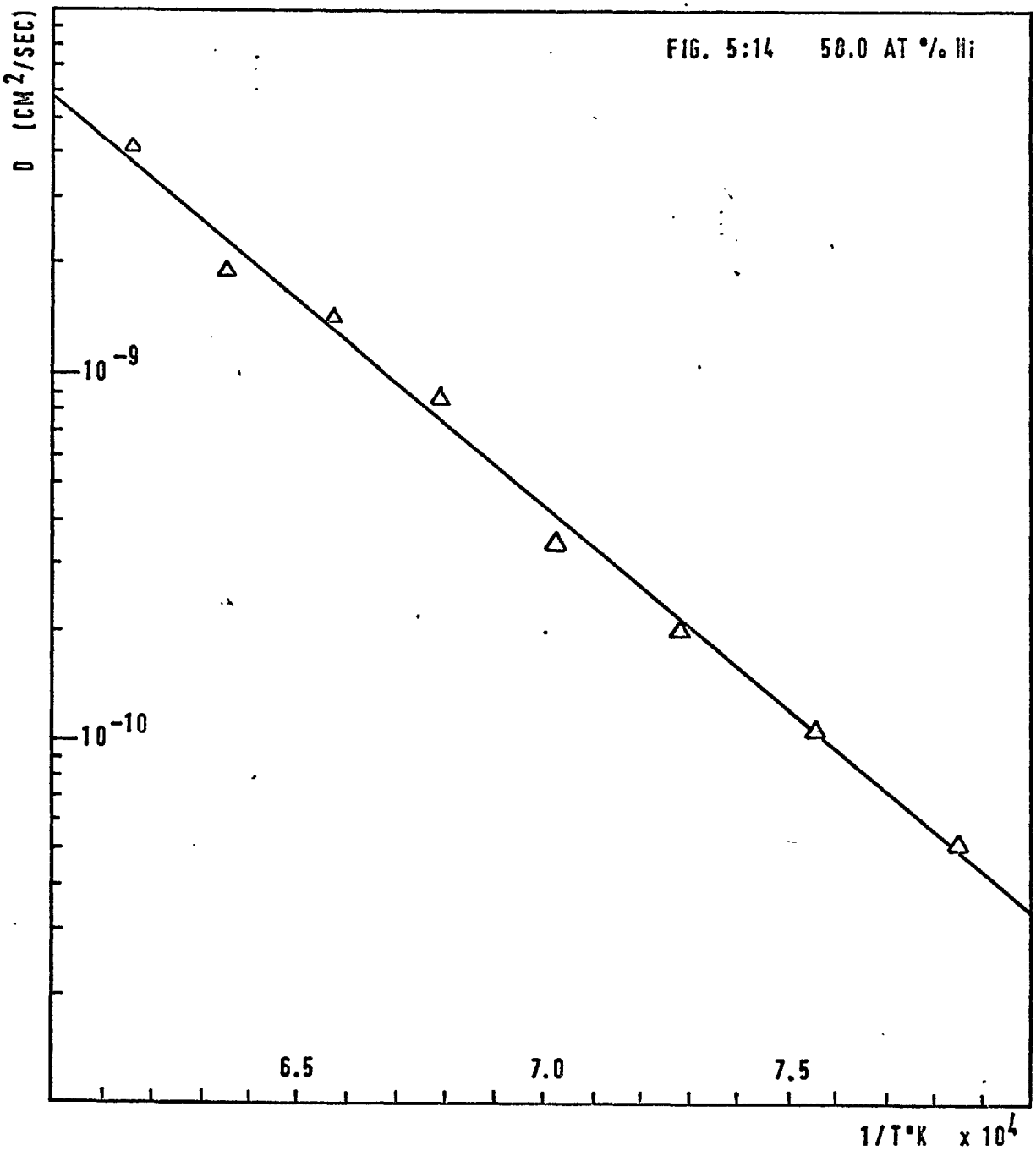
FIG. 5:14 58.0 AT % Ni
D (CM 2/SEC)
10 -9
10 -10
6.5
7.0
7.5
1/T°K x 10 4

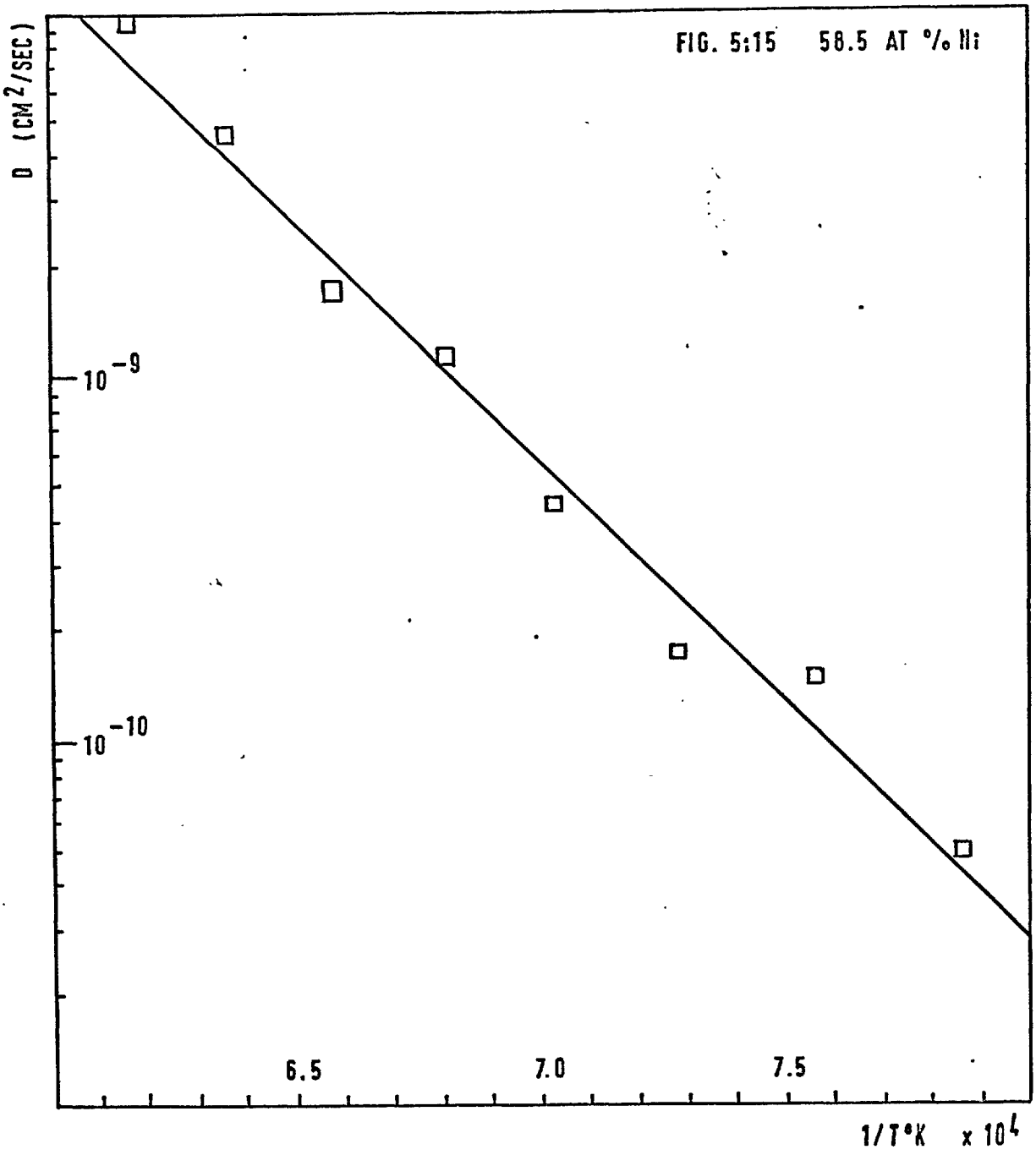
FIG. 5:15 58.5 AT % Ni
D (CM²/SEC)
10⁻⁹
10⁻¹⁰
6.5
7.0
7.5
1/T°K x 10⁴

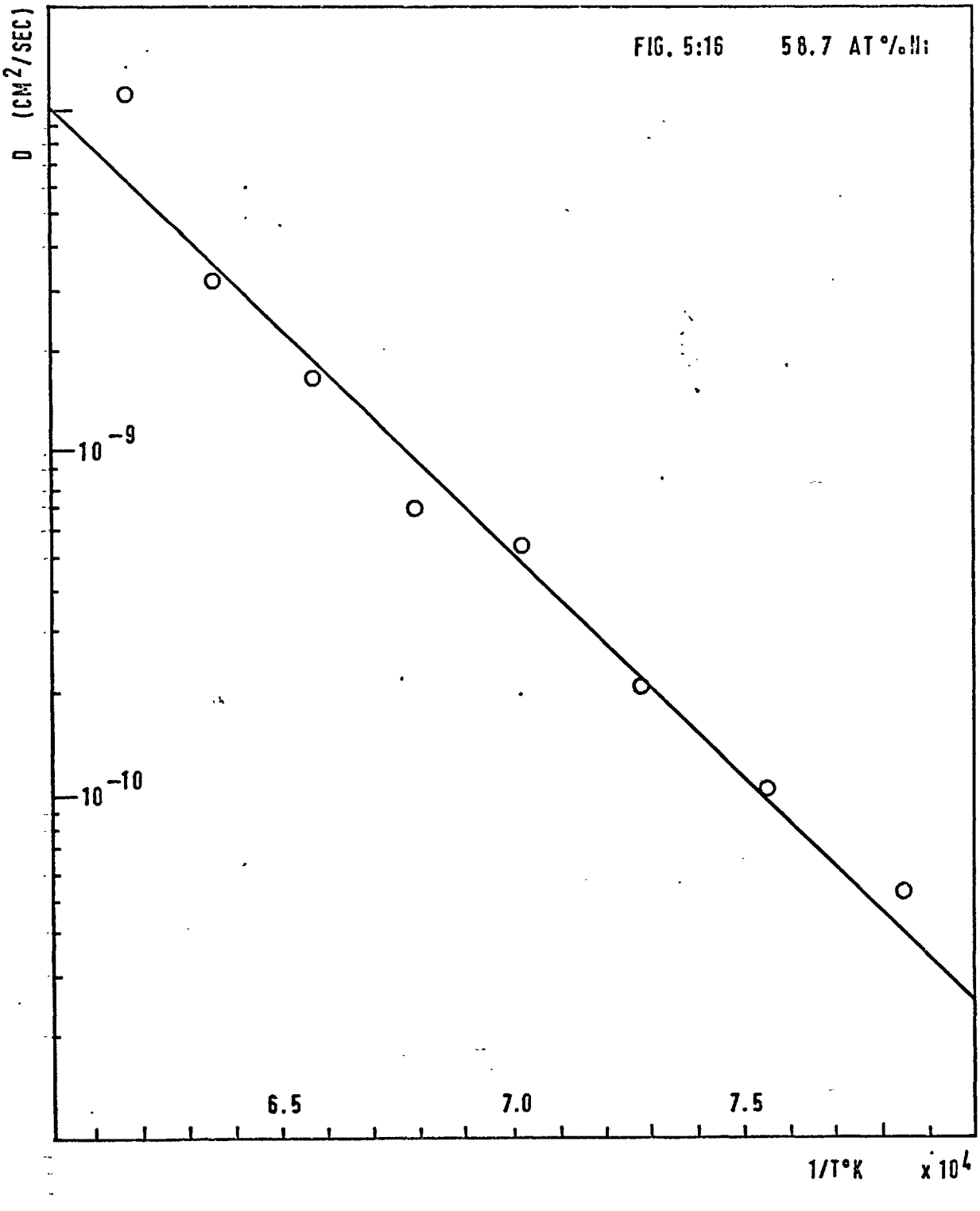
FIG. 5:16 58.7 AT %Ni
D (CM²/SEC)
10⁻⁹
10⁻¹⁰
6.5
7.0
7.5
1/T°K x 10⁴

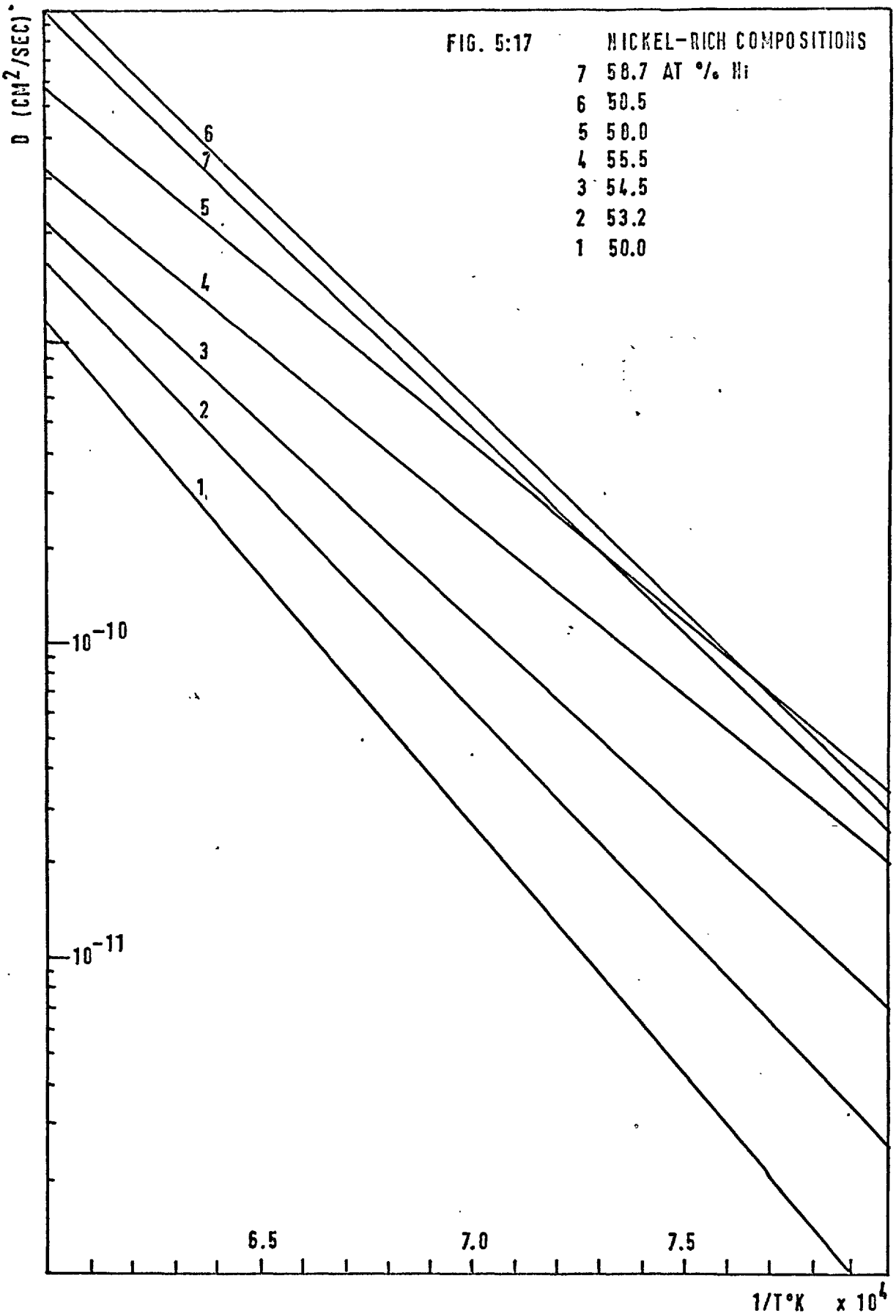
FIG. 5:17
NICKEL-RICH COMPOSITIONS
7 58.7 AT % Ni
6 58.5
5 58.0
4 55.5
3 54.5
2 53.2
1 50.0
D (CM²/SEC)
10⁻¹⁰
10⁻¹¹
6.5
7.0
7.5
1/T°K x 10⁴

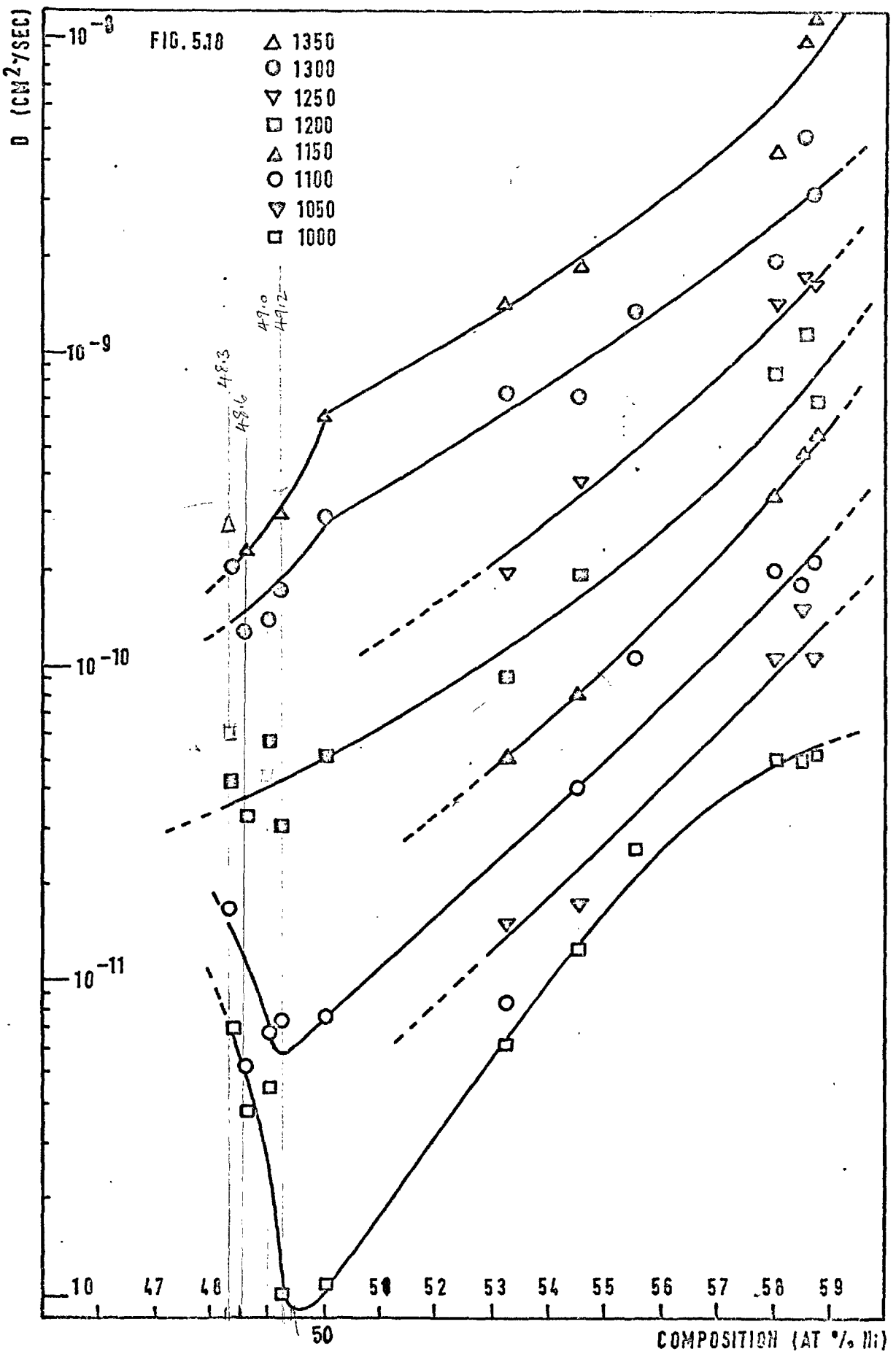
FIG. 5.18
D (CM2/SEC)
10-8
10-9
10-10
10-11
1350
1300
1250
1200
1150
1100
1050
1000
48.3
49.0
49.2
49.6
10
47
48
50
52
53
54
55
56
57
58
59
50
COMPOSITION (AT % Ni)

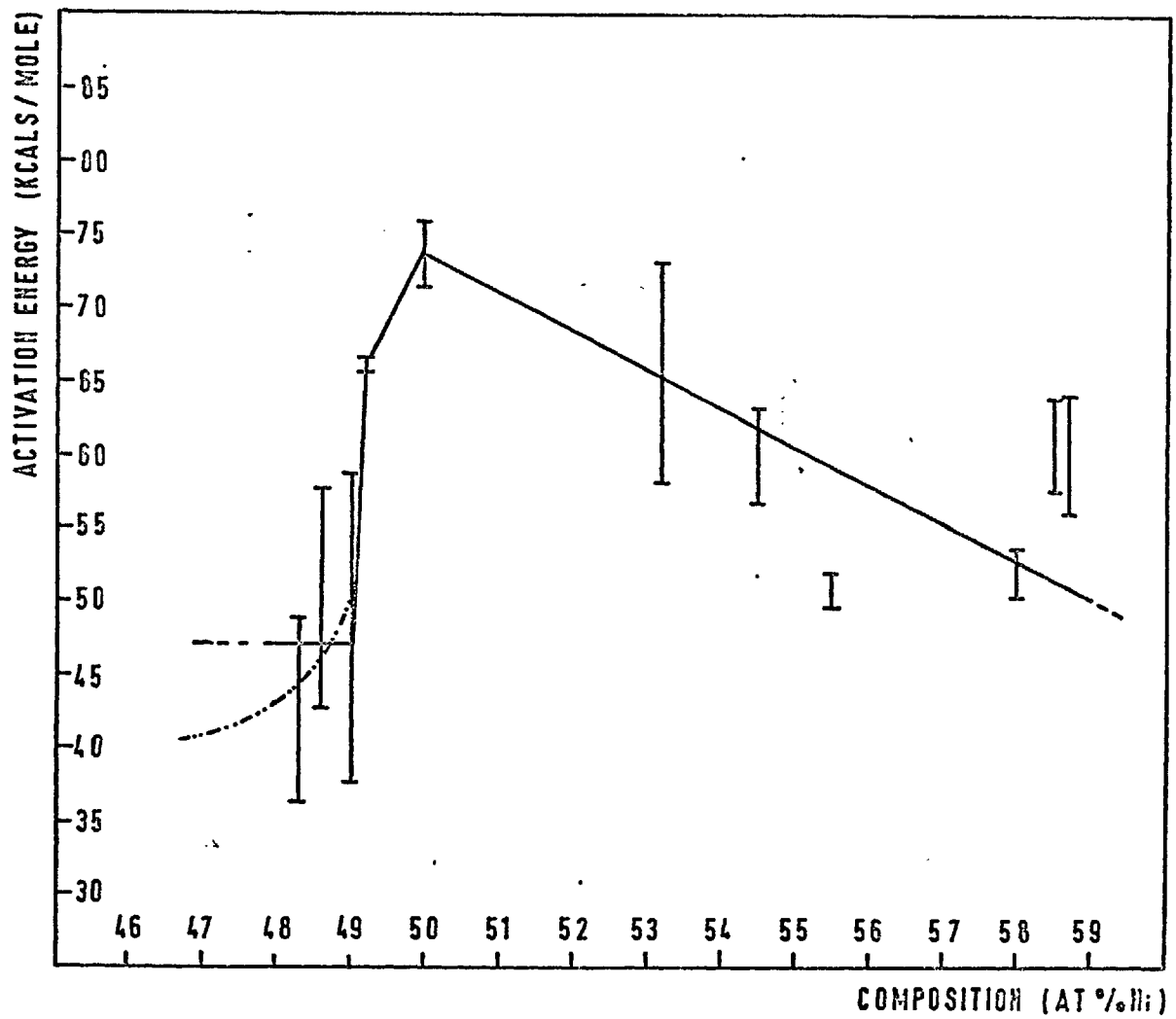

FIG. 5.19 ANALYSIS (A)

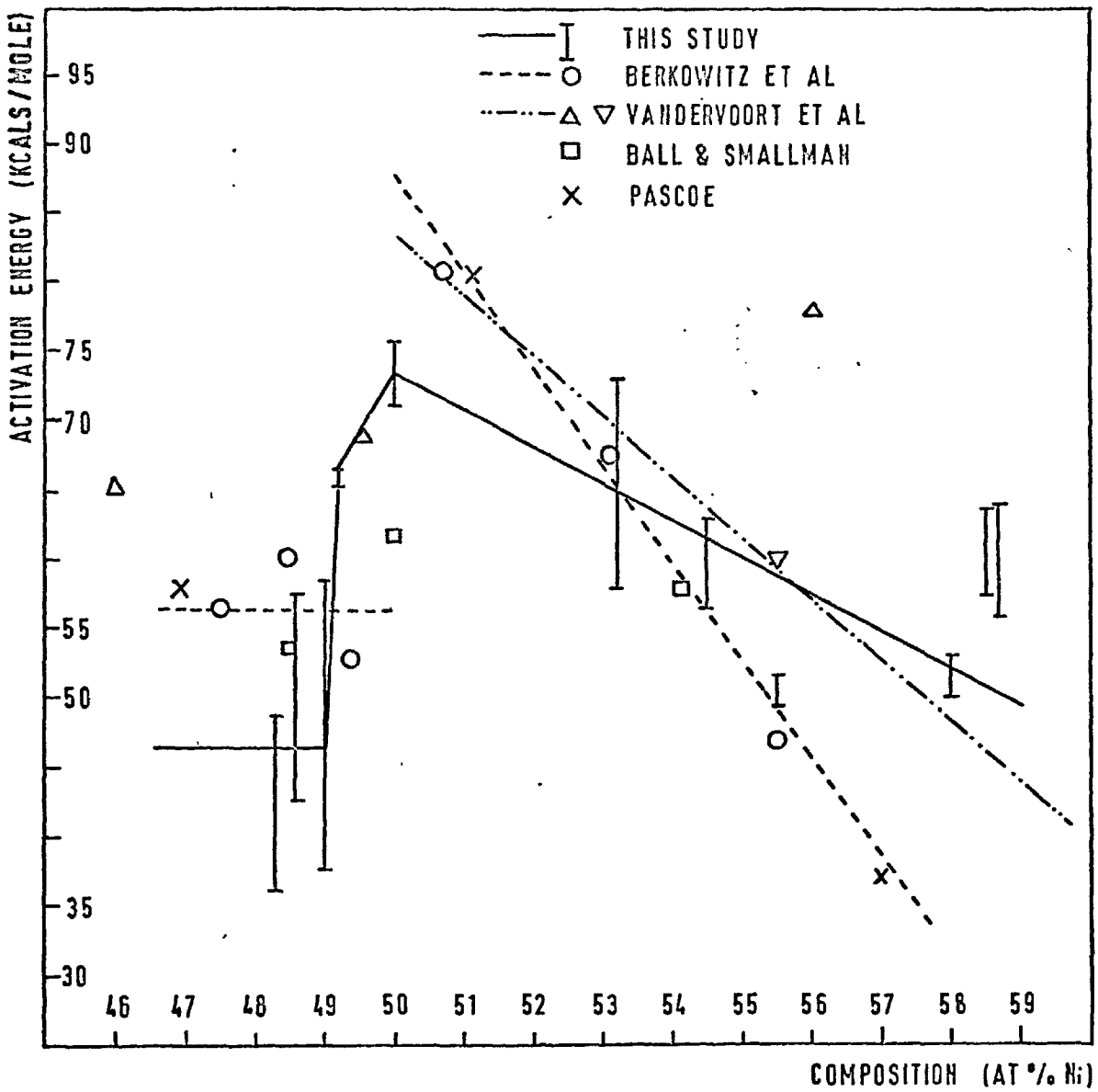

FIG. 5:20 ANALYSIS (A) & PREVIOUS WORK

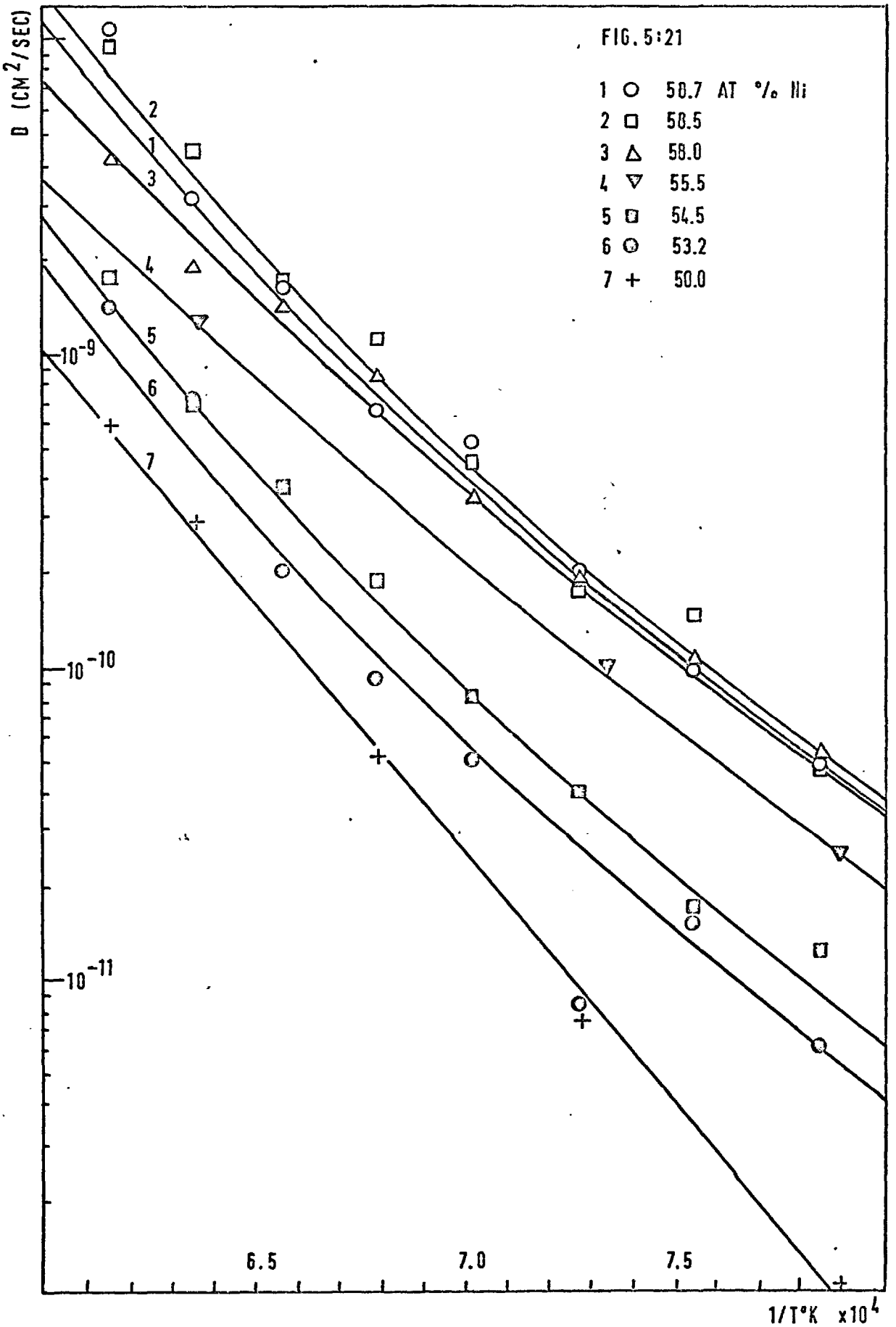
FIG. 5:21
1 ○ 58.7 AT % Ni
2 □ 58.5
3 △ 58.0
4 ▽ 55.5
5 ◫ 54.5
6 ⊙ 53.2
7 + 50.0
D (CM²/SEC)
10⁻⁹
10⁻¹⁰
10⁻¹¹
6.5
7.0
7.5
1/T°K x10⁴

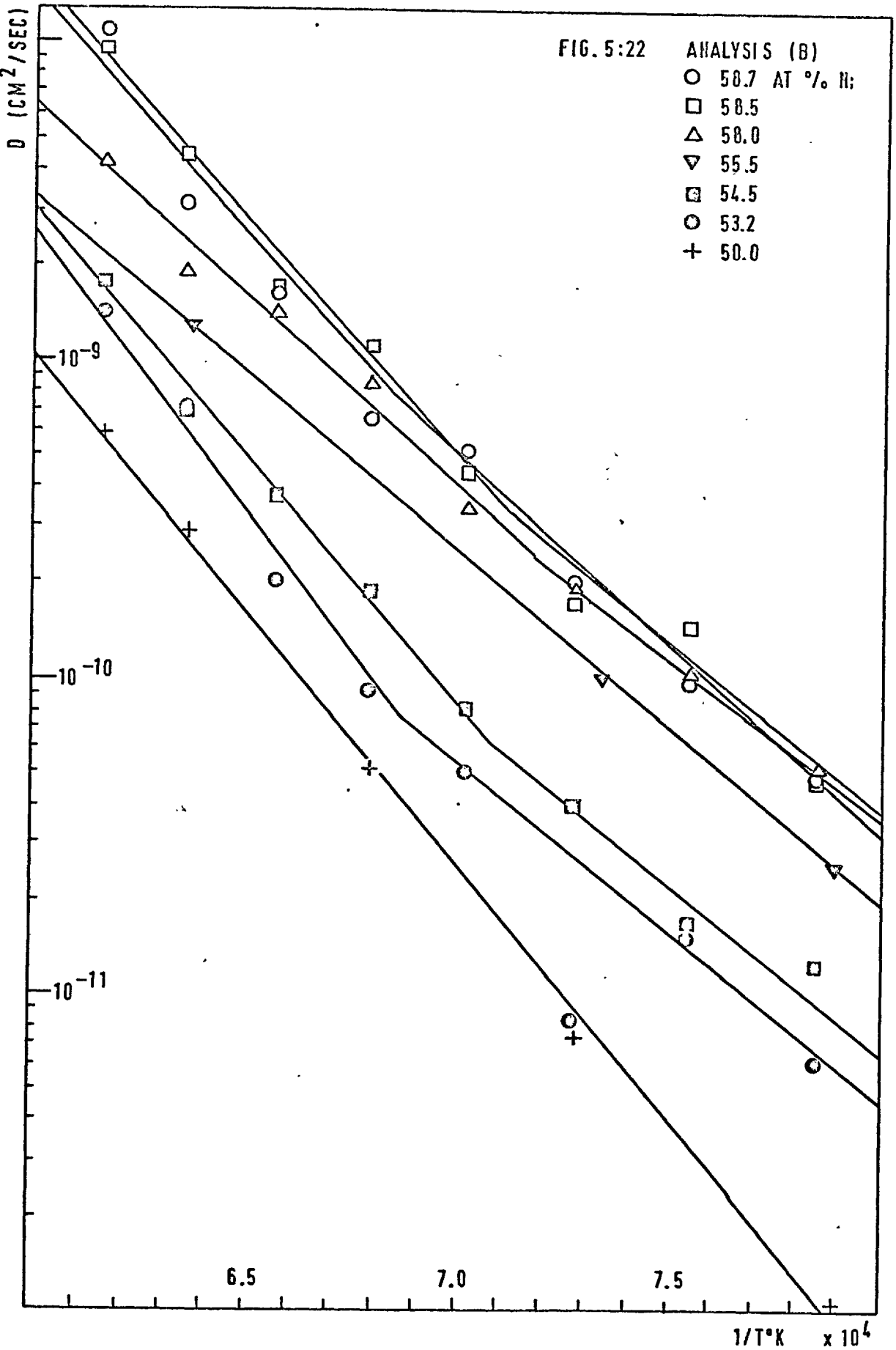
FIG. 5:22
ANALYSIS (B)
50.7 AT % N;
58.5
58.0
55.5
54.5
53.2
50.0
D (CM²/SEC)
10⁻⁹
10⁻¹⁰
10⁻¹¹
6.5
7.0
7.5
1/T°K x 10⁴

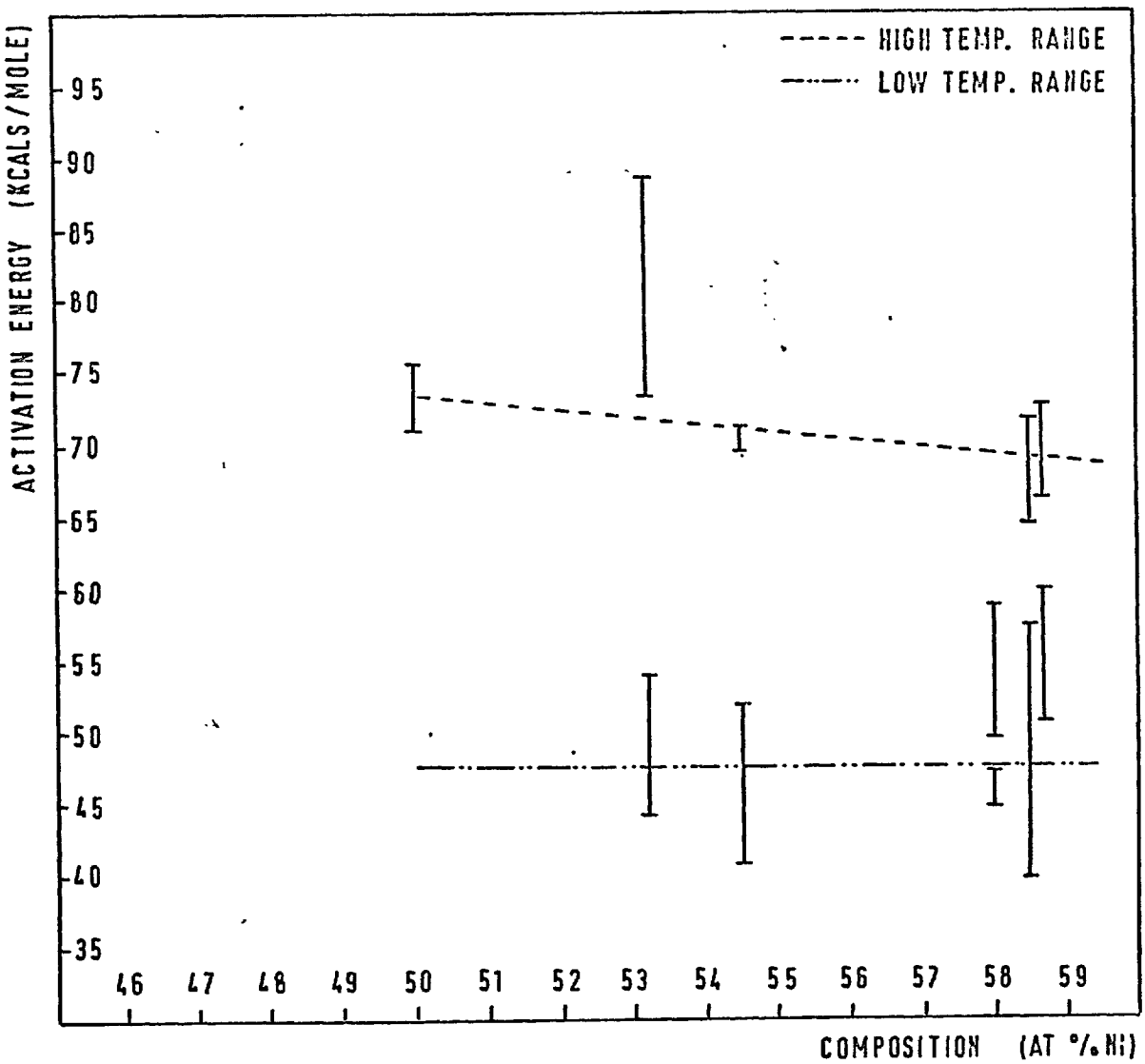

FIG. 5:23 ANALYSIS (B)

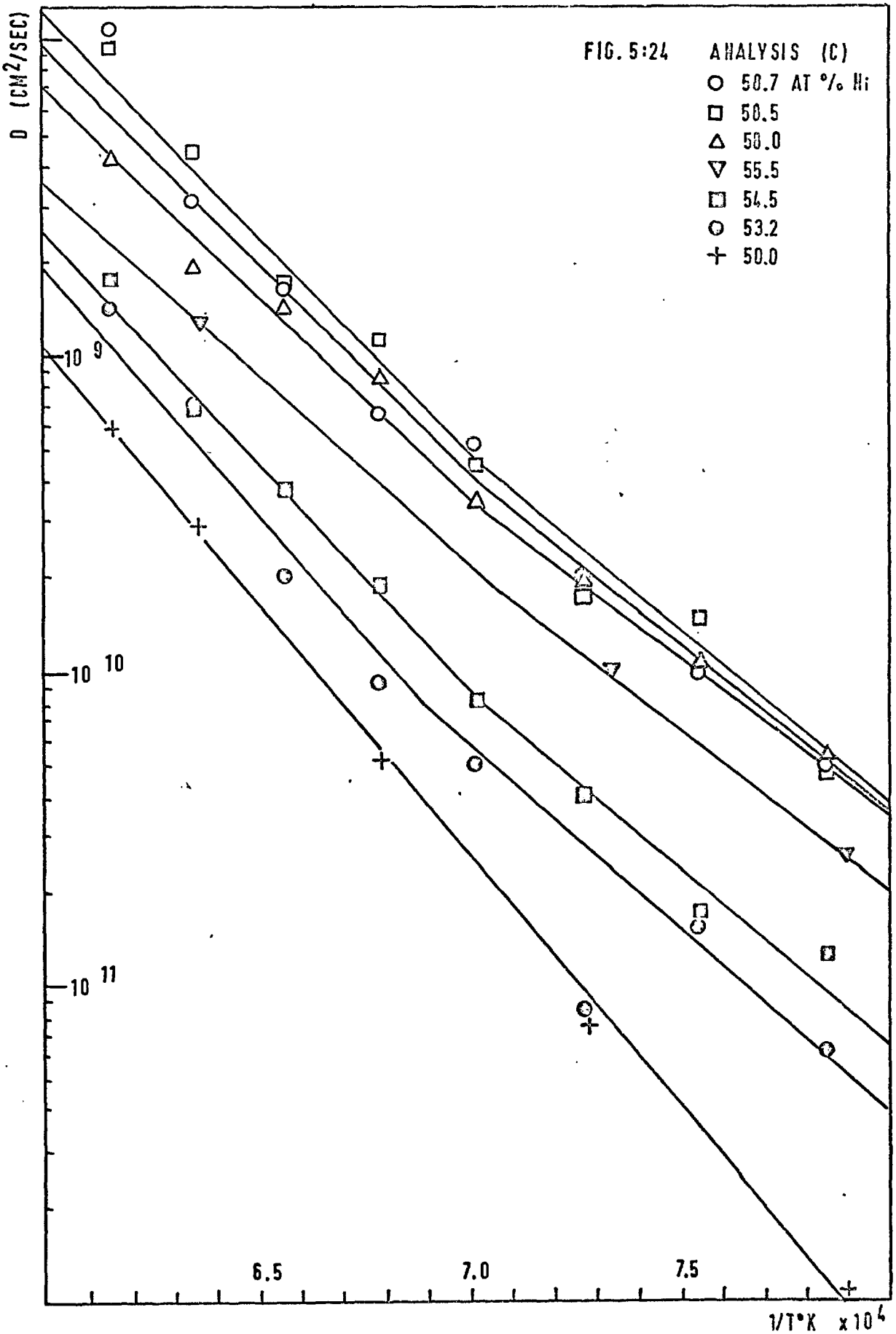
FIG. 5:24 ANALYSIS (C)
50.7 AT % Ni
50.5
50.0
55.5
54.5
53.2
50.0
D (CM2/SEC)
10 9
10 10
10 11
6.5
7.0
7.5
1/T°K x 10 4

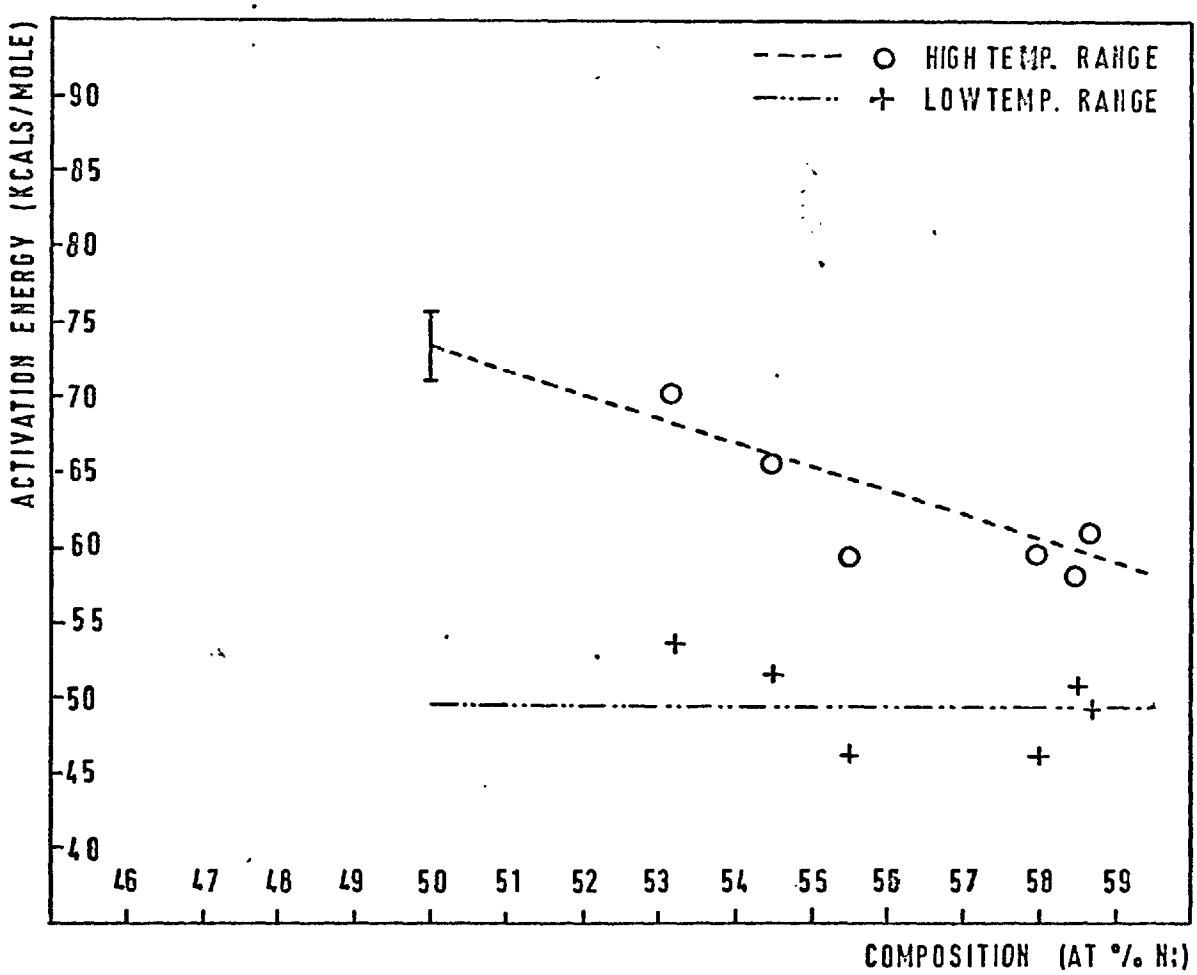

FIG. 5:25 ANALYSIS (C)

at. % Ni	T_s °K	Q Kcals/mole	D_o and limits cm^2/sec		ΔS	ΔG	Q/T_s	$\Delta G/T_s$
48.3	1901	42.5 ± 6.3	0.00012	0.08582 0.00001	-8.29	58.2	22.4	30.6
48.6	1903	50.1 ± 7.4	0.00104	0.01404 0.00008	-4.02	57.8	26.3	30.3
49.0	1906	47.9 ± 10.7	0.00053	0.02634 0.00001	-5.19	57.7	25.1	30.3
49.2	1907	65.9 ± 0.5	0.2302	0.3895 0.1360	6.70	53.1	34.6	27.9
50.0	1911	73.4 ± 2.3	4.461	9.826 2.025	12.58	49.4	38.4	25.8
53.2	1884	65.5 ± 7.5	0.6296	8.732 0.0454	8.24	49.9	34.8	26.5
54.5	1860	59.8 ± 3.2	0.1504	0.4637 0.0488	5.86	51.0	32.2	27.4
55.5	1837	50.5 ± 1.1	0.01356	0.0477 0.0038	1.08	48.6	27.5	26.4
58.0	1793	51.7 ± 1.7	0.0352	0.0637 0.0194	2.99	46.4	28.8	25.9
58.5	1784	60.6 ± 3.1	1.096	3.845 0.3128	9.82	43.0	34.0	24.1
58.7	1782	59.8 ± 3.9	0.7254	2.876 0.183	9.00	43.8	33.6	24.6

TABLE 5.1

TEMP RANGE	at. % Ni	T_s °K	Q Kcals/mole	D_o and limits cm^2/sec		ΔS	ΔG	Q/T_s	$\Delta G/T_s$
HIGH	53.2	1884	80.9 ± 7.7	102.9	1310.0 8.266	18.84	45.4	43.0	24.1
	54.5	1860	70.4 ± 0.8	4.795	6.267 3.664	12.74	43.7	37.8	23.5
	58.0	1793	54.0 ± 4.6	0.0749	0.346 0.016	4.49	45.9	30.2	25.6
	58.5	1784	68.0 ± 3.6	12.76	23.62 6.900	14.70	41.8	38.1	23.4
	58.7	1782	69.4 ± 3.1	18.94	53.95 6.653	15.49	41.8	38.9	23.5
LOW	53.2	1884	49.0 ± 4.8	0.0017	0.0106 0.0003	-2.99	54.7	26.0	29.0
	54.5	1860	46.2 ± 5.6	0.0009	0.0073 0.0001	-4.30	54.2	24.8	29.1
	58.0	1793	45.8 ± 1.2	0.0037	0.0059 0.0023	-1.48	48.5	25.6	27.0
	58.5	1784	48.4 ± 8.7	0.0113	0.2976 0.0004	0.74	47.1	27.2	26.4
	58.7	1782	55.1 ± 4.7	0.1384	0.7939 0.0241	0.57	54.1	31.0	30.4

TABLE 5.2

TEMP RANGE	at. % Ni	T_s ^oK	Q Kcals/Mole	D_o cm^2/sec	ΔS	ΔG	Q/T_s	$\Delta G/T_s$
HIGH	53.2	1884	70.1	3.5050	12.00	47.5	37.2	25.2
	54.5	1860	65.6	1.1920	10.00	47.0	35.2	25.2
	55.5	1837	54.3	0.0068	4.30	46.4	29.6	25.2
	58.0	1793	59.3	0.0412	7.90	45.2	33.1	25.2
	58.5	1784	58.2	1.0180	10.80	38.9	32.6	21.8
	58.7	1782	61.0	2.2400	9.70	43.6	34.2	24.4
LOW	53.2	1884	53.6	0.0010	0.52	52.6	28.4	27.9
	54.5	1860	51.4	0.0006	-0.42	52.2	27.6	28.1
	55.5	1837	46.2	0.0003	-1.96	42.6	25.1	23.2
	58.0	1793	46.1	0.0004	-1.60	49.0	25.7	27.3
	58.5	1784	50.6	0.0013	3.20	44.9	28.4	25.2
	58.7	1782	49.2	0.0030	1.07	47.3	27.6	25.5

TABLE 5.3

CHAPTER 6 DISCUSSION

In the results section the data was interpreted in three different ways. To summarise, these were:

Analysis (A): A least squares analysis of the log D vs 1/T data assuming a single Arrhenius-type relation holding over the temperature range in which measurements were made.

Analysis (B): A least squares analysis of the same data but for a given composition assuming two separate linear relationships, each describing a dependence over two consecutive temperature ranges, and

Analysis (C): A third analysis, again assuming two linear relationships, but suggesting that the dependences derived for each composition bear some progressive relationship one to another.

6.1 ANALYSIS (A)

The relationships calculated from analysis (A) for each composition, are shown collectively in Figs. 5:10, which presents the data for all the aluminium-rich compositions; Fig. 5:17 shows the data for all the nickel-rich compositions. In order to provide continuity the figures for the stoichiometric composition have been included in both graphs.

In the light of the suggestion made by Cooper (1963A), that there is limited substitution of aluminium for nickel in aluminium-rich alloys (see Section 2.4.2), a change in the diffusion behaviour at this limit might be expected. Fig. 5:10 shows that there is such a change between compositions 49.2 and 49.0 at. % Ni, which is in agreement with Cooper's suggested limit of substitution between 49.5 and 48.5 at. % Ni.

This change in diffusion behaviour from the substitution alloys to the defect aluminium-rich alloys takes the form of marked reduction in the activation energies, which are reflected in Figs. 5:10 and 5:17 by the slopes. Such a reduction is to be expected providing the mechanism involves vacancies, since the constitutional vacancies in the aluminium-rich compositions significantly increase the overall vacancy concentrations in these alloys.

The difference between the values of D for the stoichiometric composition and for 49.2 at. % Ni alloy (the latter being the only aluminium-rich composition studied here which exhibits a substitutional defect structure) is contrary to what might be expected. It would seem reasonable to expect any form of disordering of the ordered stoichiometric structure to have the effect of enhancing diffusion since such small degrees of local disorder would more readily permit atomic movements. This would be true for most of the diffusion mechanism that are likely to apply to these alloys (see Sections 2.2 & 6.4). In fact Fig. 5:10 shows that, except at very low temperatures, the stoichiometric alloy exhibits the higher value of D.

The argument that the disordering associated with the non-stoichiometric substitutional defect should have the effect of increasing D is, however, supported by the data for the nickel-rich alloys (Fig. 5:17 & 5:18). With the exception of the isolated values for the extreme nickel-rich compositions, these results show that D increases progressively, at any one temperature, with increasing departure from stoichiometry. This is to be expected since the degree of disorder would increase with the increase in substitutional defect concentrations and departure from stoichiometry. The minor discrepancies amongst the data for the three most nickel-rich compositions cannot be considered surprising on

studying the data scatter from which the temperature dependences were calculated (Figs. 5:14, 5:15 & 5:16).

The composition dependences at all the temperatures at which diffusivities were measured are shown collectively in Fig. 5:18. They further illustrate features which have already been mentioned, namely:

a) that D increases with departure from stoichiometry, except in aluminium-rich alloys at high temperatures,

b) that the formation of constitutional vacancies in these aluminium-rich alloys has the expected effect of enhancing diffusivities, but only at low temperatures, and

c) that the uncertainties in the form of the derived temperature or composition dependences arise from the considerable data scatter, especially for the most aluminium-rich compositions.

A comparison between the results from this study and those of Berkowitz et al (1954), who studied cobalt diffusion in NiAl compounds (see Section 2.5.3), reveals that D from both studies are of the same order of magnitude. However, the composition dependences of D from the study of Berkowitz et al show minima at the stoichiometric composition at all temperatures; a feature which is only exhibited by the lower temperature results of this study (Fig. 5:18). This discrepancy between the two studies originates from the unexpected decrease in D with departure from stoichiometry shown by the high temperature data of this study.

A theory of substitutional diffusion in an ordered phase, presented by Kikuchi & Sato (1964), and supported by, amongst others, the study of Berkowitz et al, predicted an inverse cusping in these composition dependences, which converge on the stoichiometric composition. This study only shows a true cusping, minimising at the stoichiometric composition, for the 1000°C dependence. However it is of

interest that no such inverse cusping has been found amongst the data for the comparatively more accurate studies in AgMg (Hagel & Westbrook 1965: Domian & Aaronson 1964).

6.2 ANALYSES (B) & (C)

While carrying out the least squares treatment of analysis (A) on the results for nickel-rich compositions, it became obvious that, in general, standard deviations were negative at either extreme of the temperature range over which measurements were made, and positive over the middle of this temperature range. Such behaviour can be taken as evidence of some degree of curvature in the D vs 1/T plots. Furthermore, visual examinations of the data, and the least squares lines drawn through them from analysis (A), clearly indicate the possibility of curvature, (see Section 5.9). Consequently the data for these nickel-rich alloys were accordingly treated by analyses (B) & (C).

The data for the stoichiometric and aluminium-rich compositions was not treated by analyses (B) & (C), either because there was not detectable curvature (Figs. 5:8 & 5:9), or because the data was considered to be insufficient to justify such a treatment (Figs. 5:5, 5:6 & 5:7).

No previous study in intermetallic compounds has been interpreted in terms of curvature in the log D vs 1/T plots. However, an examination of the published results of these studies reveals that there is evidence of curvature in the following systems:

a) NiAl, 49.4 at. % Ni (Berkowitz et al 1954), although the data in this case in insufficient.

b) AgMg, three compositions (Hagel & Westbrook 1965). Here curvature has been ignored on the grounds that it arose

from the two lowest temperature measurements only; a declaration which cannot be considered valid (see Fig 6:1, after Hagel & Westbrook 1965). An earlier study (Hagel & Westbrook 1961) showed only limited evidence in the 52.0 at. % Mg composition. The studies of Domian & Aaronson (1964 & 1965) indicate only limited evidence of curvature.

c) AuCd (Huntington et al 1961: Gupta 1961).

d) CuZn (Kuper et al 1956).

In the latter two cases the curvature has been attributed to the effects of ordering changes as the critical transformation temperature was approached. No such transformation is known to occur in the remaining systems, (see Section 2.4.3).

The existence of curvature in the log D vs 1/T plots for intermetallic systems cannot at present be established or disproved. No study has yet generated detailed, accurate data, and over a sufficiently wide temperature range, to justify firm conclusions concerning this curvature. However, curvature can arise from effects other than true 'anomalous' diffusion behaviour, namely:

a) Small grain sizes, and

b) Excessively high dislocation densities.

Grain boundary diffusion contributions to the measured volume diffusion (see Section 2.3.1) in this study is not considered responsible for the observed curvature. Autoradiography (see Section 3.2.4) could have provided proof of the absence of boundary effects, but suitable facilities were not available. Nevertheless it is considered significant that the values of D, which were high compared to the least squares dependences, did not correspond to specimens of small grain size. Nor was there any evidence of non-linearity in the log I vs x^2 penetration plots (as distinct from specimen

oxidation effects, see Section 5.4), which generally characterise grain boundary contributions.

It has been shown by Le Claire (1965) that, in general, dislocation densities in excess of $10^{10}/cm^2$ are required before a significant contribution to the measured volume diffusion can be expected. On the basis of studies which have been made in f.c.c. metals it is generally assumed that a well-annealed metal will not have densities in excess of $10^6/cm^2$. The studies of dislocation behaviour in NiAl (Ball & Smallman, 1968) and the deformation work by Pascoe (1966) indicate that excessively high dislocation densities are very unlikely in annealed and slowly cooled alloys. Therefore it is not considered likely that the curvature observed in this study arose from dislocation contributions.

On the assumption that this curvature is in fact representative of the diffusion behaviour, it would be reasonable to interpret the data in terms of true 'anomalous' diffusion: hence analysis (B). This analysis was unsatisfactory, essentially because of insufficient results on which to base two separate least squares treatments. The analysis generated two series of values of the activation energy (Q) which did not show the expected agreement with empirical relationship, $Q = 34T_s$ (see also Sections 5.9 & 6.3). For this reason analysis (C) was carried out, assuming that a simple proportionality between Q and T_s exists for each of the two separate temperature ranges.

The significance of the three sets of results generated by the three separate analyses appear in subsequent sections in which the values of activation energies, entropies and Gibb's free energies of diffusion are discussed.

6.3 THE ACTIVATION ENERGY

6.3.1. Proportionality Between Q and T_s

The empirical relationship, $Q = 34T_s$, is generally found to be a good approximation, to within 20% (see Section 2.3.10). Such a correlation is to be expected since both Q and the T_s are related to the binding energy between atoms. The notable exceptions are those systems which exhibit 'anomalous' diffusion, in which case the value of Q derived from the low temperature data generally falls below the empirically expected value, (see also Sections 2.3.10, 2.3.12 and 6.3.3).

In this study the activation energies predicted by the empirical law are generally in reasonable agreement with those obtained from analyses (A), (B) & (C) of the experimental data. However, the agreement is not good, more especially in connection with analysis (B), showing variations as large as 25% in some cases (see Tables 5.1, 5.2 & 5.3).

The results from analysis (A) shown in Table 5.1 indicate an average proportionality constant of 33 $\pm$ 17%, for the stoichiometric and all the substitutional compositions. An average value of 25 $\pm$ 6% was indicated for the three remaining aluminium-rich compositions. This apparent discrepancy for these defect structure alloys is considered reasonable since the empirical law was established with reference to normal vacancy concentrations. In other words the constitutional vacancies, producing an excess vacancy concentration in these alloys, have the effect of lowering Q, and hence the proportionality constant.

It is felt that no significance can be attached to the poor agreement between the empirically predicted values of Q and those produced from analysis (B); the inaccuracies preclude detailed discussion. Suffice to note that the

consistently low values generated for the low temperature range are in agreement with accepted 'anomalous' diffusion behaviour.

As might be expected from the manner in which analysis (C) was carried out, the agreement found in this instance was higher than for the results of analysis (B). The agreement was good for the higher temperature range. For the lower temperature range an average value of approximately 27 was calculated, being consistent with 'anomalous' diffusion behaviour.

These results indicate that a single activated process could be responsible for diffusion in all compositions of the compound. If this were true then the value of D at the solidus temperature can be written:

$$D_s = D_o \exp(-Q/RT_s) \qquad (6.1)$$

It follows that, if a plot of log D_o vs Q/T_s for all compositions were linear, D_s would be constant and the slope would have a constant value of 0.22 (i.e 1/2.303 R). This relationship, suggested by Paxton & Wolfe (1964), holds true for a number of b.c.c. systems: for example Peart & Tomlin (1962) have shown it to apply for niobium diffusion in the titanium-iron system; it also applied to zirconium and niobium diffusion in zirconium (Federer & Lundy 1963), and to chromium diffusion in the titanium-chromium system (Mortlock & Tomlin 1959).

A graph of log D_o vs Q/T_s, drawn from the results of analysis (A), is shown in Fig. 6:2. The indications are that both the aluminium-rich and the nickel-rich results are best described by straight lines. These have been drawn by the least squares method, giving slopes of 0.28 $\pm$ 3% and 0.26 $\pm$ 10% respectively. A least squares analysis of both

sets of results gives a slope of 0.30 ± 8%. The difference between this figure and those representing each side of stoichiometry could be indicative of different activated processes for each set of alloys. The values of D_s, calculated from the intercepts, are all of the order of 10^{-10} ± 50% cm^2/sec, which is much smaller than the expected value of 10^{-7} cm^2/sec.

Graphs of log D_o vs Q/T_s, using the results from analysis (B) & (C) for nickel-rich compositions, are shown in Figs. 6:3 & 6:4 respectively. A least squares analysis for the high and low temperature data together, for each graph, yields slopes of 0.28 and 0.30 respectively. The fact that there is no significant difference between these slopes indicates that, if diffusion in these alloys is 'anomalous', a similar activated process is responsible for diffusion over the whole temperature range. The values of D_s are again of the order of 10^{-10} cm^2/sec.

However it could be considered that, within experimental error these plots (Figs. 6:2, 6:3 & 6:4) are linear; this implies constancy of D_s. From equation 6.1 we can write:

$$\ln D_s = \ln(\gamma a^2 f \nu) + \Delta S/R - Q/RT_s$$

$$= \ln(\gamma a^2 f \nu) - \Delta G/RT_s$$

Since γ, a, f and ν can be considered constants within one system, constancy of D_s means constancy of $(\Delta G/RT_s)$, i.e:

$$\Delta G = C T_s$$

where C is a proportionality constant. Gibbs (1963A & B) has shown that in systems in which the empirical relationship,

$Q = 34T_s$, breaks down, a constant proportionality between ΔG and T_s was still valid.

In this study it has been possible to make an estimate of ΔG using the calculated values of Q, which has been assumed equal to ΔH, and an approximation for ΔS by means of the equation:

$$\Delta G = \Delta H - T\Delta S$$

Values of ΔS were estimated using the calculated values of D_o (see Section 5.8), in the equation:

$$D_o = \gamma a^2 \nu \exp(\Delta S/R)$$

(see Section 2.3.10, equation 2.14). For this calculation it was necessary to assume that:

a) the values of lattice parameters (a) measured by Bradley & Taylor (1937),

b) the vibration frequency (ν) was equal to the Debye frequency in nickel (9.53×10^{12}/sec: Gibbs 1963A),

c) the correlation factor (f) was unity.

The results of these calculations for each of the three analyses, (A), (B) and (C), are shown in Tables 5.1, 5.2 & 5.3 respectively.

In summary they show that where constancy of Q/T_s breaks down, the values of $C = \Delta G/T_s$, although not constant, do not show so pronounced a variation one to another. In view of the number of assumptions that were made in order to calculate ΔS, and the inaccuracies in the measured values of D_o, it is considered likely that these variations in C arise from experimental inaccuracies. The most that can be said therefore is that a higher degree of constancy is exhibited by C than by Q/T_s. Unfortunately there is insufficient data on

which to base more definite conclusions.

6.3.2. The Compositional Dependence of Q

The form of the compositional dependence of Q in intermetallic compounds is a subject on which a great many experimentally substantiated but differing conclusions have been presented. This is true of several studies made of CsCl-type crystals, including NiAl (see Section 2.5.3). In an attempt to predict the form of such a dependence Domian & Aaronson (1964 & 1965) calculated theoretical values of Q as a function of composition, using AgMg as a model for the CsCl intermetallic compounds. For this calculation the unit jump process was assumed to be the six-jump cycle and not the nearest-neighbour vacancy-atom interchange. The validity of this assumption, and a discussion of the applicability of the six-jump cycle mechanism to diffusion in intermetallic compounds is discussed in Section 6.4.

The theoretical development required a quantitative knowledge of the summed enthalpies of vacancy formation (ΔH_f) and motion (ΔH_m), for both silver and magnesium, in 'disordered' AgMg. No experimental values are available for these quantities since AgMg is ordered up to its melting temperature. Domian & Aaronson used an empirical scaling rule to estimate these enthalpies, using data from the isomorphous compound CuZn containing 48 at. % Zn; for example, for magnesium in 'disordered' AgMg:

$$(\Delta H_f + \Delta H_m)_{Mg}/(T_m)_{AgMg} = Q_{Zn}/(T_m)_{CuZn}$$

and similarly for silver. However, published works (summarised by Hagel 1967) indicate a strong tendency for diffusivities in zinc containing compounds to be abnormally

high, with correspondingly low values of Q; they should not therefore be used as standards for other systems. On these grounds the procedure adopted by Domian & Aaronson (1964 & 1965) may not be valid.

However their development enabled them to make theoretical calculations of both magnesium and silver diffusivities. From these, assuming an Arrhenius type temperature dependence, theoretical values of Q were obtained for each of three different possible paths of the six-jump cycle mechanism.

With respect to the present study one of the most significant findings of this theoretical treatment was the prediction that Q should increase with temperature. This gives very strong support for the existence of curvature exhibited in some of the ln D vs 1/T plots from the present study (see Section 5.9). Domian & Aaronson, who did not consider that their experimental work supported such behaviour, modified their theoretical Q values to average values.

The theoretical model predicted a linear variation of these average values of Q with increasing departure from the stoichiometric composition. This was in agreement with experimental data for AgMg. The theoretical values were, however, some 7% lower than the experimental figures, which was not considered surprising in view of the approximations on which the heuristic model was developed.

This theoretical development is particularly relevant to the present study. It is however more relevant to the nickel-rich than to the aluminium-rich compounds, since the former have the same substitutional defect structure as the AgMg compounds. The values of Q, generated from analysis (A) (Figs. 5:19 & 5:20), indicate a linear dependence with composition for nickel-rich compositions, which is in

agreement with both the experimental and theoretical results for AgMg (Hagel & Westbrook 1961 & 1965: Domian & Aaronson 1964 & 1965). However insufficient accuracy in the present values of Q have not permitted this linearity to be established beyond question.

The results for aluminium-rich compositions show a marked decrease in Q beyond Cooper's limit of substitution at 50.8 at. % Ni (Figs 5:19 & 5:20). Since this study included only one composition within Cooper's limit it has not been possible to confirm the linearity predicted for these substitutional aluminium-rich alloys. For compositions beyond Cooper's limit there is, unfortunately, insufficient data to determine the form of the composition dependence with any confidence. There seem to be two possibilities: either the rate at which Q falls with increasing aluminium content gradually decreases so that in the limit Q becomes constant, or that this decrease is linear until a 'plateau' of Q values is reached. These two possibilities are illustrated in Fig. 5:19. In either case the suggestion is that for the extreme aluminium-rich compositions Q is constant.

Comparing these results with those of Berkowitz et al (1954 & Fig. 5:20), several distinct differences emerge:

a) the value of Q for the stoichiometric composition is some 10% lower than that reported by Berkowitz et al,
b) for nickel-rich alloys the decrease in Q from this stoichiometric composition is less rapid in the present study,
c) for aluminium-rich alloys the prediction of Berkowitz et al that a 'plateau' of Q values extends to the stoichiometric composition is incompatible with the more detailed results from the present study, and
d) that this 'plateau' value may be as much as 20% lower

than that suggested by Berkowitz et al.

For these aluminium-rich compounds the behaviour postulated by the present study is considered the more valid in view of the defect structural changes that occur in the region of Cooper's limit. The behaviour also supports a theory that a vacancy mechanism is responsible for diffusion in these alloys (see also Section 6.4).

6.3.3. Activation Energies and 'Anomalous' Diffusion

The suggestion of possible 'anomalous' diffusion behaviour for nickel-rich alloys in this study (see Sections 5.9 & 6.2) has generated two values of Q for each composition. The variation of these Q values with composition, from analyses (B) and (C), are shown in Figs. 5:24 & 5:25 respectively. The reduced accuracy with which these Q values were calculated, arising from the division of the data into two separate temperature ranges, precluded a meaningful mathematical treatment of their variation with composition. Suggested dependences are shown in Figs. 5:24 & 5:25.

Bearing in mind that inaccuracies may render a detailed consideration of these dependences suspect, two general features are indicated:

a) the high temperature values of Q are approximately 30% higher than those calculated for the lower temperature range, and

b) the low temperature values could be independent of composition.

In view of the suspicion of 'anomalous' diffusion behaviour in this study it is felt that a comparison between the characteristics of 'anomalous' diffusion now established in other systems and those of this study would be of value. It has now been established that curved 'Arrhenius' plots do describe diffusion in certain b.c.c. systems. For example,

self diffusion in β-zirconium (Federer & Lundy 1963), β-titanium (Murdock et al 1964: Gibbs et al 1964), γ-uranium (Rothman et al 1960: Peterson & Rothman 1965) and in vanadium (Peart 1965: Lundy & McHague 1965). The characteristics of 'anomalous' diffusion are now well established and can be summarised as:

a) positive curvature in lnD vs 1/T plots,

b) the values of Q and D_o derived from the higher temperature data are generally of the same order of magnitude as those of 'normal' diffusion (see Section 2.3.10), and

c) abnormally low values of Q and D_o typify the lower temperature behaviour (see Sections 2.3.12 and 5.9).

Analyses (B) and (C) in this study indicate 'normal' values of Q and D_o, within the experimental error, over the higher temperature range, consistent with 'anomalous' behaviour. Furthermore the calculated values for the lower temperature range are abnormally low. These values of Q, however, were not low by as much as the factor of two which is common for 'anomalous' diffusion. The values of D_o are nearly all between two and four orders of magnitude smaller than would be expected of 'normal' diffusion, which again is consistent with 'anomalous' diffusion characteristics (see Tables 5.2 & 5.3).

It has been suggested (Tiwari & Sharma 1967) that 'anomalous' diffusion behaviour in β-zirconium, β-titanium and in γ-uranium could be due to anomalous temperature dependences of the elastic constants. This suggestion was based on Zener's theory of the entropy of diffusion (see Section 2.3.11) and the observation that most of these b.c.c. metals exhibited an anomalous elastic constant change with temperature. Furthermore it seemed that the temperature at which the two anomalies occurred were synonymous in each

metal, as far as could be determined from the data.

Tiwari & Sharma (1967) have proposed an explanation of the negative entropies associated with most 'anomalous' diffusion behaviour. They showed that the anomaly in elastic constant behaviour gave rise to a positive value of β (see equation 2.15, Zener's equation, in Section 2.3.11) close to the temperature of the anomaly; this in turn gave rise to negative values of ΔS. They, like Dienes (1953, see also Section 2.3.12), postulated two components of ΔS, a formation entropy (ΔS_f), and a migrational entropy (ΔS_m) which could be negative. It follows that ΔS can therefore be negative when ΔS_m is negative and is greater than ΔS_f.

Support for a suggestion of 'anomalous' diffusion behaviour in NiAl would clearly be implied if the compound exhibited anomalous elastic constant behaviour. Such behaviour has been observed in certain intermetallic compounds whose ordered phases are isomorphous with NiAl, namely in: CuZn (Artman 1952), AuCd (Zirinski 1956) and TiNi (Wasilewski 1965). However these anomalies occur as the temperature of their diffusionless transformation to lower-symmetry structures is approached. This behaviour has been explained as inidative of low stability of the CsCl structure in these compounds (Zener 1947). No anomalous elastic constant behaviour was observed in a compound of NiAl containing 49.4 at. % Ni (Wasilewski 1966). This can be taken as further evidence of the stability of the CsCl structure in this compound. It also implies that 'anomalous' diffusion behaviour in NiAl, at least of this composition, would not be expected. It might therefore be considered significant that the present study indicates no evidence of curvature in the ln D vs 1/T plot for an alloy of this composition (see Fig. 5:8).

Since this data on elastic constants in NiAl is limited to only one composition the values of ΔS from the present study have been plotted against Q/T_s to test the constancy of β - the temperature dependence of the elastic constant (see Section 2.3.11). It is however more conventional to plot ΔS vs Q, but this would only be valid for systems in which T_m is constant; in this study the values of T_s, which replace T_m, are of course not constant. Figs. 6:5, 6:6 and 6:7 show the three graphs generated from analyses (A), (B) and (C) respectively, and serve to illustrate how sensitive the calculations of ΔS were to experimental inaccuracies. It is therefore considered that it might be fallacious to draw any firm conclusion from this doubtful data. However a general feature of these graphs is the absence of strong evidence of non-linearity. Thus there is no real evidence for non-constancy of β.

It remains a possibility that diffusion in NiAl is not 'normal'. The fact that the evidence of 'anomalous' behaviour could be due to effects other than true 'anomalous' diffusion has already been discussed in Section 6.2. It is not felt likely that these effects - of grain boundaries and high dislocation densities - are significant. Thus on the basis of the available information it is concluded that 'anomalous' diffusion probably occurs in NiAl.

An attempt has been made to interpret 'anomalous' diffusion in terms of two separate mechanisms. Kidson (1963) suggested that low Q and D_o values could be identified with the migration of vacancy-impurity pairs, or 'extrinsic' vacancies, instead of thermal or 'intrinsic' vacancies. Since the latter type exist in greater quantities at higher temperatures this hypothesis has been used to explain 'anomalous' diffusion behaviour predominating at lower temperatures; at higher temperature values of Q and D_o

approach those of 'normal' diffusion.

An important possibility arises from considerations of the Kidson effect; namely that variations in impurity contents could generate inaccuracies in D since such variations would be reflected in the concentrations of 'extrinsic' vacancies. In support of this suggestion Murdock (1965) has found that for titanium self diffusion, the lower the impurity level the lower the value of D.

6.3.4. A Comparison of Activation Energies

The limited previous studies of self diffusion in NiAl have already been discussed and the values of Q were compared with those from this study earlier in this chapter. However, a considerable number of predictions of Q have been made as a result of mechanical deformation studies in these compounds, and these will now be discussed.

It is generally considered that the mechanism of deformation in NiAl compounds above 0.4 T_s ^{o}K is controlled by the climb of edge dislocations (Pascoe 1966: Vandervoort et al 1966: Ball & Smallman 1968). Since climb depends upon self diffusion, the activation energy for deformation in this temperature range has been compared with the activation energy measured from self diffusion studies. Fig. 5:20 shows that fair agreement exists between the two sources of Q values, which supports the mechanistic theory of deformation in these compounds. Ball & Smallman (1968) measured Q for the collapse of dislocation loops (see Fig. 5:20), which, since they were close to those of self diffusion, were interpreted as confirmation that a diffusion controlled process of dislocation climb governed the high temperature deformation in NiAl. The other values of activation energy for deformation, shown in Fig. 5:20, have been discussed in Section 2.5.3.

The absence of perfect agreement between some of the deformation values and those from self diffusion studies (Fig. 5:20) could arise from the fact that Q measured from deformation studies will represent Q for the diffusion of the slower species. This must be true since the diffusion of both constituent elements would be necessary before dislocation climb could occur. If aluminium is the slower diffusing species in NiAl then this suggestion might explain why some of the Q values from deformation studies tend to be higher than those from this study. In support of this postulation are the size factor and that in the isomorphous compound AgMg Domian & Aaronson (1965) found that the ratio of Q(Mg)/Q(Ag) was experimentally greater than unity.

6.4 THE MECHANISM OF DIFFUSION IN NiAl

A brief description of the various mechanisms of diffusion that are most common in metallic systems can be found in Section 2.2. This survey also included some of the less common mechanisms since they are relevant to this discussion.

It is perhaps true to say that no single experiment can ascertain the mechanism of diffusion in a given system but rather that it is deduced, by a process of elimination and confirmation, from the results of many different experiments. Diffusion mechanisms are generally deduced from a number of specific characteristics of diffusion behaviour; most of which have been summarised by Birchenall (1961) and are very briefly outlined below:

a) Diffusion usually occurs by that mechanism which requires the least energy.

b) Diffusion tends to occur by the motion of those defects present in greatest concentrations.

c) The Kirkendall effect (Section 2.2.3) is indicative of vacancy diffusion.

d) Measurement of the correlation factors limit the choice of mechanism.

e) Comparisons between experimentally measured frequency factors and those deduced theoretically can confirm assumed mechanisms.

f) Anisotropic diffusion behaviour may require the postulation of two types of jump without necessarily limiting the mechanism.

g) In ordered binary systems support for the six-jump cyclic mechanism is found if the ratio of the constituent diffusivities lies within a critical range.

The deduction of the diffusion mechanism in NiAl relies largely on evidence that has been generated from diffusion studies in compounds which are isomorphous with NiAl. These compounds, for example AgMg, CuZn and AuCd, were naturally chosen for more exhaustive studies since they have fewer associated experimental problems than NiAl.

For well-ordered binary alloys with a CsCl structure, which can be regarded as two interpenetrating simple cubic lattices populated exclusively by one constituent element, Slifkin & Tamizuka (1955) suggested that the diffusivities of each species should be equal. This prediction was based on the assumption that the unit process of diffusion was the nearest-neighbour vacancy-atom interchange, in which case the migration of a particular vacancy should involve an equal number of jumps with each species. Lidiard (1957) criticised such vacancy motions on the grounds that order would be disturbed, which would not satisfy the equilibrium

requirements of the alloy. Consequently mechanisms were sought which would allow vacancy motion without loss of order. Huntington et al (1961) first proposed certain cyclic motions of vacancies which are now collectively referred to as six-jump cycles. An example of such a cycle is shown in Fig. 2:2, which indicates how a vacancy makes six jumps, the net result of which is that two atoms of the same species exchange sites and one of the other species migrates across the cycle. On completion of the cycle there is no change in overall order of the lattice.

The inequalities between the diffusivities in such ordered binary systems was construed as an argument against a simple vacancy mechanism (Kuper et al 1956). However it is of interest to note that Slifkin & Tamizuka (1956) later showed that departure from perfect order could be solely responsible for this difference between diffusivities. This proposal was based on the assumption that, in non-stoichiometric alloys, the atom which jumps more readily would move preferentially when it was on a 'wrong' site. They substantiated this assumption by showing that in CuZn the ratio of the diffusivities converged to unity for perfect order.

The six-jump cycle was analysed by Elcock & McCombie (1957) and by Elcock (1958) who predicted that the ratio of diffusivities of the two constituent elements in a CsCl structure should fall within the limits of 2/3 to 3/2. In strong support of the postulation of such vacancy tracts this ratio has been demonstrated to hold for diffusion in the systems CuZn (Kuper et al 1956), AgMg (Domian & Aaronson 1965) and in AuCd (Huntington et al 1961).

Nevertheless proposals of six-jump cycles were made on the assumption that the unit process was a vacancy-atom interchange between nearest-neighbour sites. Flinn &

McManus (1961) have suggested that if next-nearest-neighbour jumps were the unit process then the approach to equilibrium long range order would be more rapid than if only nearest-neighbour jumps were permitted.

It may also be argued that since atoms in simple metals exchange by nearest-neighbour jumps, and that the constituents of some ionic crystals diffuse exclusively on their own sublattices (Lynch 1960 and Friauf 1962), diffusion in intermetallic compounds may occur by a combination of these types of behaviour (Hagel 1963) i.e. by divacancy migration.

Such considerations renewed speculation as to the dominant mechanism in ordered alloys and led Winblatt (1967) to consider these three most likely mechanisms in more detail. Using AgMg as a model he calculated theoretical energies of defect migration for the six-jump cycle, the next-nearest-neighbour jumps and for divacancy migration. These calculations involved the estimation of all the energy states between the constituent atoms and the migrating defects. In this way the total energy of migration for each mechanism was computed. For divacancy movements the necessary exchange between a vacancy on a silver site and a silver atom was not possible since the latter became trapped at the vacancy on the magnesium site. This restriction precluded the mechanism from further consideration because the divacancy would have to migrate in dipole configuration in order to contribute significantly to diffusion. Of the remaining two mechanisms considered the theoretical migration energies indicated very strong support for the six-jump cycle. Since the type of defect involved in each of these mechanisms was identical, namely the vacancy, it was reasoned that the energies of formation would be identical in each case. Since for both mechanisms the value of Q was assumed to be the sum

of the energies of formation and migration, Winblatt (1967) was able to predict that the vast majority of diffusion events would take place by means of a cyclic vacancy path.

For NiAl it could be argued that the very high ordering energy (indicated by a high heat of mixing) might preclude a six-jump mechanism on the grounds that the disordering associated with the first three jumps would not be allowed. Such an argument would favour the next-nearest-neighbour mechanism for this compound. However, Winblatt (1967) considered AgMg as his model, a compound which also exhibits strong ordering characteristics. Even if ordering is relatively stronger in NiAl than in AgMg it may not effect the migration energies sufficiently to favour the next-nearest-neighbour jumps. This supposition is supported by the results of Winblatt (1967) which predict that migration energies for the next-nearest-neighbour mechanism would be as much as 50% higher than those for the six-jump cycle.

The existence of constitutional vacancies in NiAl compounds with aluminium compositions in excess of 50.7 at. % indicates that aluminium atoms only substitute nickel atoms to a limited extent. This could be construed as an objection to the six-jump cycle in NiAl since there would presumably be an increased resistance to unit jumps which result in aluminium atoms residing on nickel atom sites. On these grounds an argument that a mechanism other than the six-jump cycle could be dominant in NiAl would be stronger for aluminium-rich alloys than for nickel-rich. Furthermore only the nickel-rich alloys exhibit the same defect structure as AgMg for which the theoretical calculations were carried out.

It is however very probable that the dominant mechanism in aluminium-rich compositions does involve the

migration of the constitutional vacancies. It can therefore be assumed that Q will be the sum of a vacancy formation and migration energy. It follows that in extreme aluminium-rich compositions the formation energy becomes negligible since the concentration of constitutional vacancies far exceeds that of thermal vacancies. Assuming this argument to be valid the 'plateau' value of Q described for these compositions (see Section 6.3.2 and Fig. 5:19) can be identified with the migrational energy. In which case the results of the present study indicate a migration energy between 40 and 46 Kcals/mole. The average of this range is 43 Kcals/mole, which is lower than the value of 56 Kcals/mole predicted by Berkowitz et al (1954). It is felt that more confidence can be attached to the figure from this study since it has been derived from more detailed data.

If E_m for the stoichiometric composition is assumed to be equal to this average value of 43 Kcals/mole, then the value of Q at this composition indicates a value for E_f of 30 Kcals/mole. This in turn would imply a value of 1.4 for the ratio E_m/E_f, in fair agreement with a value of 1.35 suggested by Wasilewski (to be published). The value of this ratio calculated from the data of Berkowitz et al (1954) is approximately 2.0. In most metallic systems the ratio does not exceed unity (Ball & Smallman 1968). The present study however has predicted a figure greater than unity, which is consistent with what appears to be a characteristic of compounds with a CsCl structure.

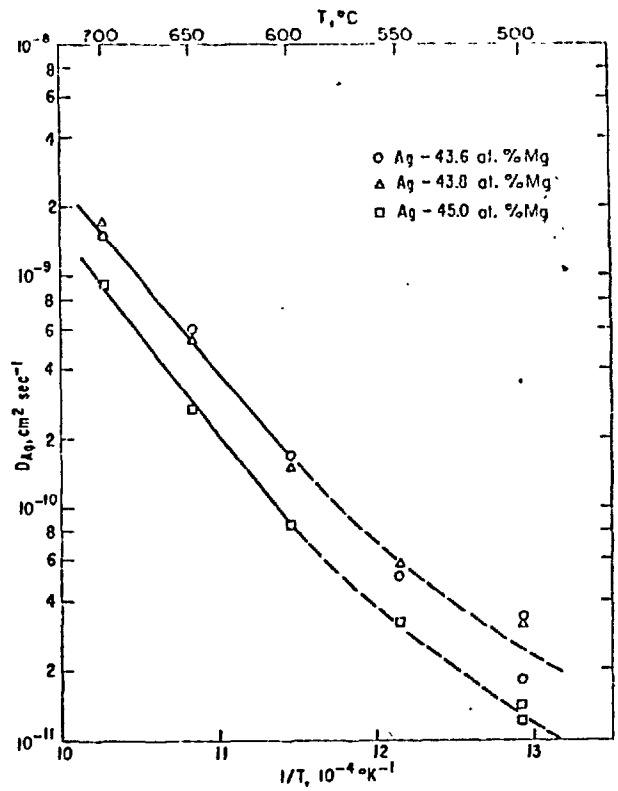

FIG. 6:1 SILVER DIFFUSION IN SILVER RICH AgMg
(AFTER HAGEL & WESTBROOK 1965)

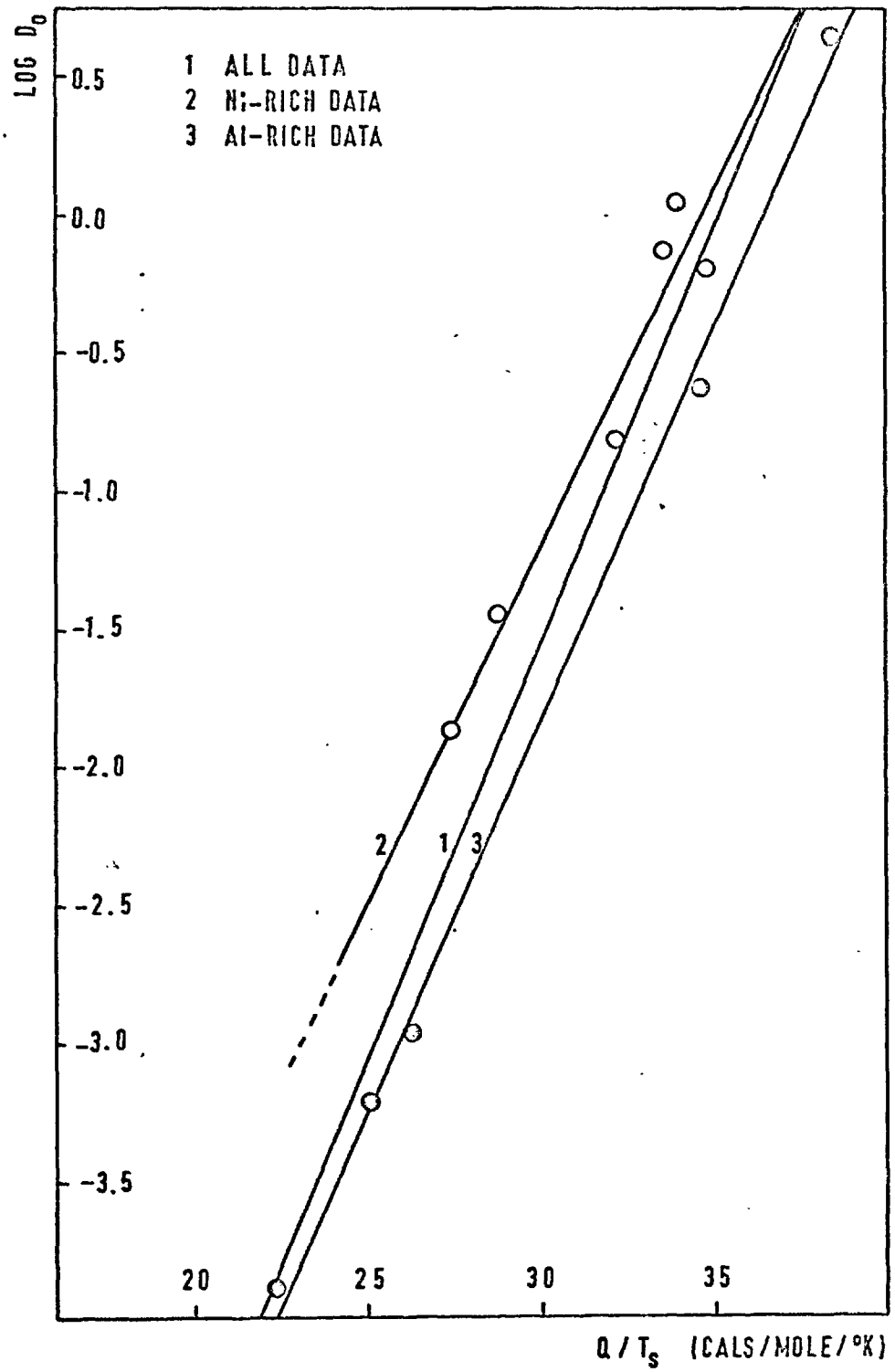

FIG. 6:2 ANALYSIS (A)

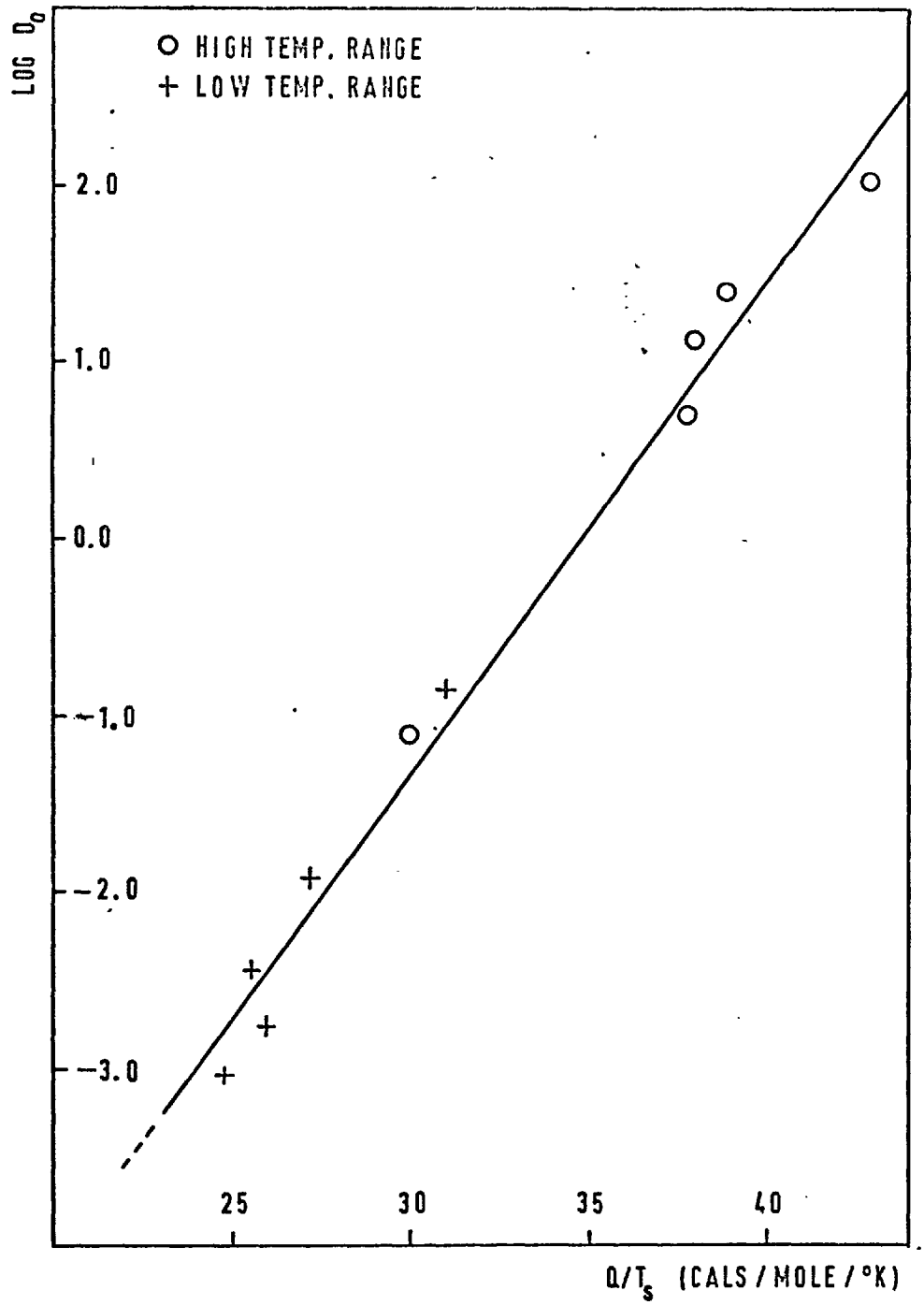

FIG. 6:3 ANALYSIS (B)

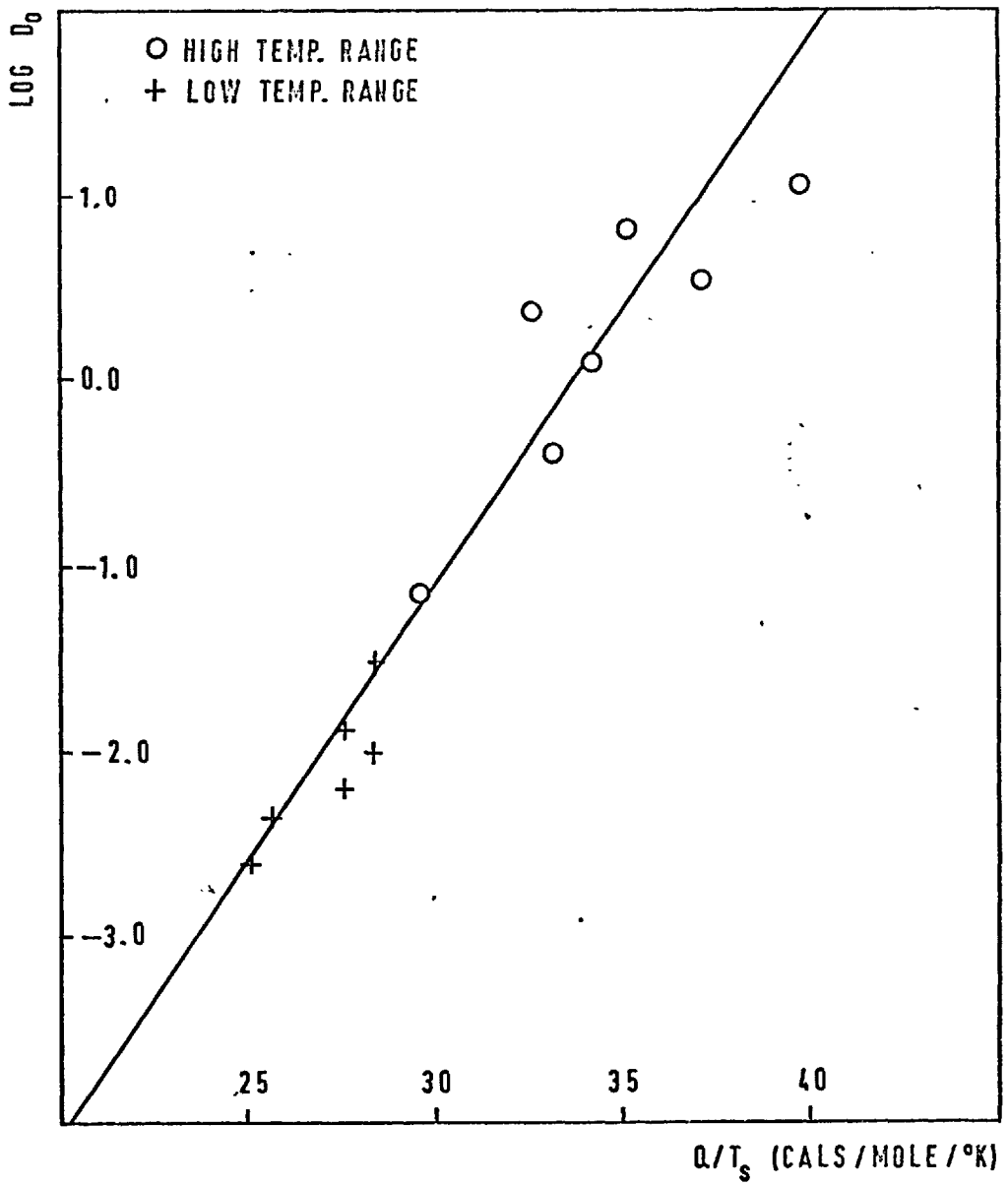

FIG. 6:4 ANALYSIS (C)

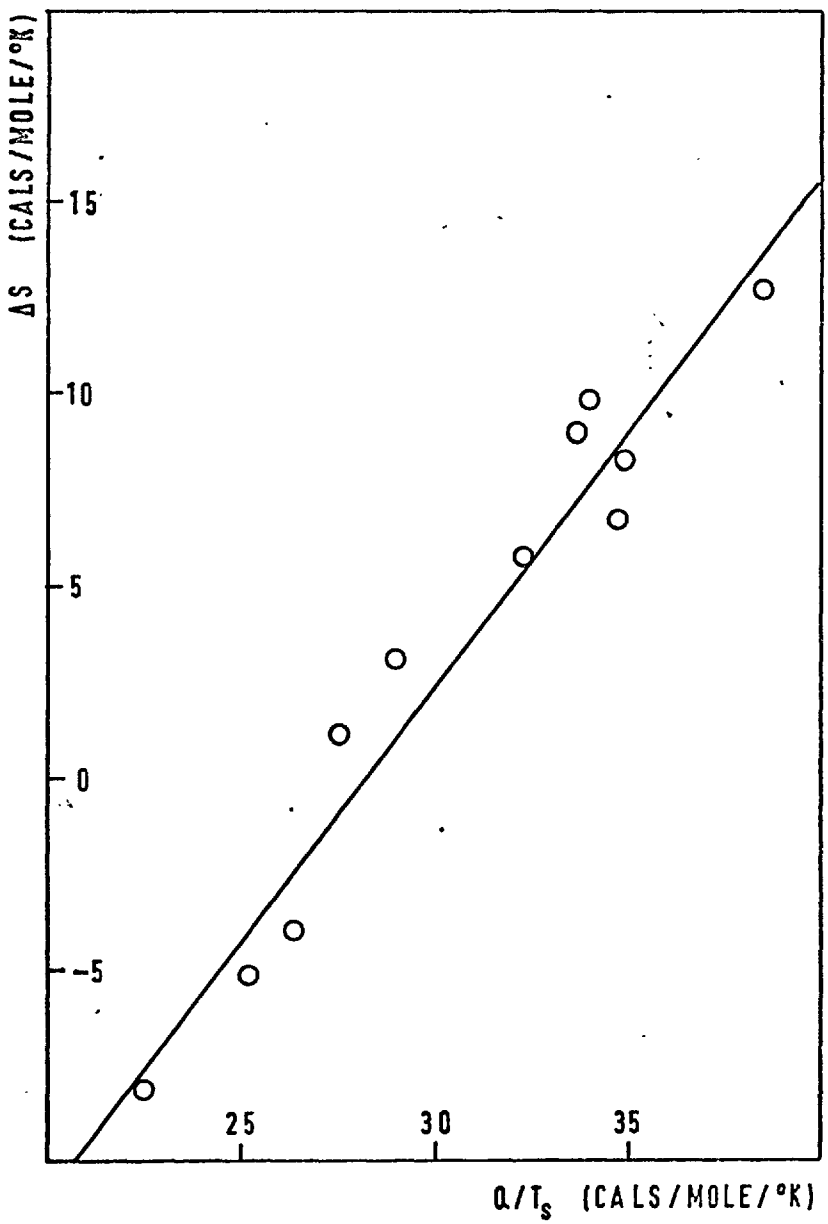

FIG. 6:5

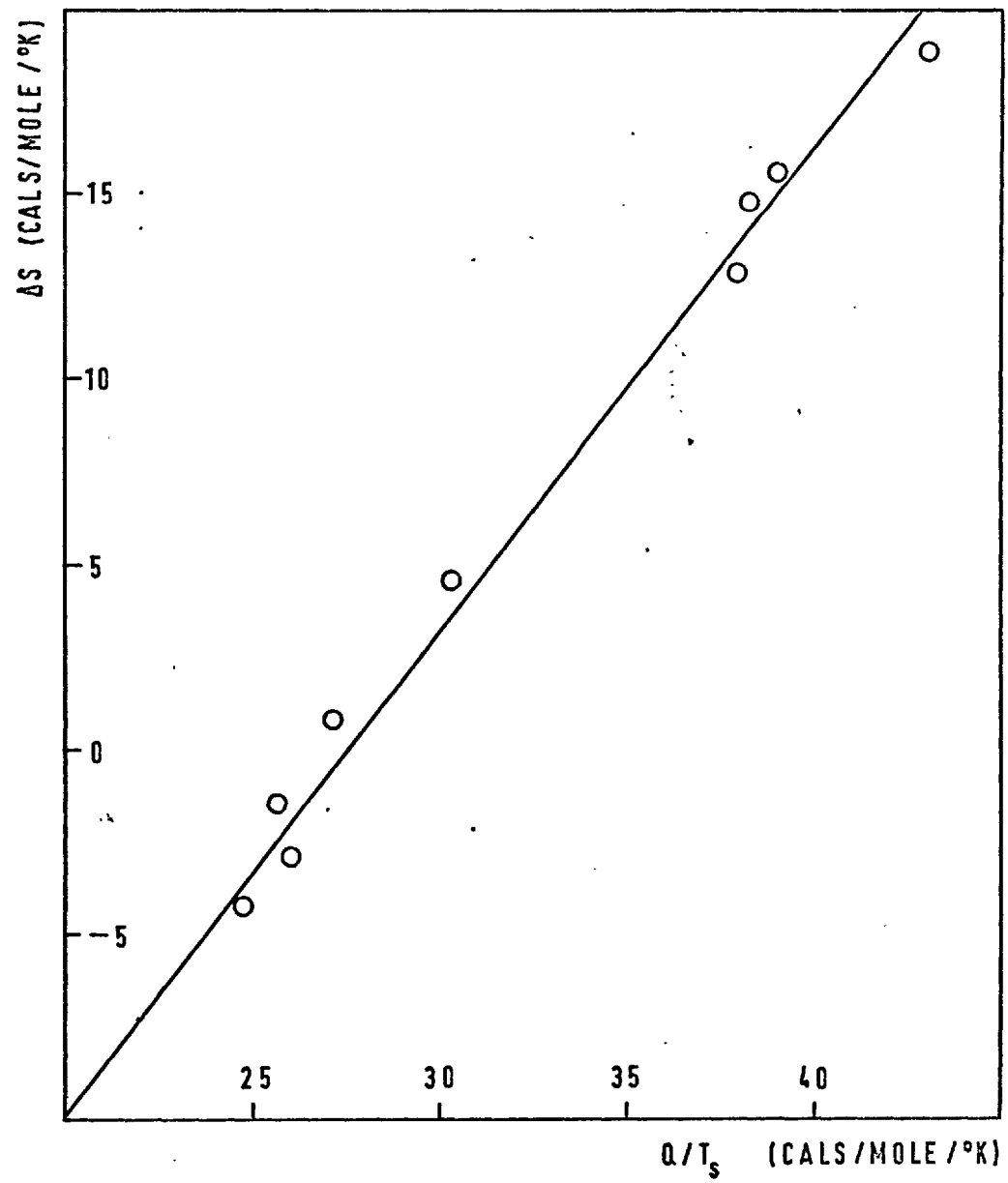

FIG. 6:6

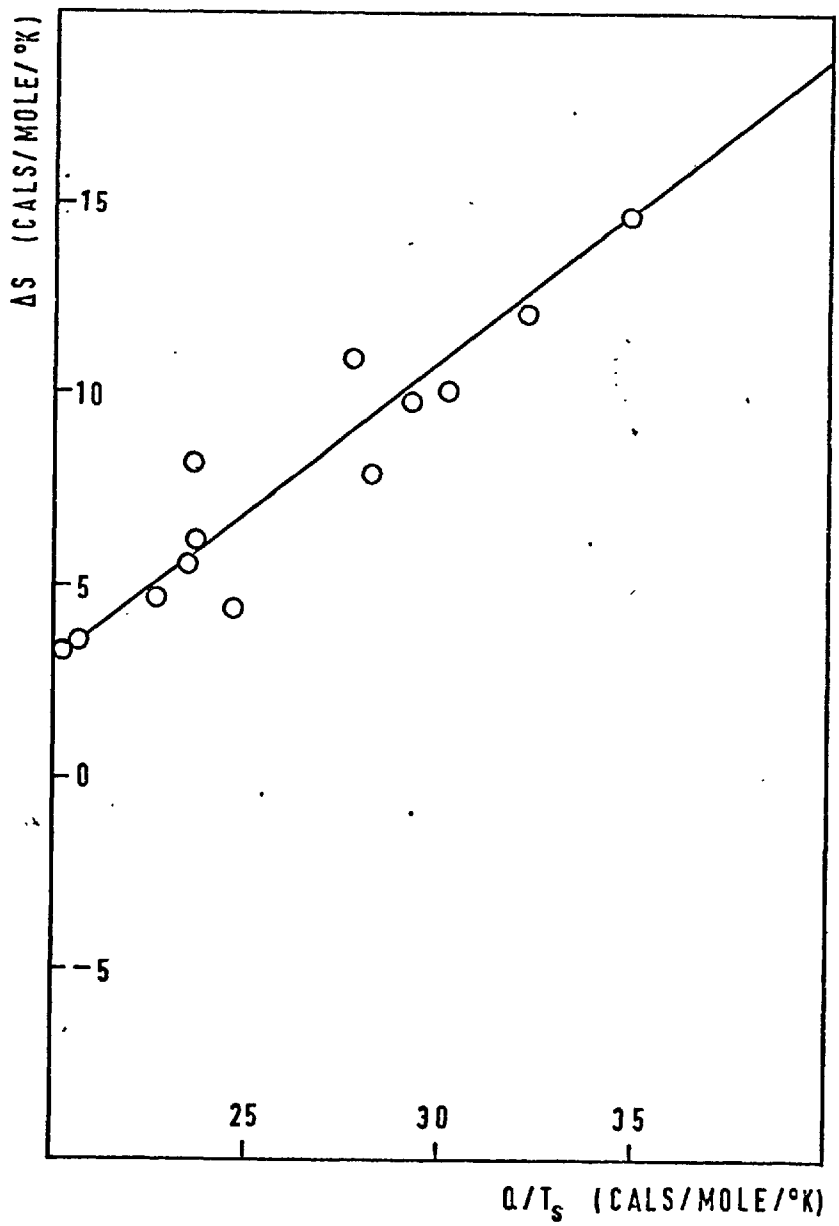

FIG. 6:7

CHAPTER 7 CONCLUSIONS AND SUGGESTIONS FOR FUTURE WORK

7.1 CONCLUSIONS

A modified Bridgman technique may be used to produce ingots of NiAl, of varying compositions, and with grain sizes large enough for self diffusivity measurements. A precasting technique was found necessary to control purity and composition.

It was found that high standards of atmosphere control were required in order to restrict specimen oxidation during the diffusion anneals. Such specimen oxidation causes severe loss of accuracy in self diffusivity measurements.

The results indicate that the log D vs 1/T dependences may be curved, in which case a simple Arrhenius-type relationship would not be applicable. The inaccuracies in the measured diffusion coefficients have not permitted the form of these dependences to be established beyond question. However, from the information available it is concluded that 'anomalous' diffusion behaviour probably occurs in nickel-rich compositions of NiAl. The results, interpreted in terms of 'anomalous' diffusion, were consistent with patterns of behaviour exhibited in systems in which 'anomalous' diffusion has been established.

A comparison of activation energies for self diffusion in aluminium-rich alloys has led to the conclusion that the mechanism of diffusion was by the motion of vacancies, and that the constitutional vacancies contribute significantly to diffusion. So much so that in extreme aluminium-rich compositions a 'plateau' of activation energies was indicated. The value of this 'plateau' was identified with the activation energy of motion of vacancies. It is

concluded that the mechanism of diffusion in NiAl is probably by six-jump cyclic vacancy tracks, which have been postulated for other intermetallic compounds with the CsCl structure.

The activation energies of self diffusion were consistent with the prediction that high temperature deformation mechanisms are governed by diffusion.

7.2 SUGGESTIONS FOR FUTURE WORK

In view of the fact that it has not been possible to establish beyond question that 'anomalous' diffusion occurs in NiAl, it is felt that a more exhaustive re-examination of nickel self diffusion might be of value. However, it does not appear that a sufficiently high degree of accuracy would be guaranteed, because of material handling difficulties, and that such a study might not therefore be justified. It is suggested that if this study were undertaken then it should initially be confined to one composition, preferably a non-stoichiometric nickel-rich alloy, and that the diffusion coefficient should be measured at frequent temperature intervals over as wide a temperature range as possible. If the accuracies in this initial study proved sufficient to establish either 'anomalous' or 'normal' diffusion behaviour, then clearly a study over the whole composition range would be justified in order to determine whether the same type of diffusion occurs in all compounds.

There appears to be both theoretical and experimental evidence that the activation energy of self diffusion in other isomorphous, intermetallic compounds is temperature dependent, implying that 'anomalous' diffusion occurs. This evidence has so far been ignored and the results interpreted

assuming 'normal' diffusion behaviour. It would clearly be of value to redetermine self diffusivities in AgMg, for example, paying particular attention to attaining high accuracies. Since AgMg does not have so many associated experimental difficulties as NiAl relatively greater accuracies should be guaranteed. If 'anomalous' diffusion behaviour were established, it should therefore be possible to determine whether two linear log D vs 1/T dependences describe the behaviour or whether the activation energy varies continuously with temperature, as indicated by theoretical predictions.

Finally it would clearly be of interest to determine aluminium self diffusivities in NiAl. The postulation of the six-jump cycle mechanism for diffusion in NiAl would be supported providing the ratio of the diffusivities was between 2/3 and 3/2. Furthermore any significant variation of this ratio with composition would imply a change in mechanism. Owing to both expense and experimental difficulties it is felt that the measurement of aluminium diffusivities in NiAl would be difficult to justify.

8. ACKNOWLEDGMENTS

The author would like to thank both his supervisor, Dr. C.W.A. Newey, and Dr. G.F. Hancock for their valuable advice and assistance throughout the investigation.

The provision of laboratory facilities in the Metallurgy Department by Professor J.G. Ball, and the financial support of the Ministry of Aviation, are also gratefully acknowledged.

9. APPENDICES

9.1 APPENDIX I : ERRORS IN DENSITY MEASUREMENT

ELEMENT	ELEMENT VALUE	ABSOLUTE ERROR	FRACTIONAL ERROR
W_A	1.50g	1×10^{-4}	0.67×10^{-4}
W_{PD}	0.13g	1×10^{-3}	
W_{PSD}	1.00	1×10^{-3}	
W_{SD}	0.90	$(2)^{\frac{1}{2}}\times10^{-3}$	
W_A-W_{SD}	0.60	4.6×10^{-4}	8.0×10^{-4}
$W_A/(W_A-W_{SD})$	3.00		$((8\times10^{-4})^2+(0.67\times10^{-4})^2)^{\frac{1}{2}}$
			8.0×10^{-4}g
$\rho_D(W_A/(W_A-W_{SD}))$			$((8.0\times10^{-4})^2\times2)^{\frac{1}{2}}$
i.e. ρ_S	6.00g/cc	7.0×10^{-3}	11.3×10^{-4}

W_A is the weight of specimen in air
W_{PD} is the weight of the pan in dibromoethane
W_{PSD} is the weight of both the pan and specimen in dibromoethane
W_{SD} is the weight of the specimen in dibromoethane
ρ_D is the density of dibromoethane
ρ_S is the specimen density

Thus the errors on an average density measurement will have an absolute error of 7.0×10^{-3}g or a fractional error of 0.11%.

9.2 APPENDIX II : ERRORS IN D MEASUREMENTS

ELEMENT	ELEMENT VALUE	ABSOLUTE ERROR	FRACTIONAL ERROR
W		1×10^{-4}	
WD	0.003 g	$(2)^{\frac{1}{2}}\times10^{-4}$	4×10^{-2}
WD^2	2.5×10^{-4} g^2	1.4×10^{-6}	5.7×10^{-2}
$D(WD^2)$	300.0×10^{-6}	2.0×10^{-6}	66×10^{-4}
I_n			15×10^{-3}
$\log I_n$	3.0	6.5×10^{-3}	
$D(\log I_n)$	1.0	9.2×10^{-3}	92×10^{-4}
t	370,800 sec.	180.0	49×10^{-4}
ρ	6.0 g/cc	7.0×10^{-3}	11×10^{-4}
r	0.5 cm	5.0×10^{-3}	1×10^{-2}
r^4			200×10^{-4}

(With reference to equation 5.1, the total fractional error in D is given by the square root of the sum of the squares of the elemental fractional errors.)

D	1.9×10^{-12} $cm^2/sec.$	4.3×10^{-4}	2.3×10^{-2}

Thus for this particular specimen the error is:

$$D = 1.9 \pm 0.04 \times 10^{-12} \text{ cm}^2/\text{sec or } 2.3\%.$$

The average error found from similar calculations was $\pm$ 3%, the largest was $\pm$ 5% and the smallest was $\pm$ 1%. The example given above is typical of these calculations.

9.3 APPENDIX III : THE GROWTH OF SINGLE CRYSTALS OF THE INTERMEDIATE PHASES NiAl AND Ni_3Al

JOURNAL OF MATERIALS SCIENCE 2 (1967) 365–370

The Growth of Single Crystals of the Intermediate Phases NiAl and Ni_3Al

B. R. MCDONNELL, R. T. PASCOE, G. F. HANCOCK, C. W. A. NEWEY
Department of Metallurgy, Imperial College, London, SW7, UK

Received 10 January 1967, and in revised form 2 May

Single crystals of stoichiometric NiAl, nickel-rich Ni_3Al, and aluminium-rich $Ni_3(Al, Ti)$ have been grown by a modified Bridgman technique; a strain-anneal method has also been used to produce small, single crystals of non-stoichiometric NiAl.

1. Introduction

The intermediate phases based on the stoichiometric compositions NiAl and Ni_3Al are currently the subject of considerable research, both in the field of high-temperature alloys and in fundamental studies of the properties of structures which exhibit long-range order and which exist over a range of composition. Detailed investigations of these materials require them in the form of high-purity single crystals.

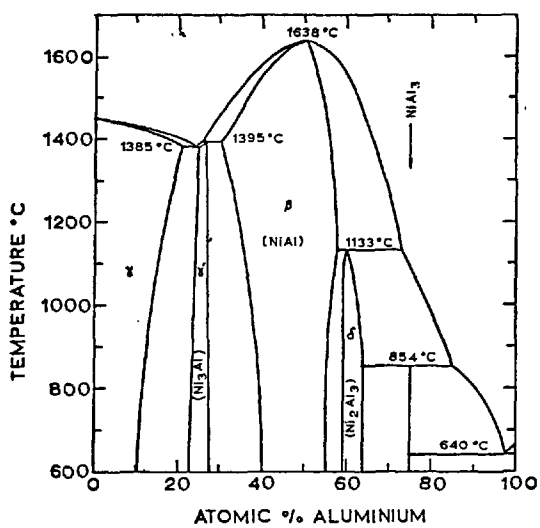

Figure 1 The Ni/Al phase diagram (after Hansen [1]).

The Ni/Al phase diagram, fig. 1, shows that the β' phase, NiAl, exists over a wide range of composition, with a maximum melting point of 1638° C at the stoichiometric composition. The γ' phase, Ni_3Al, also exists over a range of

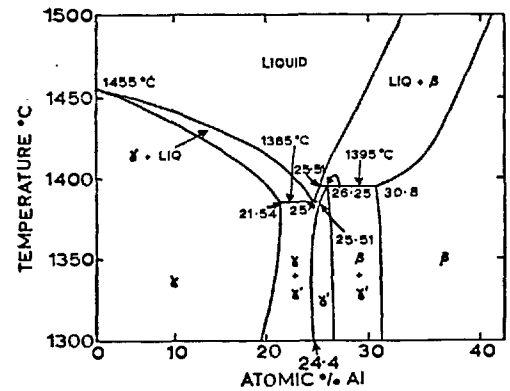

Figure 2 The nickel-rich region of the Ni/Al system (after Phillips [2]).

composition, see fig. 2; compositions between 24.4 and 25.51 and between 25.51 and 26.25 at. % Al are produced via a eutectic reaction at 1385° C and a peritectic reaction at 1395° C respectively.

This paper describes a modified Bridgman technique which has been used to grow single crystals of stoichiometric NiAl and Al-rich Ni_3Al alloys from the melt, and a strain-anneal technique for the production of single crystals of non-stoichiometric NiAl.

2. The Production of Ni/Al Alloys

In the production of high-purity Ni/Al alloys of the required composition and volume, for use as starting material for the growth of single crystals from the melt, two serious difficulties were encountered: the strong affinity which aluminium has for oxygen and the violent exothermic reaction which occurs when nickel and

aluminium are melted together. These problems were overcome by casting the alloy under a very pure argon atmosphere in a horizontal, water-cooled, copper boat using rf induction heating.

The apparatus, see fig. 3, was basically the "silver boat" equipment obtained from Stanelco Industrial Services Ltd* (early versions of this equipment were described by Sterling and Warren [3]) used in conjunction with a 25 kW rf generator. The closed system containing the boat and charge was traversed manually through the rf coil. The original, multitube, silver boat was replaced by a more simple boat, see fig. 3, which was constructed from a single copper tube. High-purity argon was produced by passing argon of commercial purity through P_2O_5 to remove water, and over titanium and chromium chips at 1000° C to remove oxygen and nitrogen respectively. Gaseous contamination of the closed system was reduced as much as possible by evacuating to a pressure of 10^{-5} torr prior to melting the main charge of 99.99 wt % Al and 99.999 wt % Ni. The first ingot of a series was often contaminated by the small traces of oxygen remaining in the system and was discarded. The alloy was produced and consolidated by moving the boat and accessories through the coil; careful manipulation of the boat was required to produce an ingot of satisfactory shape and homogeneity. The eddy currents induced in the melt only provided good mixing in the top half of the ingot, and homogeneity was improved by turning the ingot over and remelting.

Sterling and Warren [3] attempted to produce single crystals from the melt using the horizontal boat method, but were unsuccessful.

3. Growth of Single Crystals from the Melt

3.1. NiAl (β Phase)

The Ni/Al phase diagram, fig. 1, indicates that stoichiometric and near-stoichiometric NiAl alloys have a congruent melting point; consequently, single crystals of these compositions can be produced from the melt more readily than other compositions of the phase. In the present work, this has been achieved using the Bridgman technique; although, hitherto, this technique has not been used successfully for the growth of crystals with melting points above 1500° C because of the problems associated with container materials. The alternative methods of growing crystals from the melt, the floating-zone and Czochralski techniques, were considered to be impracticable because of the considerable technical problems involved.

The apparatus developed in the present work, fig. 4, was similar to that described by Hall [5] for the growth of iron-alloy single crystals, but, to withstand operating temperatures of 1700° C and to minimise the loss of aluminium at these temperatures, it differed in several important features.

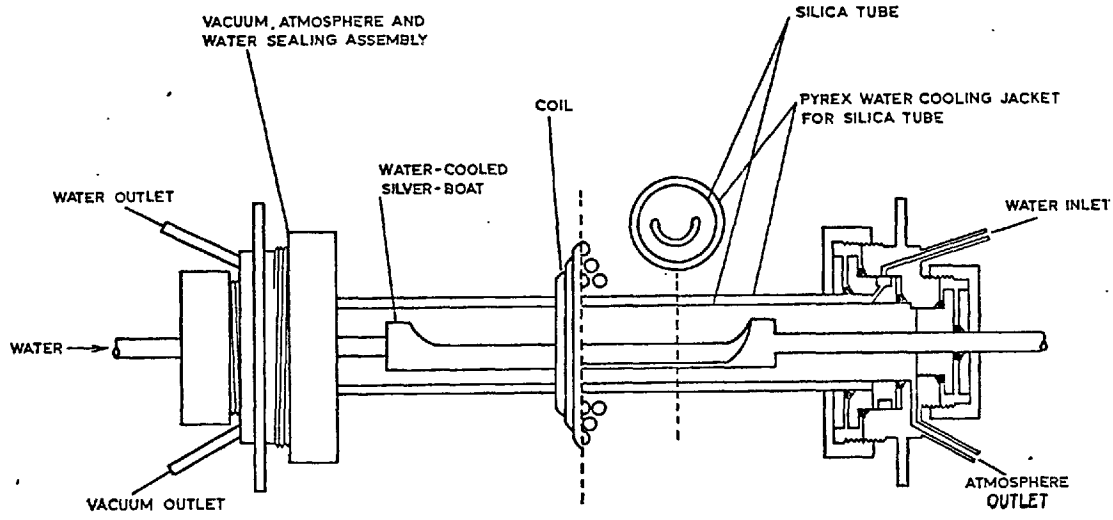

Figure 3 Schematic diagram of the horizontal casting apparatus.

*Address: Boreham Wood, Herts, UK.

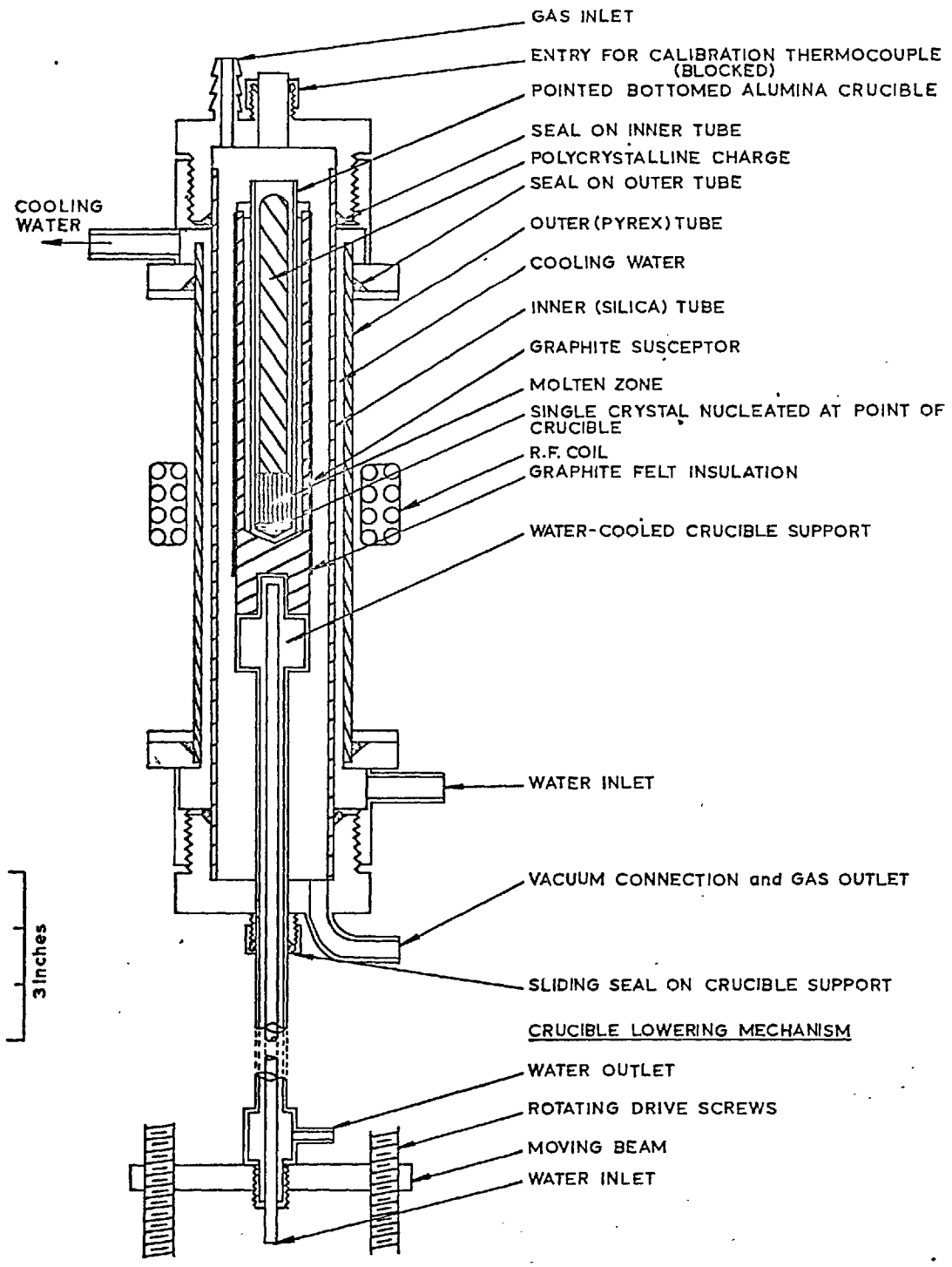

Figure 4 Schematic diagram of modified Bridgman apparatus (1 in. = 2.5 cm).

To ensure a constant alloy feed, the ingot produced in the horizontal boat was ground to fit easily into a tapered, alumina crucible with a pointed bottom. The charge was heated by rf

currents induced in a nuclear-purity graphite susceptor in the form of a tube around the crucible; a small gap between the susceptor and crucible minimised reduction of the alumina by the graphite. The crucible and susceptor were contained in a gas-tight, water-cooled jacket consisting of concentric silica (inner) and Pyrex tubes. Crystal growth was achieved by lowering the crucible and assembly, at the required temperature, through the rf coil by means of a mechanical drive. The crystal was grown in an argon atmosphere of commercial-purity argon; no attempt was made to purify the argon in this case, since carbon is a very efficient oxygen-getter at the operating temperatures used (about 1700° C). The apparatus was degassed by evacuating to a pressure of 10^{-4} torr at dull-red heat prior to carrying out the growth procedure.

During the initial experiments with this apparatus, the radiation from the susceptor was sufficient to cause devitrification and collapse of the silica tube. This problem was overcome by the incorporation of a radiation shield of graphite felt (Le Carbone (GB) Ltd,* Grade RVG200). This shield, sewn as a sleeve around the susceptor using graphite thread, proved to be extremely efficient and reduced considerably the power required to maintain the molten zone at 1700° C.

A control thermocouple was not used because its presence in the crucible would have interfered with the feeding of material into the molten zone. Instead, the power supplied by the rf generator was calibrated against temperatures achieved in blank experiments under growth conditions, and the operating temperature during crystal growth was then controlled by the power supplied. The temperature was found to be constant to within 20° C in successive calibrations at 1700° C.

The most satisfactory conditions for producing NiAl single crystals were a growth rate of 0.2 mm/min using an rf coil which heated a small zone of the susceptor about 2.5 cm wide; this size of zone prevented excessive volatilisation of aluminium from the melt and chemical attack of the crucible by the melt. Single crystals, 6 cm in length and 1 cm in diameter, have been grown; they did not adhere to the crucible and their surfaces were quite clean and oxide-free. The growth faces of these crystals were close to {100} and {110} – the most closely packed planes in the NiAl crystal structure.

3.2. Ni_3Al (γ' Phase)

According to the phase diagram, when alloys of composition between 24.4 and 25.0 at. % Al are cooled from the melt, primary γ dendrites separate out. At the eutectic temperature, the remaining liquid freezes as a two-phase mixture of $\gamma + \gamma'$. The final, single-phase, γ' structure is achieved by a solid-state transformation involving the precipitation of γ' in the primary γ dendrites and transformation of the eutectic to massive γ'.

Kear and Copley [6], using a 22.5 at. % Al alloy, have shown that, if growth is promoted from one end of a molten ingot by gradient cooling, the final cast structure is such that the primary γ dendrites are continuous throughout the crystal in the growth direction; consequently, on annealing, transformation of the residual γ should result in a homogeneous single crystal of γ'.

Provided the phase diagram is correct, in detail it should also be possible to grow single crystals of 25.51 at. % Al from the melt, since, at this unique composition, solidification occurs through the reactions liquid $\rightarrow \gamma' +$ liquid $\rightarrow$ γ' without the formation of any intermediate β. It may also be possible to grow crystals of compositions in the range 25.51 to 26.25 at. % Al, provided that a single nucleus of the β phase can be produced on cooling through the $\beta +$ liquid field, and that the nucleation and growth of γ' from this nucleus can be suitably controlled on cooling through the peritectic temperature. A considerable experimental difficulty for these compositions is the prevention of large amounts of segregation during growth from the melt. Thornton [7] has recently described a technique for producing single crystals of ζ Cu/Ge and ζ Ag/Sn, both of which are the products of a peritectic reaction. His technique involves a three-stage melting procedure which is difficult to apply to materials with melting points greater than about 1100° C.

In the present work, Ni_3Al (22.8 at. % Al) and a number of Ni_3 (Al, Ti) single crystals were grown using the modified Bridgman apparatus, but employing a higher growth rate (0.5 mm/min) than for the growth of NiAl crystals. The starting material was supplied by

*Address: Portslade, Sussex, UK.

International Nickel Ltd* in ingot form and this was machined to a loose fit in the pointed-bottomed crucible.

The composition of the binary alloy is similar to that of the nickel-rich crystals produced by Kear [6]. According to fig. 2, the composition of this alloy and also that of the crystals grown by Kear is in the $\gamma' + \gamma$ phase field. After a homogenisation anneal at 1200° C for 48 h, optical microscopy showed the apparent presence of small traces of γ at the original dendrite boundaries. However, electron-probe microanalysis was unable to detect any change in nickel or aluminium composition on traversing these boundaries.

Table I lists the compositions of the $Ni_3(Al, Ti)$ crystals which were grown. Since titanium atoms are substituted for aluminium atoms on the Ni_3Al crystal lattice, alloys 1 and 2 can be regarded as aluminium-rich; the presence of a small amount of titanium is not expected to have a significant effect on the phase diagram and so these alloys should solidify by a peritectic reaction. Chemical analysis indicated that, after homogenisation at 1300° C for 48 h, there was no significant segregation (0.2% along a 7 cm length of crystal).

TABLE I

Alloy No.	Aluminium (at. %)	Titanium (at. %)
1	22.05	4.3
2	21.34	4.94
3	20.52	4.4

Alloy 3 is essentially stoichiometric and again no significant segregation was observed.

The above results are to be contrasted with those for the binary alloys, where no success was achieved with the growth of crystals having compositions lying between stoichiometric and the aluminium-rich limit of the phase field.

All crystals produced had growth axes close to <211>, in contrast to the work of Kear and Copley [6] where growth axes close to <100> were invariably found.

4. The Strain-Anneal Technique

Since in the NiAl phase field, fig. 1, the liquidus and solidus diverge rapidly with departure from stoichiometry, particularly on the aluminium-rich side, it was felt that a solid-state method would provide the best means of growing single crystals of non-stoichiometric NiAl. The strain-anneal technique [4], which is based on the controlled recrystallisation and grain growth of a work-hardened polycrystalline sample of the required composition, was chosen. In its conventional form, this method consists of introducing a previously determined, "critical", tensile strain into a fine-grained, strain-free specimen; the specimen is then annealed at successively higher temperatures in a stepwise fashion or by passing it through a steep temperature gradient.

Hot-extruded NiAl with a grain size of 50 μm, supplied by International Nickel Ltd, was cut into specimens of typical dimensions 15 × 2.5 × 2.5 mm using a diamond-impregnated slitting wheel.

The brittle nature of NiAl in tension, at temperatures below which appreciable recovery occurs, prevented the use of a tensile pre-strain, and so the specimens were pre-strained in compression using apparatus which is described elsewhere [8]. The deformed specimens were then annealed in batches by placing them in a closed-end, alumina tube, over which was passed a temperature-gradient furnace. The furnace, which had a gradient of 150° C/cm at an operating temperature of 1500° C, was traversed at 0.5 cm/h. The specimens were annealed in a stream of argon which was purified by the process described earlier.

A critical strain value that leads to the growth of a single crystal was not found; this was probably a consequence of the slight inhomogeneities of deformation produced during the pre-straining of the long, narrow specimens. It was found, however, that specimens with large grains were often obtained after strains of greater than 0.5% and that many of the grains were sufficiently large for useful single crystals to be isolated, see fig. 5.

Useful single crystals were grown in a range of compositions containing excess nickel and these have been used in studies of slip systems. No satisfactory, aluminium-rich, single crystals have yet been grown, although considerable grain growth has been observed. The growth of aluminium-rich crystals is complicated by their vacancy defect structure, which renders these alloys completely brittle at room temperature, even in compression. Specimens of these compositions must, therefore, be strained at an elevated temperature; 650° C was found to be

*Address: Wiggin Street, Birmingham 16, UK

Figure 5 Effects of the strain-anneal treatment on grain size; each specimen has been given the same annealing treatment (heated to 1500° C in a travelling gradient). Top – specimen undeformed before annealing. Bottom – specimen given 1% plastic strain in compression before annealing.

the most effective, because the initial rate of work-hardening is greatest at this temperature, and a high rate of work-hardening aids a uniform distribution of strain. The specimens were rapidly cooled to room temperature immediately after deformation at 650° C, to prevent recovery

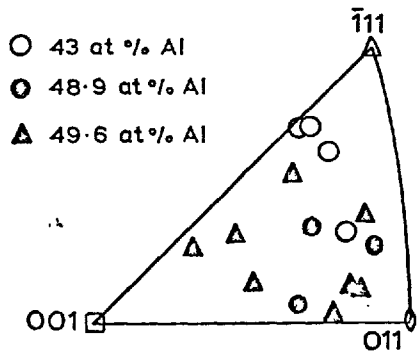

Figure 6 Orientations of the compression axes of polycrystals related to the resultant single crystals grown by the strain-anneal technique.

reducing the stored energy introduced by the deformation.

Crystalline perfection, indicated by the sharpness of X-ray reflections, was higher for crystals grown by the solid-state method than for those grown from the melt. This difference could be removed by annealing the melt-grown crystals at 1500° C in an argon atmosphere for about 12 h. There was no obvious relationship in the strain-anneal specimens between the orientations of the crystals produced and their original compression axes, see fig. 6; crystals with orientations covering a wide area of the unit stereographic triangle were produced.

Acknowledgements

The authors would like to thank Professor J. G. Ball for the provision of research facilities at Imperial College, and the Science Research Council for a Grant for Special Research, and the Ministry of Aviation for support.

The provision of materials by International Nickel Ltd (Ni_3Al, high-purity Ni, and extruded NiAl), British Aluminium Research Laboratories (high-purity Al), and Dr D. A. Young of Imperial College (graphite rod and felt) are also gratefully acknowledged.

References

1. M. HANSEN, "Constitution of Binary Alloys" (McGraw-Hill, 1958), p. 118.
2. H. W. L. PHILLIPS, Annotated Equilibrium Diagram No. 18, Institute of Metals (1958).
3. H. F. STERLING and R. W. WARREN, *Metallurgia* 67 (1963) No. 404.
4. "Art and Science of Growing Crystals", edited by J. J. Gilman (Wiley, 1963), p. 415.
5. R. C. HALL, *Trans. Met. Soc. AIME* 209 (1957) 1267.
6. B. KEAR and S. COPLEY, Pratt & Witney Aircraft Report No. 66-026 (September 1966).
7. P. H. THORNTON, *Trans. Met. Soc. AIME* 236 (1966) 592.
8. R. T. PASCOE, K. C. RADFORD, R. D. RAWLINGS, and C. W. A. NEWEY, *J. Sci. Instr.* 44 (1967) 366.

10. REFERENCES

M.R. Acher & R. Smoluchowski (1951) J. Appl. Phys. 22, 1260.
R.P. Agarwala, S.P. Murarka & M.S. Anand (1968) Acta Met. 16, 61.
W.O. Alexander & N.B. Vaughn (1937) J. Inst. Met. 61, 247.
S. Arrhenius (1889) Z. Phys. Chem. 4, 226.
R.A. Artman (1952) J. Appl. Phys. 23, 475.

A. Ball & R.E. Smallman (1966) Acta. Met. 14, 1349.
A. Ball & R.E. Smallman (1968) Acta Met. 16, 233.
J. Bardeen (1949) Phys. Rev. 76, 1403.
J. Bardeen & C. Herring (1951) Atom Movements. A.S.M. Cleveland.
R.M. Barrer (1941) Diffusion in and Through Solids, Cambridge Univ. Press.
A.E. Berkowitz, F.E. Jaumot & F.C. Nix (1954) Phys. Rev. 95, 1185.
C.E. Birchenall (1959) Trans. A.I.M.E. 227, 784.
C.E. Birchenall & R.F. Mehl (1947) Trans. A.I.M.M.E. 171, 147.
J.M. Blakely (1963) Progress in Material Science. 10, 395.
L. Boltzman (1894) Ann. Physik. 53, 959.
H.P. Bonzel (1965) Acta Met. 13, 1084.
R.J. Borg & C.E. Birchenall (1960) Trans A.I.M.E. 218, 980,
A.J. Bradley & G.C. Seeger (1939) J. Inst. Met. 64, 81.
A.J. Bradley & A. Taylor (1937) Proc. Roy. Soc. A159, 56.
W.L. Bragg & E.J. Williams (1935) Proc. Roy. Soc. A151, 540.
A.R. Brosi, C.J. Borkowski, E.E. Conn & J.C. Griess (1951) Phys. Rev. 81, 391,
F.S. Buffington & M. Cohen (1954) Acta Met. 2, 660.
F.S. Buffington, K. Hirano & M. Cohen (1961) Acta Met. 9, 434.

H.C. Carslaw & J.C. Jaeger (1959) Trans. A.I.M.E. 122, 11.

S. Chandrasekhar (1943) Rev. Mod. Phys. 15, 63.
R. Collongues (1956) Inst. Itern. de Chimie Solvay - 10ieme Conseil de Chimie, Brussels.
K. Compaan & Y. Haven (1956) Trans. Faraday Soc. 52, 786.
M.J. Cooper (1963A) Phil. Mag. 8, 805.
M.J. Cooper (1963B) Phil. Mag. 8, 811.
M.J. Cooper (1964) Phil. Mag. 10, 735.
J. Crank (1956) Mathematics of Diffusion, Clarendon Press, Oxford.

L.S. Darken (1948) Trans. A.I.M.E. 175, 184.
L.S. Darken (1951) Atom Movements, A.S.M, Cleveland.
G.T. Dienes (1953) Phys. Rev. 89, 185.
H.A. Domian & H.I. Aaronson (1964) Trans. Met. Soc. A.I.M.E. 230, 44.
H.A. Domian & H.I. Aaronson (1965) Diffusion in Body Centered Cubic Metals, A.S.M.
J.E. Dorn & A.R. Wazzen (1965) J. Appl. Phys. 36, 222.

F. Einsen & C.E. Birchenall (1957) Acta Met. 5, 265.
E.W. Elcock (1959) Proc. Phys. Soc. 73, 250.
E.W. Elcock & C.N. McCombie (1958) Phys. Rev. 109, 605.

J.I. Federer & T.S. Lundy (1963) Trans. A.I.M.E. 227, 592.
A. Fick (1855) Uber Diffusion Pagg. Ann. 94, 59.
J.C. Fisher (1951) J. Appl. Phys. 22, 74.
J.C. Fisher, J.H. Hollomon & D. Turnbull (1948) Trans. A.I.M.E. 175, 184.
P.A. Flinn & G.M. McManus (1961) Phys. Rev. 124, 54.
R.J. Friauf (1962) J. Appl. Phys. 33, 494.

H.C. Gatos & A.D. Kurtz (1954) J. Metals. 6, 616.

S.D. Gertstriken, I. Ya. Dekhtyar, N.P. Plotnikova, L.F. Slastnikova & T.K. Yatsenko (1958) Issled. po Zharoproch. Splavam, Akad. Nauk S.S.S.R. 3, 68.

S.D. Gertstriken & I. Ya Dekhtyar (1956) Fiz. Metal, i Metallored., Akad. Nauk S.S.S.R. 3, 242.

S.D. Gertstriken, T.K. Yatsenko & L.F. Slastnikova (1961) Sb. Nauchn. Rabot Inst. Metallofiz, Akad. Nauk Ukr. S.S.S.R. 13, 93.

G.B. Gibbs (1963A) C.E.G.B. Research & Develop. Dept., Berkeley Nucl. Labs. Report No. RD/B/N.152.

G.B. Gibbs (1963B) C.E.G.B. Research & Develop. Dept., Berkeley Nucl. Labs. Report No. RD/B/N.159.

G.B. Gibbs, D. Graham & D.H. Tomlin (1964) Phil. Mag. 8, 1269.

E.M. Grata (1960) Symp. Mechanical Properties of Intermetallic Compounds, ed. Westbrook, Wiley, 358.

J. Groh & G. Von Hevesy (1920) Ann. Physik. 63, 85.

J. Groh & G. Von Hevesy (1920) Ann. Physik. 65, 216.

S.R. de Groot (1952) Thermodynamics of Irreversible Processes, New York.

P.L. Gruzin (1952) Dokl. Akad. Nauk S.S.S.R. 86, 289.

D. Gupta (1961) Phd thesis, Univ. of Illinois.

L.N. Guseva (1951) Dokl. Akad. Nauk S.S.S.R. 77, 145.

L. Guttman (1956) Solid State Physics 3, 415.

R.A. Harlow & Otto Gamba (1964) Atomics International, Report No. NNA-SR-8, 387.

W.C. Hagel (1962) Trans. Met. Soc. A.I.M.E. 224, 430.

W.C. Hagel (1963) General Electric Research Laboratory Report No. 63-RL-3320M.

W.C. Hagel (1967) Intermetallic Compounds ed. Westbrook, Wiley.

W.C. Hagel & J.H. Westbrook (1961) Trans. Met. Soc. A.I.M.E, 221, 951.

W.C. Hagel & J.H. Westbrook (1965) Diffusion in Body Centered Cubic Metals, A.S.M.

M. Hansen (1958) Constitution of Binary Alloys, McGraw-Hill.

K. Hirano, R. Agarwala & M. Cohen (1962) Acta Met. 10, 857.

K. Hirano, M. Cohen & B. Averbach (1961) Acta Met. 9, 440.

K. Hirano, D. Duhl & M. Cohen (1963) Acta Met. 11, 1.

R.E. Hoffman (1951) Atom Movements, A.S.M., Cleveland.

R.E. Hoffman, F.W. Pikus & R.A. Ward (1956) J. Metals, 8, 483.

D.F. Holcomb & R.E. Norberg (1955) Phys. Rev. 98, 1074.

J.B. Hudson & R.E. Hoffman (1961) Trans. A.I.M.E. 221, 761.

W. Hume-Rothery & G.V. Raynor (1962) The Structure of Metals and Alloys, Institute of Metals.

H.B. Huntington, N.C. Miller & V. Nerses (1961) Acta Met. 9, 749.

M.C. Inman (1954) The Measurement of Self Diffusion Coefficients in Binary Alloys. Proc. of Radioactive Conf., Oxford.

F.E. Jaumot & R.L. Smith (1956) Trans. A.I.M.E. 206, 164.

W. Jost (1952) Diffusion in Solids Liquids & Gases, Ac. Press, New York.

W. Kass & M. O'Keeffe (1966) J. Appl. Phys. 37, 2377.

T.S. Ke (1947) Phys. Rev. 71, 553.

G.V. Kidson (1963) Can J. Phys. 41, 1563.

G.V. Kidson (1965) Diffusion in Body Centered Cubic Metals, A.S.M.

R. Kikuchi (1961) J. Phys. Chem. Sol. 20, 35.

R. Kikuchi & H. Sato (1964) Theory of Substitutional Diffusion in an Ordered Phase, talk presented at 93rd A.I.M.E. Annual Meeting.

E.O. Kirkendall (1942) Trans. A.I.M.E. 147, 104.

S.N. Kriukov & A.A. Joukhovitsky (1953) Dokl. Akad. Nauk S.S.S.R. 90, 379.

G.C. Kuczynski (1948) J. Appl. Phys. 19, 308.

A.B. Kuper, D. Lazarus, J.R. Manning & C.T. Tomizuka (1956) Phys. Rev. 104, 1536.

A.D. Kurtz, B.L. Averbach & M. Cohen (1955) Acta Met. 3, 442.

U.S. Landergren (1956) Trans. A.I.M.E. 206, 73.

I. Langmuir (1934) J. Franklin Inst. 217, 543.

E.P. Lautenslager, D.A. Kiewit & J.O. Brittain (1965) Trans. Met. Soc. A.I.M.E. 233, 1297.

D. Lazarus (1955) Phys. Rev. 93, 973.

D. Lazarus (1960) Solid State Physics, 10, 106.

D. Lazarus (1962) Energetics. 1, 1.

A.D. Le Claire (1948) Progress in Metal Physics, 1, chapt. 7.

A.D. Le Claire (1953) Acta Met. 3, 452.

A.D. Le Claire (1965) Diffusion in Body Centered Cubic Metals, A.S.M.

C. Leymonie (1963) Radioactive Tracers in Physical Metallurgy, Chapman & Hall, London.

A.B. Lidiard (1955) Phil. Mag. 46, 1218.

A.B. Lidiard (1957) Phys. Rev. 106, 823.

A.B. Lidiard & A.D. Le Claire (1956) Phil. Mag. 1, 518.

H. Lipson & A. Taylor (1939) Proc. Roy. Soc. A173, 232.

T. Liu & H. Drickamer (1954) J. Chem. Phys. 22, 312.

T.S. Lundy, J.I. Federer, R.E. Pawel & F.R. Winslow (1965) Diffusion in Body Centered Cubic Metals, A.S.M.

T.S. Lundy & C.J. McHargue (1965) Trans. A.I.M.E. 233, 243.
D.W. Lynch (1960) Phys. Rev. 118, 468.

J.R. MacEwan, J.U. MacEwan & L. Yaffe (1959) Can. J. Chem. 37, 1629.
C.A. Mackliet (1958) Phys. Rev. 109, 1964.
S.M. Makin, A.H. Rowe & A.D. Le Claire (1957) Proc. Phys. Soc. 708, 545.
O. Manley (1960) J. Phys. Chem. Solids. 13, 244.
J.R. Manning (1958) Phys. Rev. Let. 1, 365.
J.R. Manning (1959) Phys. Rev. 116, 819.
C. Matano (1933) Japan J. Phys. 8, 109.
R.F. Mehl (1936) Trans. A.I.M.E. 122, 11.
R.F. Mehl (1937) J. Appl. Phys. 8, 174.
A.J. Murdock & D.H. Tomlin (1959) Phil. Mag. 4, 628.
J.F. Murdock (1965) Diffusion in Body Centered Cubic Metals, A.S.M.
J.F. Murdock, T.S. Lundy & E.E. Stansbury (1964) Acta Met. 12, 1033.
T. Muto & Y. Takagi (1955) Solid State Physics, 1, 194.

F.C. Nix & F.E. Jaumot (1951) Phys. Rev. 83, 1275.
A.S. Nowick (1952) Phys. Rev. 88, 9.
A.S. Nowick (1953) Progress in Metal Physics, 4, chapt. 1.

L. Onsager (1931) Phys. Rev. 37, 405.
L. Onsager (1932) Phys. Rev. 38, 2265.
L. Onsager & R.M. Fuoss (1932) J. Phys. Chem. 36, 3689.

R.M. Paine, A.J. Stonehouse & M.B. Bever (1960) Wright Air Development Command Technical Report, WADC TR 59-29.
H.R. Paneth (1950) Phys. Rev. 80, 708.
R.T. Pascoe (1966) PhD thesis, Univ. of London.

R.T. Pascoe & C.W.A. Newey (1968) Metal Science Journal, 2, 138.

H.W. Paxton & R.A. Wolfe (1964) Carnegie Inst. of Tech. Report No. NR. 031-184.

R.F. Peart (1965) Diffusion in Body Centered Cubic Metals, A.S.M.

R.F. Peart & D.H. Tomlin (1962) Acta Met. 10, 123.

N.L. Peterson & S.J. Rothman (1965) Diffusion in Body Centered Cubic Metals, A.S.M.

W.M. Portnoy, H. Letaw & L. Slifkin (1954) Rev. Sci. Inst. 25, 865.

G.M. Pound, W.R. Bittler & H.W. Paxton (1961) Phil. Mag. 6, 473.

T.J. Renouf (1964) Phil. Mag. 9, 781.

J.E. Reynolds, B. Averbach & M. Cohen (1957) Acta Met. 5, 29.

S.A. Rice et al (1958) Phys. Rev. 112, 804.

S.A. Rice et al (1959) J. Chem Phys., 31, 139.

W.C. Roberts-Austin (1896) Phil. Trans. Roy. Soc. A187, 383.

W.C. Roberts-Austin (1896) Proc. Roy. Soc. A59, 281.

S.J. Rothman, L.T. Loyd, R. Weil & A.L. Harkness (1960) Trans. A.I.M.E. 218, 605.

R.C. Ruder & C.E. Birchenall (1951) Trans. A.I.M.E. 191, 142.

A.V. Savitski (1964) Physics of Metals & Metallography, 16, 77.

J. Steigman, W. Shockley & F.C. Nix (1939) Phys. Rev. 56, 13.

W. Seith (1955) Diffusion in Metallen, Berlin.

F. Seitz (1948) Phys. Rev. 74, 1513.

A.U. Seybolt & J.H. Westbrook (1964) Acta Met. 12, 449.

J.A. Sheppard (1963) Brit. Weld. Journal, 10, 603.

P.G. Shewmon (1963) Diffusion in Solids, McGraw-Hill.

G.A. Shirn, E.S. Wadja & H.B. Huntington (1953) Acta Met. 1, 513.

L. Slifkin, D. Lazarus & C.T. Tomizuka (1952) J. Appl. Phys. 23, 1032.

L. Slifkin & C.T. Tomizuka (1955) Phys. Rev. 97, 836.

L. Slifkin & C.T. Tomizuka (1956) Phys. Rev. 104, 1803.

A.D. Smigelskas & O.E. Kirkendall (1947) Trans. A.I.M.E. 171, 130.

J.C. Smithells (1949) Metals Reference Book, Butterworths, London.

R. Smoluchowski & H. Burgess (1949) 76, 309.

H.F. Stirling & R.W. Warren (1963) Metallurgia, 67, 404.

N.S. Stoloff & R.G. Davies (1966) Progress in Material Science, 13, 1.

G.P. Tiwari & B.D. Sharma (1967) Scripta Met. 1, 131.

C.T. Tomizuka (1959) Methods in Experimental Physics, Acad. Press, New York, 5.

Tret'yakov & Khomyakov (1959) Russ. J. Inorg. Chem., 4, 5.

D. Turnbull (1951) Atom Movements. A.S.M., Cleveland.

P.A. Turner, R.T. Pascoe & C.W.A. Newey (1966) J. Material Science, 1, 113.

R.R. Vandervoort, A.K. Mukherjee & J.E. Dorn (1966) Trans. A.S.M. 59, 931.

G.A. Vinyard (1957) J. Phys. Chem. Sol. 3, 121.

R.J. Wasilewski (1965) Trans. Met. Soc. A.I.M.E. 233, 1691.

R.J. Wasilewski (1966) Trans. Met. Soc. A.I.M.E. 236, 455.

M.S. Wechslers (1957) Acta Met. 5, 150.

J. Weertman (1957) J. Appl. Phys. 28, 362 & 1185.

Cyril Wells (1951) Atom Movements, A.S.M.

C. Wert (1950) Phys. Rev. 79, 601.
C. Wert & C. Zener (1949) Phys. Rev. 76, 1169.
G.W. West (1964) Phil. Mag. 9, 979.
J.H. Westbrook (1957) J. Electrochem. Soc. 104, 369.
J.H. Westbrook (1960) Symp. Mechanical Properties of Intermetallic Compounds, ed. Westbrook, Wiley.
J.H. Westbrook (1965) High Strength Materials, ed. Zackay, Wiley.
J.H. Westbrook & W.C. Hagel (1963) Trans. Met. Soc. A.I.M.E. 221, 193.
J.H. Westbrook & D.L. Wood (1963A) J. Inst. Met. 91, 174.
J.H. Westbrook & D.L. Wood (1963B) General Electric Research Report No. 63-RL-3324M.
E.P. Wigner (1932) Phys. Rev. 40, 749.
W.D. Wilkinson (1965) Laboratory Handbook, ed. Parr.
G.P. Williams Jr. & L. Slifkin (1958) Phys. Rev. Letters, 1, 234.
P. Winblatt (1967) Acta Met. 15, 1453.
D.L. Wood & J.H. Westbrook (1960) Wright Air Development Division Technical Report WADD TR-60-184.
D.L. Wood & J.H. Westbrook (1962) Trans. Met. Soc. A.I.M.E. 224, 1024.

A. Ya Shinyayav (1964) Phys. Met. & Metallography, 15, 93.
S. Yukawa & M.J. Sinnott (1955) Trans. A.I.M.E. 203, 996.

C. Zener (1947) Phys. Rev. 71, 846.
C. Zener (1948) Elasticity and Anelasticity in Metals, Univ. of Chicago Press.
C. Zener (1950) Acta Cryst. 3, 346.
C. Zener (1951) J. Appl. Phys. 22, 372.
C. Zener (1952) Imperfections in Nearly Perfect Crystals, Wiley, New York.

A.A. Zhukhovitsky (1956) Conf. Acad. Sci. U.S.S.R. on Peaceful Uses of Atomic Energy, U.S. Atomic Energy Commission.

S. Zirinski (1956) Acta Met. 4, 164.